Interface of Abiotic and Microbial Reactions for Enhanced Detoxification of Trichloroethene and Hexavalent Chromium

by

Srivatsan Mohana Rangan

A Dissertation Presented in Partial Fulfillment
of the Requirements for the Degree
Doctor of Philosophy

Approved September 2022 by the
Graduate Supervisory Committee:

Rosa Krajmalnik-Brown, Co-Chair
Anca G. Delgado, Co-Chair
César I. Torres
Leon van Paassen

Arizona State University

December 2022

ABSTRACT

Trichloroethene (TCE) and hexavalent chromium (Cr (VI)) are ubiquitous subsurface contaminants affecting the water quality and threatening human health. Microorganisms capable of TCE and Cr (VI) reductions can be explored for bioremediation at contaminated sites. The goal of my dissertation research was to address challenges that decrease the efficiency of bioremediation in the subsurface. Specifically, I investigated strategies to (i) promote improve microbial reductive dechlorination extent through the addition of Fe^0 and (ii) Cr (VI) bio-reduction through enrichment of specialized microbial consortia. Fe^0 can enhance microbial TCE reduction by inducing anoxic conditions and generating H_2 (electron donor). I first evaluated the effect of Fe^0 on microbial reduction of TCE (with ClO_4^- as co-contaminant) using semi-batch soil microcosms. Results showed that high concentration of Fe^0 expected during *in situ* remediation inhibited microbial TCE and ClO_4^- reduction when added together with *Dehalococcoides mccartyi*-containing cultures. A low concentration of aged Fe^0 enhanced microbial TCE dechlorination to ethene and supported complete microbial ClO_4^- reduction. I then evaluated a decoupled Fe^0 and biostimulation/bioaugmentation treatment approach using soil packed columns with continuous flow of groundwater. I demonstrated that microbial TCE reductive dechlorination to ethene can be benefitted by Fe^0 abiotic reactions, when biostimulation and bioaugmentation are performed downstream of Fe^0 addition. Furthermore, I showed that ethene production can be sustained in the presence of aerobic groundwater (after Fe^0 exhaustion) by the addition of organic substrates. I hypothesized that some lessons learned from TCE Bioremediation

can be applied also for other pollutants that can benefit from anaerobic reductions, like Cr (VI). Bioremediation of Cr (VI) has historically relied on biostimulation of native microbial communities, partially due to the lack of knowledge of the benefits of adding enriched consortia of specialized microorganisms (bioaugmentation). To determine the merits of a specialized consortium on bio-reduction of Cr (VI), I first enriched a culture on lactate and Cr (VI). The culture had high abundance of putative *Morganella* species and showed rapid and sustained Cr (VI) bio-reduction compared to a subculture grown with lactate only (without *Morganella*). Overall, this dissertation work documents possible strategies for synergistic abiotic and biotic chlorinated ethenes reduction, and highlights that specialized consortia may benefit Cr (VI) bio-reduction.

ACKNOWLEDGMENTS

Firstly, I would like to convey my gratitude to my advisors Dr. Rosa Krajmalnik-Brown and Dr. Anca G. Delgado, who inspired me to pursue PhD in Environmental Engineering. You have guided me and supported me constantly in my ups and downs throughout my program at ASU. I am grateful for all the support, motivation and critical feedback from you, which were instrumental in my scientific contributions. Thank you very much for providing emotional support beyond academic responsibilities whenever I needed it. I am immensely honored to have been your student. Sincere thanks to Dr. César I. Torres and Dr. Leon van Paassen, my committee members for providing timely valuable thoughts and feedback on my research. Thank you very much for being very flexible and supportive.

Thanks to Dr. Greg Lowry and Dr. Laurie Lapat-Polasko for collaborating with me in the chlorinated ethenes and perchlorate remediation work. Your thoughts and insights were very valuable. Dr. Bruce Rittmann, thanks for being an inspiration and participating as a committee member in my comprehensive exam. I am thankful to my mentees Aatikah Mouti, Ibrahim Ibrahim, Anton Sachs, Zandrian McMacken, Erik Barraza Cordova and Sarah Sachs (undergraduate students), and Shefali Rao and Maheshwar Suresh Mane (master's students) for your dedicated work and contributions to this work. Thanks to Dr. Sofia Esquivel-Elizondo, Dr. Georgios Papacharalampos, Dr. Khemlal Nirmalkar, Dr. Diana Calvo Martinez, Dr. Devin Bowes and Dr. Sanchari Saha for helping me in various aspects of my research. Special thanks to my fellow PhD students Aide Robles, Evelyn Moni Miranda and Sayalee Joshi for being my support

system professionally as well as personally. I would like thank all members of the Biodesign Swette Center for Environmental Biotechnology and Biodesign Center for Health Through Microbiomes for making my workplace comfortable and memorable. Carole Flores and Sarah Arrowsmith, thank you very much for making the lab a safe and comfortable place to work. Christopher Muse, thanks for being my go-to person for help with analytical instruments and reactor design. Your creativity, and dedication to work has impressed me several times.

I sincerely thank the Center for Bio-mediated & Bio-inspired Geotechnics (CBBG) for providing funding, and an amazing platform for research collaborations, outreach activities and leadership roles. I have enjoyed unique opportunities to work with undergraduate students (REU program) and high school teachers (RET program), and participate in outreach activities. I can certainly say that my experience with CBBG has been very rewarding. The CBBG team has gone above and beyond for being inclusive and making sure I have all the resources for my research and career advancement. Thanks to the ASU graduate college for supporting my final semester with the prestigious Graduate Completion Fellowship.

I would like to thank my friends outside the laboratory, who were my family away from home. Big thanks to Dr. Raghu Pradeep Narayanan, Dr. Soma Chaudhary, Dr. Sree Ganesh Balasubramani, Dr. Sanchari Saha, Dr. Pritha Bisarad, Leeza Abraham, and Skanda Vishnu Sundar for your moral support and being my well-wishers. I would not have survived my grad school life without you all. Bharath Sampathkumar, Sam Asir Nandakumar, Vishal Jaitra, Venkatesh Janakiraman, and Ashwin Agathya, Praveen

Muruganandam and Arul Ravichandran, I have enjoyed your friendship, support, and all our weekend meetups.

I would not have been here without the love and support from my family. To my father, thanks for trusting me, and providing constant support and motivation throughout my life. You have always gone above and beyond to make sure I have everything I need to pursue my ambitions. To my mother, your selflessness and encouragement have made me who I am, and I can't thank you enough for everything you have done for me throughout my life. To my brother, growing up with you is one of the most memorable things in my life. I have learned many things from you since my childhood days and I continue to do so. Thanks for being an amazing brother and my best friend. To my cousins Poovannan Dhasarathi and Madhumitha Poovannan, you are the reason why I never felt home-sick, being far away from home. Your care, love, and emotional support helped me a great deal during my grad school at ASU. Thanks to my mother-in-law, for being a friend and well-wisher, and all her encouragement.

To my wife, Himalini Srinivasan, thanks for all the patience, motivation and encouragement to pursue this PhD. Your love, and support are my greatest strengths. I dedicate this work to you Himu!

TABLE OF CONTENTS

Page

LIST OF TABLES

Table Page

LIST OF FIGURES

Figure Page

Figure Page

CHAPTER 1

INTRODUCTION

About one third of the world's population relies on groundwater as a source of drinking water and water for irrigation (Li et al., 2021a). Yet, chemical contamination of groundwater and associated sediments is a ubiquitous problem affecting the water quality and health of millions of people around the world. Trichloroethene (TCE), perchlorate (ClO_4^-) and hexavalent chromium (Cr (VI)) are some of the most common groundwater contaminants affecting the global human population (Oleszkiewicz and Elektorowicz, 1993; Saha et al., 2011; Cao et al., 2019). My overall research goals were focused on enhancing anaerobic bioremediation of TCE, ClO_4^-, and Cr (VI) in soil and groundwater. Chapters 2 and 3 investigate the application of zero valent iron (Fe^0) and D*ehalococcoides mccartyi*-containing cultures for enhancing reductive dechlorination of TCE and ClO_4^- reduction. Chapter 4 addresses the contribution of enriched Cr (VI)-reducing microorganisms and fermentative microorganisms on the rate and capacity of microbial Cr (VI) reduction to shed light into the benefits of bioaugmentation for bioremediation of Cr (VI). Chapter 5 addresses the need for reliable, accurate, and cost-effective analytical method for simultaneous quantification 9 environmentally-important anions including Cr (VI) and ClO_4^-, at low μg L^{-1} in aqueous media.

1.1 Bioremediation of chlorinated ethenes

Chlorinated ethenes contamination is widespread in groundwater resources globally, primarily due to improper disposal and accidental spills of chlorinated organic solvents, including tetrachloroethene (PCE) and trichloroethene (TCE) (Pankow and

Cherry, 1996; McCarty, 2010; Stroo et al., 2012). PCE is a probable human carcinogen, and TCE is a known human carcinogen, and these two chemicals can cause harmful acute and chronic effects on the central nervous system, liver, lungs and kidney in humans and animals (Lash et al., 2014; ATSDR, 2019; Todd et al., 2019).

Bioremediation *via* anaerobic microbial reductive dechlorination is a widely used technique for remediation of chlorinated ethenes in soil and groundwater (Ellis, 2000; Löffler et al., 2013). Microbial reductive dechlorination of TCE is a process by which organohalide-respiring bacteria remove a chlorine atom from TCE and replace it with a hydrogen atom to transform TCE to primarily *cis*-DCE (occasionally to *trans*-DCE or 1,1-DCE), VC and finally to ethene, in a sequential manner (Figure 1.1).

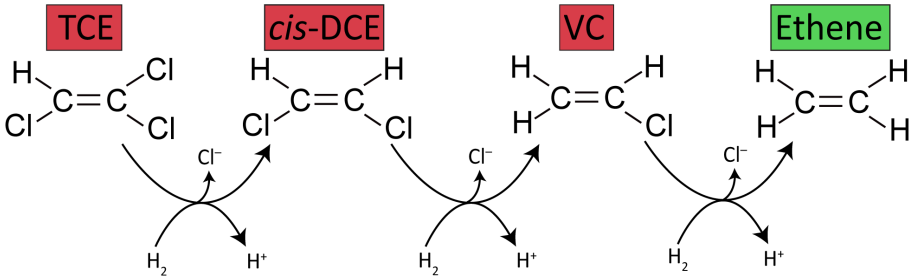

Figure 1.1. Pathway of microbial TCE reductive dechlorination to ethene mediated by organohalide-respiring bacteria.

Several organohalide-respiring bacteria can mediate TCE reductive dechlorination to DCE including species of *Geobacter (Sung et al., 2006)*, *Dehalobacter* (Schumacher and Holliger, 1996), *Desulfitobacterium* (Villemur et al., 2006), *Desulfuromonas* (Krumholz, 1997), *Sulfurospirillum* (Nijenhuis et al., 2005), *Dehalogenimonas* (Moe et al., 2016), and *Dehalococcoides* (Maymo-Gatell et al., 1997). Reductive dechlorination of *cis*-DCE and VC to produce non-toxic ethene is unique to certain species of *Dehalogenimonas* (Yang et al., 2020) and *Dehalococcoides* (Maymo-Gatell et al., 1997). Hence, anaerobic

bioremediation of chlorinated ethenes to ethene is contingent upon *Dehalococcoides mccartyi* (*D. mccartyi*) (Maymo-Gatell et al., 1997) and/or *Dehalogenimonas etheniformans* (Yang et al., 2020; Chen et al., 2022). In the past decades, TCE anaerobic bioremediation efforts in the field have primarily relied on *D. mccartyi* (Lu et al., 2006; Lee et al., 2008b).

1.2 Bioremediation of Perchlorate (ClO_4^-)

ClO_4^- often co-occurs with TCE due to their common usage in military sites operated by the U.S department of defense (U.S. Department of Defense, 2005; Stephenson, 2007; Rangan et al., 2020). 84% of the ClO_4^--contaminated Superfund sites in the U.S contain TCE as a co-contaminant (US EPA, 2017). ClO_4^- is an oxyanion widely used as an oxidizer in solid propellant rockets and missiles, and manufacture of munitions and fireworks (Gullick et al., 2001). Consumption of ClO_4^- can affect the thyroid gland by interfering with uptake of iodide, which is essential for thyroid hormone production (Coates and Achenbach, 2004; Environmental Toxicology Section., 2004).

The high reduction potential of ClO_4^- (E^0 = 1.287 V) makes it a favorable electron acceptor for perchlorate-reducing bacteria (Urbansky, 2000; Coates and Achenbach, 2004). Microbial ClO_4^- reduction involves sequential reduction of ClO_4^- to chlorate (ClO_3^-), chlorite (ClO_2^-) and finally to Cl^- and O_2. The O_2 generated from microbial ClO_4^- reduction is also usually reduced by perchlorate reducing bacteria to yield H_2O. The pathway of microbial ClO_4^- reduction is shown in Figure 1.2.

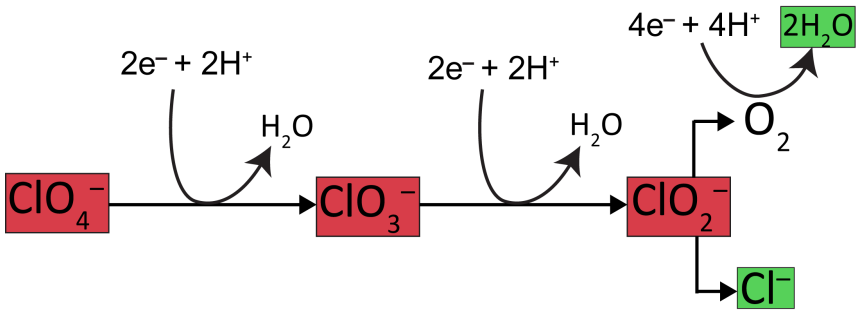

Figure 1.2. Pathway of microbial ClO_4^- reduction mediated by perchlorate-reducing bacteria.

1.3 Zerovalent iron (Fe^0)-enhanced bioremediation of TCE and ClO_4^-

Anaerobic bioremediation of TCE and ClO_4^- is often challenged by oxic conditions in the subsurface (Song and Logan, 2004; Amos et al., 2008a; Lyon and Vogel, 2013). Fe^0 is a reactive metal with strong reducing capability ($E^0 = -0.44$ V) (Fu et al., 2014). Fe^0 rapidly reduces dissolved O_2, thereby inducing anoxic conditions in the subsurface (Huang and Zhang, 2005). In the absence of O_2, Fe^0 reduces water molecules to generate H_2 (Lampron et al., 1998). Microbial TCE and ClO_4^- reductions can benefit from the Fe^0-induced anoxic conditions and H_2 production. H_2 is the obligate electron donor for TCE reductive dechlorination by *D. mccartyi* and a favorable electron donor for microbial ClO_4^- reduction by perchlorate-reducing bacteria. These characteristics of Fe^0 make it a good candidate to enhance anaerobic bioremediation of TCE and ClO_4^-, especially in aerobic aquifers. Figure 1.3 shows synergistic reactions between Fe^0, organohalide-respiring bacteria and perchlorate-reducing bacteria.

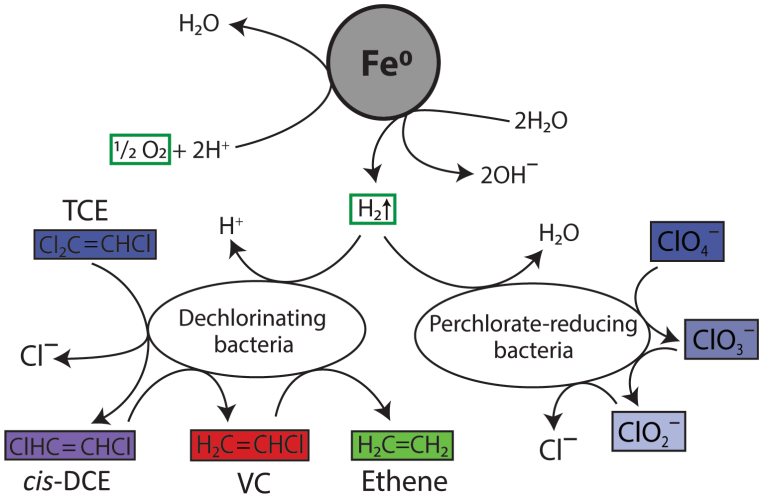

Figure 1.3. Synergistic reactions between abiotic Fe^0 reductions and TCE and ClO_4^- microbiological dechlorination.

However, these benefits could be offset by the Fe^0 induced oxidative stress and toxicity to microorganisms (Auffan et al., 2008; Yang et al., 2013; Velimirovic et al., 2015; Xie et al., 2017). The synergy between Fe^0 abiotic reactions and simultaneous microbiological TCE and ClO_4^- reductions is poorly understood and seldom addressed in the literature. Chapter 2 of my dissertation focused on addressing this gap of knowledge. I evaluated the effects of Fe^0 and its oxidation product Fe^{2+} on simultaneous microbial TCE and ClO_4^- reduction. In Chapter 3, I evaluated a strategy where the application of zero valent iron (Fe^0) and bioaugmentation with *D. mccartyi*-containing cultures were decoupled in space and time, for enhanced microbial TCE reductive dechlorination.

1.4 Bioremediation of hexavalent chromium (Cr (VI))

Chromium is a transition metal that has been widely used in a variety of industrial processes such as leather tanning, electroplating, and manufacture of alloys, pigments, and dyes (Zhitkovich, 2011; Karthik et al., 2017). In aqueous systems, the most stable oxidation states of chromium are +6 (Cr (VI)) and +3 (Cr (III)) (Joutey et al., 2015;

Shekhawat et al., 2015). Cr (VI) is a potent carcinogen and highly water-soluble, commonly as chromate ion (CrO_4^{2-}) or dichromate ion ($Cr_2O_7^{2-}$), depending on the pH (Biedermann and Landolph, 1990; Zhitkovich, 2011). Cr (III) is 1000 times less mutagenic than Cr (VI) and is considered an essential element for protein metabolism and insulin action (Cefalu and Hu, 2004; Qian et al., 2016; Vincent, 2017).

Bioremediation of Cr (VI) involves microorganisms that can use Cr (VI) as terminal electron acceptor (Cr (VI)-reducing microorganisms), reducing it to Cr (III) (Krishna and Philip, 2005). The reduced Cr (III) readily forms Cr_2O_3 and/or $Cr(OH)_3$ precipitates, effectively detoxifying and immobilizing chromium in subsurface environments (Jobby et al., 2018). Cr (VI) bioremediation usually relies on biostimulation of indigenous soil microorganisms using organic substrates (Nazarova et al., 2020; Song et al., 2021). This is primarily due to the lack of knowledge in the benefits of bioaugmentation for Cr (VI) reduction. Specifically, there is a lack of understanding in the contribution of enriched Cr (VI)-reducing microorganisms and fermentative microorganisms on the rate and capacity of microbial Cr (VI) reduction. Chapter 4 of my dissertation is focused addressing this gap of knowledge and assessing the benefits of bioaugmentation with enriched Cr (VI)-reducing bacteria for bioremediation of Cr (VI).

1.5 Objectives and outline of the dissertation

Microbial TCE reductive dechlorination of chlorinated ethenes to non-toxic ethene is often challenged by oxic conditions in the subsurface (Amos et al., 2008a). Additionally, the presence of ClO_4^- as a co-contaminant can also pose challenges to microbial reductive dechlorination of chlorinated ethenes (Borden, 2007; Hatzinger and

Diebold, 2009). In such scenarios, Fe^0 can induce the required anoxic conditions by removing dissolved O_2, and produce H_2, the obligate electron donor for *D. mccartyi* and a favorable electron donor for perchlorate-reducing bacteria. However, these benefits could be offset by the Fe^0 and Fe^{2+} (from Fe^0 oxidation)-induced oxidative stress and toxicity to microorganisms.

Chapter 2. The effect of Fe^0 on simultaneous microbial TCE and ClO_4^- reduction remains a gap of knowledge in the realm of combined Fe^0 and bioremediation treatment. The main objective of this chapter was to evaluate the effects of Fe^0 and its oxidation product, Fe^{2+} on microbiological TCE and ClO_4^- reductions using semi-batch microcosms containing soil and groundwater from a TCE and ClO_4^- contaminated Superfund site. This chapter has been published in a modified form in *Environmental Science & Technology* (Rangan et al., 2020).

Chapter 3. The results from chapter 2 implied that simultaneous application of Fe^0 and *D. mccartyi*-containing bioaugmentation cultures is detrimental to microbial TCE and ClO_4^- reduction. In chapter 3, I hypothesized that the negative effects can be mitigated and microbial TCE and ClO_4^- reduction can benefit from the Fe^0-induced anoxic conditions, when bioaugmentation is performed downstream of Fe^0 application. The objective of this chapter was to evaluate a novel treatment approach where the application of Fe^0 was decoupled in space and time from the addition of organic substrates and *D. mccartyi*-containing cultures for enhanced bioremediation of TCE, using continuous-flow soil columns. This chapter has been submitted for publication in a modified form in *Environmental Science & Technology*.

Chapter 4. The Superfund site soil and groundwater utilized in Chapters 2 and 3 has a history of Cr (VI) contamination. Cr (VI) groundwater contamination is a frequently encountered global issue, due to its usage in a wide range of industrial processes. Personally, my hometown in India has a serious Cr (VI) groundwater contamination since the early 1990s. Unlike TCE bioremediation where the benefits of bioaugmentation are well established, there is a lack of understanding in the benefits of bioaugmentation for *in situ* bioremediation of Cr (VI).

The objective in chapter 4 was to evaluate the benefits of bioaugmentation of mixed culture enriched with Cr (VI)-reducing bacteria for bioremediation of Cr (VI). I developed a microbial mixed culture enriched with Cr (VI)-reducing bacteria using soil and groundwater from the superfund site. I compared the rate and extent of Cr (VI) reduction by the mixed culture enriched with potential Cr (VI)-respiring bacteria (grown with Cr (VI) and lactate) against a subculture grown with lactate only.

Chapter 5. The maximum allowable limit for Cr (VI) in groundwater and drinking water established by the World Health Organization is 50 $\mu g\ L^{-1}$. For such low concentrations, the standard EPA method for Cr (VI) quantification using ion chromatography (IC) (Method 218.7) is Cr (VI) specific and does not allow quantification of other co-occurring anions. The objective of this chapter was to develop an IC method for simultaneous quantification Cr (VI) along with toxic metal anions including ClO_4^- and other common inorganic anions (e.g. Chloride, Nitrate and Sulfate) at low $\mu g\ L^{-1}$ concentrations. This chapter has been published in a modified from in *Environmental Engineering Science* (Mohana Rangan et al., 2021).

CHAPTER 2

SYNERGISTIC ZEROVALENT IRON (Fe^0) AND MICROBIOLOGICAL TRICHLOROETHENE AND PERCHLORATE REDUCTIONS ARE DETERMINED BY THE CONCENTRATION AND SPECIATION OF Fe[a]

2.1 Abstract

Trichloroethene (TCE) and perchlorate (ClO_4^-) are co-contaminants at multiple Superfund sites. Fe^0 is often used during TCE bioremediation with *Dehalococcoides mccartyi* to establish anoxic conditions in the aquifer. However, the synergy between Fe^0 abiotic reactions and microbiological TCE and ClO_4^- reductions is poorly understood and seldomly addressed in the literature. Here, we investigated the effect of Fe^0 and its oxidation product, Fe^{2+}, at field-relevant concentrations, in promoting microbial TCE and ClO_4^- reductions. Using semi-batch microcosms with a Superfund site soil and groundwater, we showed that high Fe^0 concentration (16.5 g L^{-1}) expected during Fe^0 *in situ* injection mostly yielded TCE abiotic reduction to ethene/ethane. However, such concentrations obscured dechlorination by *D. mccartyi*, impeded ClO_4^- reduction, and enhanced SO_4^{2-} reduction and methanogenesis. Fe^{2+} at 0.25 g L^{-1} substantially delayed conversion of TCE to ethene when compared to no-Fe controls. A low concentration of aged-Fe^0 synergistically promoted microbiological TCE dechlorination to ethene while achieving complete ClO_4^- reduction.

---

[a]This chapter was published in an altered format as **Rangan, S. M.**, Mouti, A., LaPat-Polasko, L., Lowry, G. V., Krajmalnik-Brown, R., & Delgado, A. G. (2020). Synergistic zerovalent Iron (Fe0) and microbiological trichloroethene and perchlorate reductions are determined by the concentration and speciation of Fe. *Environmental Science & Technology*, *54*(22), 14422-14431.

Collectively, these results illustrate scenarios relevant at or downstream of Fe^0 injection zones when Fe^0 is used to facilitate microbial dechlorination. Results also underscore potential detrimental effects of Fe^0 and bioaugmentation cultures co-injection for *in situ* treatment of chlorinated ethenes and ClO_4^-.

2.2 Introduction

Anaerobic bioremediation of trichloroethene (TCE) through bioaugmentation with *Dehalococcoides mccartyi*-containing cultures has been utilized at many contaminated sites (Lyon and Vogel, 2013). The efficacy of *in situ* bioaugmentation is sometimes challenged by aerobic conditions in aquifers, limitations on the availability of H_2, the obligate electron donor for *D. mccartyi*, and toxicity of high TCE concentrations to reductively dechlorinating bacteria (Amos et al., 2007; Ziv-El et al., 2012; Stroo et al., 2014; Zhao and He, 2019). Coupling bioaugmentation with the chemical reductant, zero-valent iron (Fe^0), could potentially alleviate some of these challenges and bring advantages for achieving shorter remediation timeframes. Specifically, Fe^0 can reduce dissolved O_2 and, thus, decrease the oxidation-reduction potential (ORP), leading to enhanced anaerobic microbial activity (O'Carroll et al., 2013). In the absence of dissolved O_2, Fe^0 oxidation in water produces H_2, the electron donor for conversion of TCE to ethene (Liu and Lowry, 2006), and generates OH^-, which could counter balance H^+ produced from fermentation of organic substrates chlorinated ethenes (Equation 2.1):

$$Fe^0_{(s)} + 2H_2O \rightarrow Fe^{2+} + H_{2(g)} + 2OH^- \qquad \text{(Equation 2.1)}$$

Micro-scale and nano-scale Fe^0 particles also directly reduce chlorinated ethenes to ethene and ethane (Figure 2.1). The reactivity of Fe^0 is higher with the lesser chlorinated ethenes (Arnold and Roberts, 2000), while reductive dechlorination of the more

chlorinated compounds yields more energy for the microorganisms (Vogel et al., 1987). Therefore, combining Fe^0 and bioaugmentation with *D. mccartyi* could potentially negate accumulation of the microbial TCE reduction intermediates, *cis*-dichloroethene (DCE) and vinyl chloride (VC).

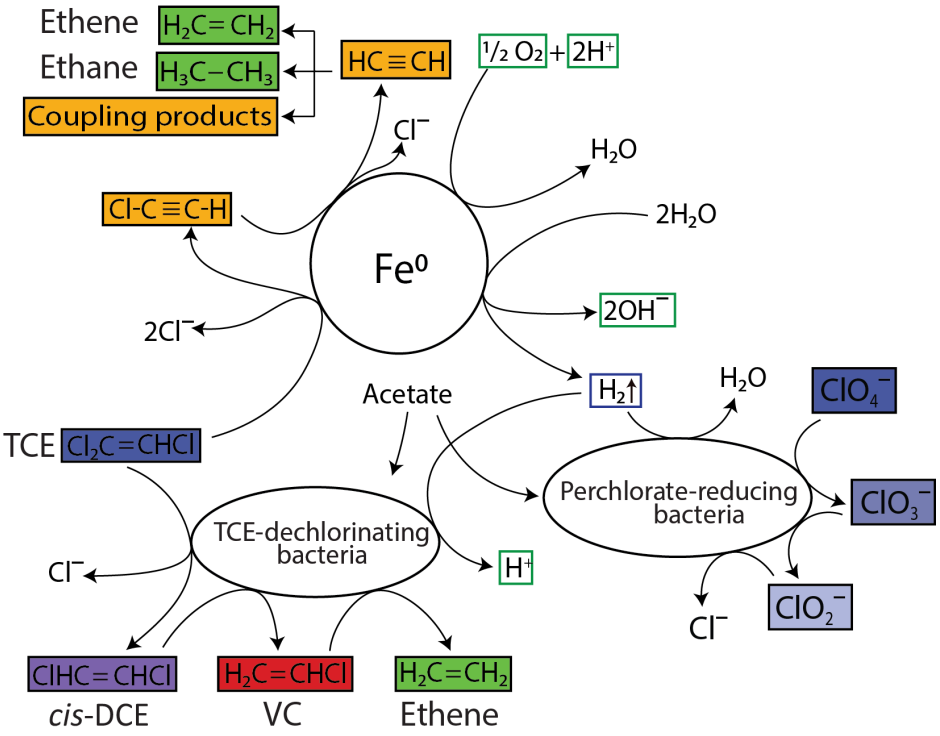

Figure 2.1 Potential synergy between abiotic Fe^0 reductions and TCE and ClO_4^- microbiological dechlorination.

Synergistic Fe^0-mediated abiotic and microbial dechlorination of chlorinated ethenes has been investigated in several laboratory studies (Rosenthal et al., 2004; Xiu et al., 2010b; Dong et al., 2019). At contaminated sites, (Chowdhury et al., 2015) reported > 99% reduction of up to 3 µmol L^{-1} TCE in groundwater after injection of a 1 g L^{-1} nano-scale Fe^0 slurry into the subsurface. In a long-term field study, (He et al., 2010a) reported that nano-scale Fe^0 stimulated microbial TCE reductive dechlorination following a rapid abiotic TCE reduction during the first two weeks post-Fe^0 injection. However,

most laboratory and peer-reviewed field studies have focused on TCE or other chlorinated ethenes as sole contaminants. The majority of US Superfund sites have multiple contaminants (US EPA, 2017). Chlorinated ethenes, including TCE, and perchlorate (ClO_4^-) co-occur in soil and groundwater, particularly in the Southwestern US, due to the common usage of these chemicals at military sites operated by the Department of Defense (U.S. Department of Defense, 2005; Stephenson, 2007). TCE has been widely employed in degreasing and cleaning of metal parts in mechanical equipment (Russell et al., 1992), while ClO_4^- is extensively used in the manufacture of munitions, explosives, and rocket propellants (Urbansky, 2002; Srinivasan and Viraraghavan, 2009). Among the 25 US Superfund sites contaminated with ClO_4^-, the majority (21 sites) are co-contaminated with TCE (US EPA, 2017). ClO_4^- can be microbially reduced to O_2 and Cl^- with available electron donors (e.g., H_2, acetate) (Bardiya and Bae, 2011). A limited number of studies have shown that concomitant microbial ClO_4^- and TCE reduction negatively impacts the activity of *D. mccartyi*, with stalling of dechlorination at *cis*-DCE or VC in monitoring wells containing ClO_4^- (Borden, 2007; Hatzinger and Diebold, 2009). Based on our review of the literature, no studies have investigated the use of Fe^0 in concert with microbial reduction of TCE and ClO_4^-. Unlike TCE, Fe^0-mediated ClO_4^- reduction is considered unfavorable due to a large activation energy barrier for the reaction (Moore et al., 2003). Theoretically, Fe^0 can support microbiological TCE and ClO_4^- reduction by creating anoxic conditions and providing H_2 in subsurface environments, as illustrated in Figure 2.1. Fe^0-aided microbial ClO_4^- reduction is still poorly understood with studies showing both enhanced

and diminished microbiological activity (Shrout et al., 2005; Son et al., 2006; Yu et al., 2006). Thus, the lack of knowledge regarding the use of Fe^0 for concomitant TCE and ClO_4^- reductions brings uncertainties in the effective design of bioremediation schemes, potentially leading to unexpected or undesired outcomes.

Despite the theoretical benefits of combining Fe^0 with microbiological TCE and ClO_4^- reduction, high concentrations of certain micro-scale Fe^0 (e.g., BASF's HQ powder at >15 g L^{-1}) and nano-scale Fe^0 products (e.g., NANOIRON nanoferstar at > 0.05 g L^{-1}) have been shown to inhibit *D. mccartyi* in pure and mixed microbial communities (Xiu et al., 2010a; Xiu et al., 2010b; Velimirovic et al., 2015) and perchlorate-reducing enrichment cultures (Shrout et al., 2005). Direct inhibition can be created from the strong reducing potential and reactive oxygen species (ROS) generated by Fe^0 and its oxidation product, Fe^{2+} (Equation 2.1) (Auffan et al., 2008; Yang et al., 2013; Velimirovic et al., 2015; Xie et al., 2017). Water-soluble Fe^{2+} ions migrate downstream from the Fe^0-injection zone (Naftz et al., 2002), scavenging O_2 and producing Fe^{3+}, as shown in Equation 2.2:

$$Fe^{2+}_{(aq)} + O_{2(aq)} + 4H^+ \rightarrow Fe^{3+} + 2H_2O \qquad \text{(Equation 2.2)}$$

The influence of Fe^{2+} on microbial TCE and ClO_4^- reduction is largely unknown. Fe^{2+} and Fe^{3+} can precipitate on microbial cell surfaces and be incorporated into the cell wall, leading to inhibition of TCE-dechlorinating and ClO_4^--reducing microorganisms (Warren and Ferris, 1998; Shrout et al., 2005). The presence of soil/sediment and groundwater is expected to diminish some of these inhibitory effects; yet the extent to which they do is greatly influenced by the biogeochemical characteristics of aquifer materials (Kirschling

et al., 2010; Pawlett et al., 2013) and has been recently recognized as a gap in Fe^0 research (Xie et al., 2017).

Indirect Fe^0 inhibition can be a result of enhanced microbial competition. For example, Fe^{3+} from Equation 2.2 is a terminal electron acceptor for iron-reducing bacteria that compete for electron donor and other resources with *D. mccartyi* (Evans and Koenigsberg, 2001; Zaa et al., 2010). Many groundwater contaminated sites are abundant in SO_4^{2-}, the electron acceptor for sulfate-reducing bacteria. H_2 derived from Equation 2.1 can also be used as an electron donor by sulfate-reducing bacteria. The concentration of SO_4^{2-} reported in groundwater is usually in a range of 10 to 1000 mg L^{-1}, while majority of the groundwater sources contain less than 500 mg L^{-1} (U.S. EPA, 2003; WHO, 2004; Miao et al., 2013). Achieving reductive dechlorination of TCE to ethene in aquifers containing a high SO_4^{2-} concentration ($\geq$ 500 mg L^{-1}) is challenging, as extensive SO_4^{2-} reduction can decrease the rates of reductive dechlorination (Pantazidou et al., 2012). Furthermore, high concentrations of the generated sulfide are inhibitory to many microorganisms (Mao et al., 2017).

The goal of this work was to investigate the effect of Fe^0 and its oxidation product, Fe^{2+}, on microbial TCE and ClO_4^- reductions in the presence of aquifer material, at field-relevant concentrations. We utilized bench-scale semi-batch microcosms containing soil and groundwater from a Superfund site co-contaminated with TCE and ClO_4^- and containing a high SO_4^{2-} concentration. We performed experiments representative of a combined Fe^0 and biostimulation/bioaugmentation scheme, including a Fe^0 injection zone containing a high Fe^0 concentration and a downstream zone

containing dissolved Fe^{2+}. Our data showed that the rapid abiotic reduction of TCE to ethene/ethane by high Fe^0 concentration obscured microbial TCE reductive dechlorination, enhanced SO_4^{2-} reduction and methanogenesis, and impeded ClO_4^- reduction. These results strongly suggest that co-injection of high concentrations of Fe^0 and bioaugmentation cultures could be detrimental to survival and activity of TCE-dechlorinating and ClO_4^--reducing microorganisms. On the other hand, a low concentration of partially oxidized (aged)-Fe^0 showed synergistic abiotic and microbiological TCE dechlorination to ethene along with complete microbiological ClO_4^- reduction.

2.3 Methods and materials

2.3.1 *Aquifer materials, Fe^0 products, and microbial inocula*

The soil and groundwater used in this study were obtained from the Phoenix-Goodyear Airport-North (PGAN) Superfund site, Goodyear, Arizona, USA (Rangan, 2017). The site was developed as a research, design, and manufacturing plant for defense and aerospace equipment in 1963 (Arizona Department of Environmental Quality, 2017). TCE and ClO_4^- were utilized during aircraft and weapon-related manufacturing, leading to soil and groundwater contamination. PGAN Superfund site has been on the US EPA's National Priority List (NPL) since 1983 (Arizona Department of Environmental Quality, 2017). For this study, soil cores in increments of 0.3-0.6 m containing silty sand, clayey sand, well graded sand, and poorly graded sand were retrieved from a depth of 25-52 m below ground surface. Equal parts of soil cores were homogenized in an anaerobic glove chamber before using in microcosm experiments. The groundwater was sampled from

the upper aquifer (34-46 m depth). The groundwater characteristics are shown in Table 2.1.

Table 2.1 Characteristics of groundwater used in this study. The data are averages of triplicate measurements.

Parameter	Value
pH	7.78 ± 0.10
Oxidation reduction potential (ORP) (mV)	150 ± 30
Conductivity (mS cm^{-1})	4.1 ± 0.02
Total dissolved solids (TDS) (parts per thousand, ppt)	2.9 ± 0.02
Salinity (ppt)	2.1 ± 0.02
Alkalinity (mg L^{-1} as $CaCO_3$)	410 ± 20
Chemical oxygen demand (COD) (mg L^{-1})	41 ± 7
TCE (μmol L^{-1})	8 ± 1.2
ClO_4^- (μmol L^{-1})	1.6 ± 0.2
SO_4^{2-} (mmol L^{-1})	11.0 ± 0.5
NO_3^- (mmol L^{-1})	1.0 ± 0.3

Two micro-scale and nano-scale Fe^0 products were utilized. The micro-scale products were Z-Loy™ MicroMetal (OnMaterials, Escondido, CA; avg. d = 2-3 μm) and carbonyl iron powder OM (BASF, Florham Park, NJ; avg. d < 10 μm). The nano-scale Fe^0 product was NANOFER STAR W™ (Nano Iron, s.r.o., Czech Republic; avg. d < 50 nm). The reductively dechlorinating enrichment cultures used in this study were ZARA-10 (Delgado et al., 2014b; Delgado et al., 2016; Delgado et al., 2017) and SDC-9™ (RNAS Remediation products, Brooklyn Center, MN) (Vainberg et al., 2009) Both cultures are enriched in reductively dechlorinating-, fermenting-, and methanogenic-microorganisms (Delgado et al., 2014b; Dang et al., 2018). ZARA-10 culture contains strains of *D. mccartyi* with *tceA*, *vcrA*, and *bvcA* reductive dehalogenase genes and *Geobacter sp*. most similar to *G. lovleyi* involved in partial TCE to *cis*-DCE reductive dechlorination (Delgado et al., 2014b). SDC-9 ™ culture contains strains of *D. mccartyi*

with *pceA*, *tceA*, and *vcrA* reductive dehalogenase genes (Dang et al., 2018; Kucharzyk et al., 2020).

2.3.2 Semi-batch microcosm experiments

Semi-batch microcosm experiments were carried out in 120 mL glass serum bottles with 25 g of soil (10.5 ± 0.2 % moisture) and 75 mL of groundwater (soil to groundwater ratio of 1:3). The experimental conditions (a total of 11) are shown in Table 2.2 and were tested in triplicates. Briefly, non-bioaugmented ("High Fe^0) and biostimulated/bioaugmented ("High Fe^0 & SDC-9" and "High Fe^0 & ZARA-10) microcosms were set up with 16.5 g L^{-1} Fe^0. Biostimulated/bioaugmented microcosms labelled "Low Fe^0 ZARA-10 & SDC-9" were established by adding 2.5 mL of spent slurry collected from the "High Fe^0" microcosms after 56 days (four semi-batch cycles). Non-bioaugmented ("Fe^{2+}") and biostimulated/bioaugmented ("Fe^{2+} & SDC-9" and "Fe^{2+} & ZARA-10) microcosms were set up with 0.25 g L^{-1} Fe^{2+}. Non-bioaugmented ("No Fe/cultures") and biostimulated/bioaugmented controls ("SDC-9") in the absence of added Fe were also assessed.

Table 2.2. Experimental conditions established in semi-batch microcosms with 25 g soil and 75 mL of groundwater. Note that conditions labelled as "High Fe^0 & SDC-9" and "High Fe^0 & ZARA-10" consisted of two sets of microcosms per culture (n = 6): one set amended with lactate and another amended with EVO.

	Concentration/Amount in microcosms								
Condition	Fe^0 (g L^{-1})	Fe^{2+} (g L^{-1})	Phosphate buffer (mM)	Yeast extract (mg L^{-1})	Lactate (mg L^{-1})	EVO (mg L^{-1})	TCE (µmol L^{-1})	ZARA-10 (mL)	SDC-9 (mL)
No Fe/cultures	0	0	0	0	0	0	140[e]	0	0
SDC-9	0	0	10	200	0	170	140	0	4[b]
Low Fe^0, ZARA-10 & SDC-9	2.5 mL[a, b]	0	10	200	560	0	100	2[b]	2[b]
High Fe^0	16.5[b, c]	0	0	0	0	0	140[e]	0	0
High Fe^0 & SDC-9	16.5[b, c]	0	10	200	560	0	140[e]	0	4[b]
	16.5[b, c]	0	10	200	0	170	140[e]	0	4[b]
High Fe^0 & ZARA-10	16.5[b, c]	0	10	200	560	0	140[e]	4[b]	0
	16.5[b, c]	0	10	200	0	170	140[e]	4[b]	0
Fe^{2+}	0	0.25[b, d]	10	200	560[b]	170[e]	100	0	0
Fe^{2+} & SDC-9	0	0.25[b, d]	10	200	560[b]	170[e]	100	0	4[b]
Fe^{2+} & ZARA-10	0	0.25[b, d]	10	200	560[b]	170[e]	100	4[b]	0

[a]Slurry containing aged Fe^0 from the "High Fe^0" microcosms after 56 days; [b]Added only at time 0; [c]Fe^0 added as combined 15 g L^{-1} micro-scale and 1.5 g L^{-1} nano-scale Fe^0 products; [d]Fe^{2+} added as $FeCl_2$; [e]Added at the beginning of the second semi-batch cycle onwards. All other amendments were added at the beginning of every semi-batch cycle.

The groundwater was sparged with N_2 for 20 min before using in the microcosms. As shown in Table 2.2, the microcosms were amended with 200 mg L^{-1} yeast extract, 560 mg L^{-1} lactate (60% syrup; Sigma-Aldrich, St. Louis, MO) and/or 170 mg L^{-1} emulsified vegetable oil (EVO; EOS Pro, EOS Remediation. LLC, Raleigh, NC), and 10 mM phosphate buffer. The microcosm bottles were sealed with butyl rubber stoppers and aluminum crimps. The microcosms were operated in semi-batch cycles (14 days per cycle). Starting on day 14 of incubation, the serum bottles were vigorously shaken and

set aside for 5 mins to allow settling of soil particles. Then, 25 mL of spent microcosm slurry (containing fine solids that did not settle) were removed and replaced with 25 mL of groundwater containing amendments at the concentrations specified in Table 2.2. Four 14-day semi-batch cycles were conducted (amounting to 56 days) and a total of 75 mL slurry liquid were replaced (representing one hydraulic retention time). To understand solid losses during the experiment, the mass of dry solids was measured in the 25 mL of spent microcosm slurry withdrawn at the end of semi-batch cycles. The microcosm spent slurry was centrifuged at 4000 RPM for 5 min to make a pellet. The pellet was dried in an oven at 105 °C overnight to remove water and the weight of dry solids was determined. Total solid losses in microcosms were 11 ± 4 % during the experiment (from three slurry removal events in four semi-batch cycles).

In the microcosms with a 16.5 g L^{-1} Fe^0, the initial TCE concentration was 8 ± 1 µmol L^{-1} (~1000 µg L^{-1}), the typical TCE groundwater concentration at the PGAN Superfund site. Starting with the second semi-batch cycle (day 14), TCE was added at 140 ± 15 µmol L^{-1} (~18 mg L^{-1}). The initial TCE concentration in all other microcosms was 100 ± 12 µmol L^{-1} (~13 mg L^{-1}). The initial ClO_4^- concentration was 2 ± 1 µmol L^{-1} (~180 µg L^{-1}). The starting pH was 7.4 ± 0.1. The pH was adjusted to 7.6 in microcosms initially amended with 16.g L^{-1} Fe^0 (Table 2.2) on day 42 (beginning of the 4th semi-batch cycle) using a 2 M HCl solution. The microcosms were incubated statically at room temperature (25 °C) in the dark.

The ability of SDC-9 and ZARA-10 cultures to reduce ClO_4^- was tested in 160 mL serum bottles containing 100 mL reduced anaerobic mineral medium without soil and

groundwater. The mineral medium was prepared as described in previous studies (Löffler et al., 2005; Delgado et al., 2012). The concentration of ClO_4^- was 20 μmol L^{-1} and 5 mM lactate was added as the electron donor and carbon source. The methodologies for chemical analyses of the microcosms were previously published (Ziv-El et al., 2011a; Delgado et al., 2014a; Ziv-El et al., 2014; Robles, 2019) and are presented in detail in the Supporting Information.

2.3.3 Microbiological analyses

Microbial biomass samples were obtained from the microcosms at the beginning and end of each semi-batch cycle. Samples of 1 mL of slurry were pelleted using an Eppendorf micro centrifuge 5415R (Hauppauge, NY) at 13200 RPM. Genomic DNA was extracted from these pellets using the MOBIO PowerSoil® DNA extraction kit (Carlsbad, CA). Quantitative real-time PCR (qPCR) was performed targeting the 16S rRNA gene of *Dehalococcoides mccartyi*, Bacteria, and Archaea using a QuantStudio 3 Real-Time PCR System (Applied Biosystems®, Foster City, CA). The primers, probes, reagent concentrations, and PCR conditions were those published (Ziv-El et al., 2011b; Delgado et al., 2016; Delgado et al., 2017). The reaction volume was 10 μL containing 4 μL of 1:10 diluted DNA as template. The reactions were setup in triplicates for experimental samples and for six-point calibration curves. Pipetting was performed using an automated epMotion 5070 liquid handling system (Eppendorf, Hauppauge, NY).

The Illumina Miseq platform was used for DNA sequencing at the Microbiome Facility at the Biodesign Institute (https://biodesign.asu.edu/microbiome-facility), Arizona State University. The primers were 515F and 806R to amplify the V4 hyper-

variable region of the 16S rRNA gene of Bacteria and Archaea (Caporaso et al., 2012a). The sequences were processed using QIIME 2 software package (Bolyen et al., 2019a). DADA2 software package was used to quality filter the raw sequences by removing phiX, chimeric, and erroneous reads (Callahan et al., 2016). Reads were truncated at 150 bases prior to processing with the dada2 denoise-single method. All other DADA2 parameters were used with the default settings (Callahan et al., 2016). Taxonomy was assigned using q2-feature-classifier (Bokulich et al., 2018b) to the Greengenes database (McDonald et al., 2012). The microbial sequences obtained from the Illumina Miseq high-throughput DNA sequencing were submitted to the National Center for Biotechnology Information (NCBI) and are available under the Bioproject number PRJNA573752 (Sequence Read Archive numbers SRX6900162–SRX6900181). A student's *t*-test with 95% confidence interval was used to determine statistically significant differences between chemical and microbiological results from various experimental conditions, where a p value < 0.05 was considered statistically significant.

2.4 Results and discussion

2.4.1 High Fe^0 concentrations rapidly converted TCE to ethene/ethane, but impaired microbiological TCE and ClO_4^- reduction

Figure 2.2 shows the time-course reductive dechlorination of TCE in semi-batch microcosms. TCE dechlorination was absent in the "No Fe/cultures" microcosms (Figure 2.2A) and *D. mccartyi* 16S rRNA genes were not detected at time 0 in this condition. The Fe^0 concentration (16.5 g L^{-1}) in "High ZVI" microcosms decreased the ORP of the groundwater from 150 ± 30 mV to < –400 mV (Table 2.3).

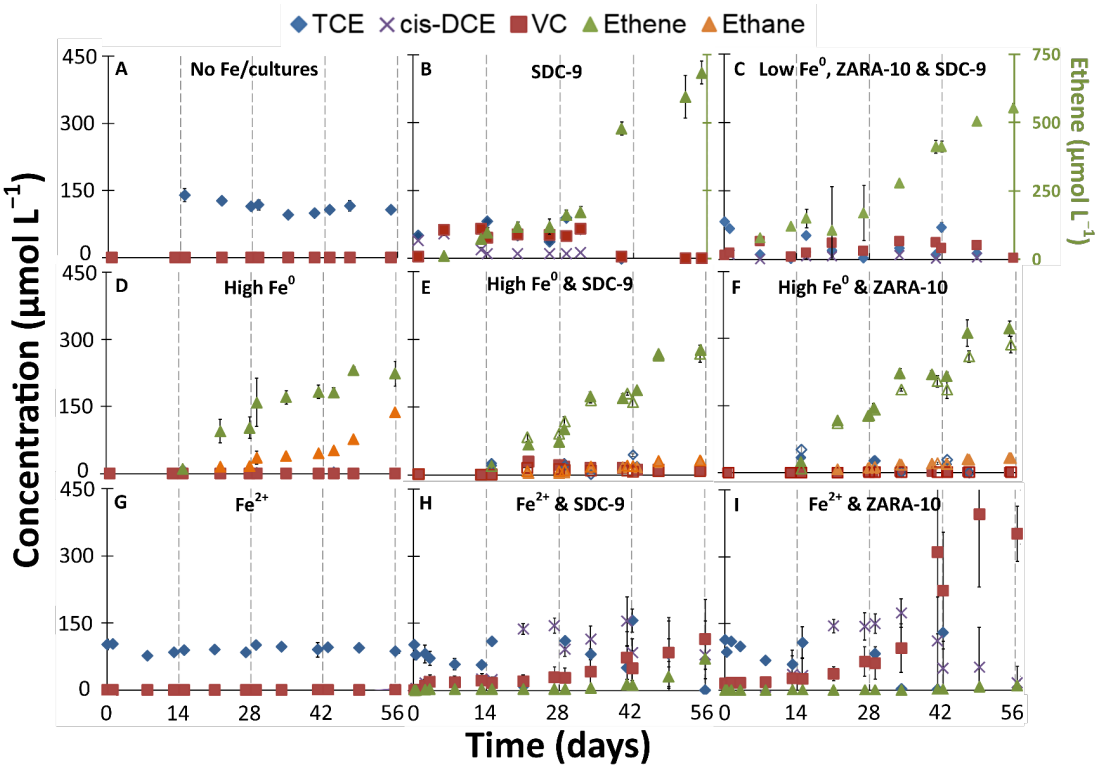

Figure 2.2 Reductive dechlorination of TCE in semi-batch microcosms with aquifer soil and groundwater. "High Fe^0" denotes combined concentrations of 15 g L^{-1} micro-scale and 1.5 g L^{-1} nano-scale Fe^0. "Low Fe^0" contained 2.5 mL spent slurry from "High Fe^0" microcosms (panel D) after 56 days. The concentration of Fe^{2+} was 0.25 g L^{-1}. In panels E and F, the filled symbols show conditions with lactate and the empty symbols show conditions with emulsified vegetable oil (Table 2.2). The dashed lines denote end/beginning of a 14-day semi-batch cycle. Ethene is plotted on the secondary y-axis in panels B and C. The data are averages of triplicate microcosms and the error bars indicate the standard deviation of the mean.

Table 2.3 ORP and pH measurements at selected timepoints in the microcosms from this study. Day 0 represents the beginning of the first semi-batch cycle. Day 42 is the end of the third semi-batch cycle and day 56 is the end of the fourth semi-batch cycle. The data are averages with standard deviation of triplicate microcosms.

	ORP (mV)			pH
Condition	**Day 0**	**Day 42**	**Day 56**	**Day 56**
No Fe/cultures	–	–45 ± 18	–137 ± 45	7.36 ± 0.04
SDC-9	–	–183 ± 2	–170 ± 5	6.81 ± 0.02
Low Fe^0, ZARA-10 & SDC-9	–206 ± 10	–240 ± 13	–194 ± 3	6.90 ± 0.02
High Fe^0	–	–526 ± 49	–348 ± 30	8.53 ± 0.05
High Fe^0 & ZARA-10*	–435 ± 82	–315 ± 12	–313 ± 11	8.53 ± 0.05
High Fe^0 & SDC-9*	–	–307 ± 30	–325 ± 14	8.86 ± 0.64
Fe^{2+}	–174 ± 5	–	–189 ± 4	6.80 ± 0.02
Fe^{2+} & SDC-9	–164 ± 1	–	–239 ± 10	6.88 ± 0.05
Fe^{2+} & ZARA-10	–160 ± 9	–	–198 ± 5	6.80 ± 0.01

*The data are averages of two sets of triplicate microcosms (one set amended with lactate and one set with emulsified vegetable oil as described in Table 2.2); Symbol "–" = not measured.

All "High Fe^0" microcosms showed rapid dechlorination of TCE to ethene and ethane (Figure 2.2D-F). The ethene:ethane molar ratio was 1:0.6 in the non-bioaugmented "High Fe^0 microcosms (Figure 2.2D). *cis*-DCE was not detected in any of the sampling events and only low concentrations of VC (0.8 ± 0.1 to 29 ± 2.0 μmol L^{-1}) were detected in the SDC-9 and ZARA-10 bioaugmented "High Fe^0" microcosms (Figures 2.2E-F), indicating the dominance of Fe^0 in TCE reduction. First-order TCE dechlorination rate constants (k_{obs}) during the fourth semi-batch cycle in the "High Fe^0" microcosms confirmed a mainly abiotic mechanism for TCE reduction (Figure 2.3). The k_{obs} values for TCE were similar (4.3-4.8 × 10^{-2} h^{-1}; $p \geq 0.56$), regardless of the presence of dechlorinating enrichment cultures, suggesting a negligible contribution of the bioaugmented microorganisms in "High Fe^0" microcosms. A similar k_{obs} value (5.3 × 10^{-2} h^{-1}) was achieved in (Xiu et al., 2010b) in experiments with a dechlorinating

enrichment culture, 1 g L^{-1} nano-scale Fe^0, and an initial TCE concentration of ~152 µmol L^{-1}.

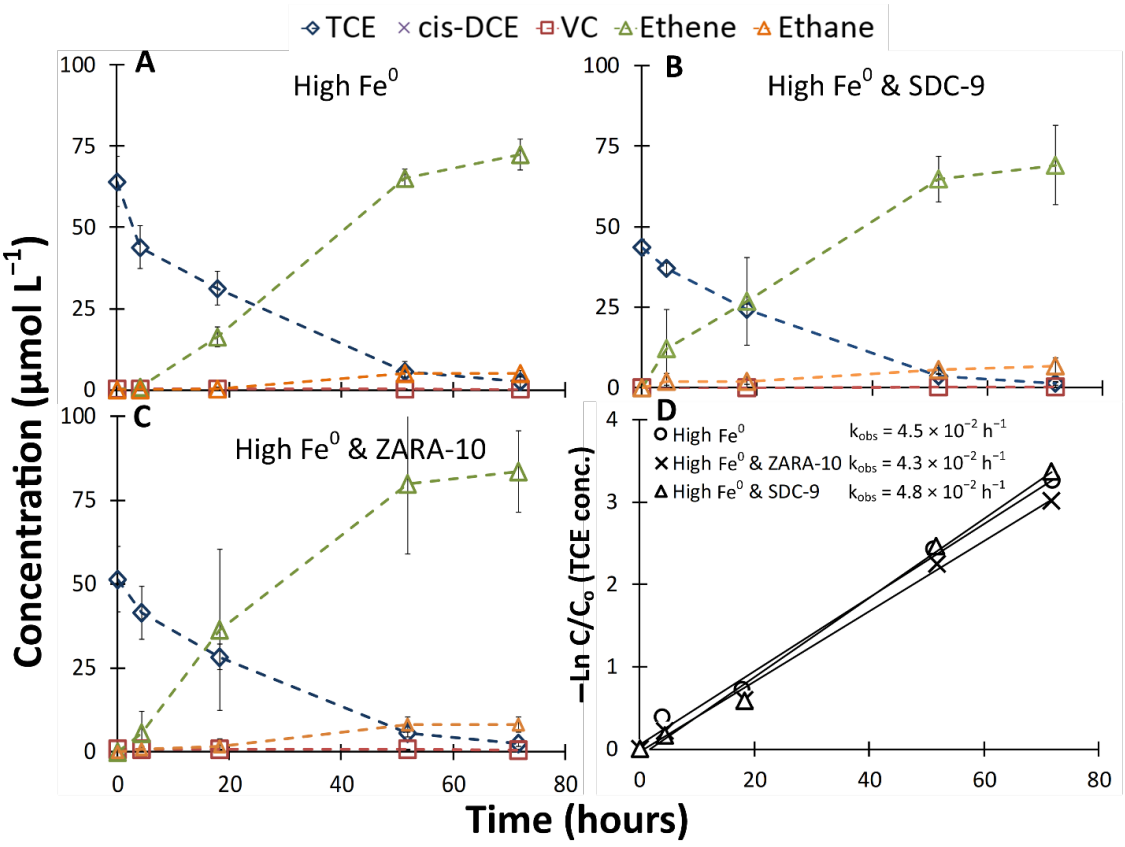

Figure 2.3. Rapid TCE reduction during the fourth semi-batch cycle (days 42-45 in Figure 2.2) in Fe^0 microcosms (A) without or (B-C) with reductively dechlorinating cultures, SDC-9 and ZARA-10. (D) First order TCE dechlorination rates (k_{obs}). The data are average of triplicate microcosms and error bars indicate the standard deviation of the mean.

The co-contaminant ClO_4^- was present in the PGAN Superfund site groundwater at a concentration of 1.6 ± 0.2 µmol L^{-1}. Adsorption of ClO_4^- on the iron oxides or Fe^0-mediated abiotic ClO_4^- reduction was likely negligible, as demonstrated in prior studies (Moore et al., 2003; Shrout et al., 2005; Son et al., 2006; Yu et al., 2006). Neither culture reduced ClO_4^- in anaerobic medium without soil (Figure 2.4), indicating that ClO_4^- reduction was driven by the indigenous soil and groundwater microorganisms.

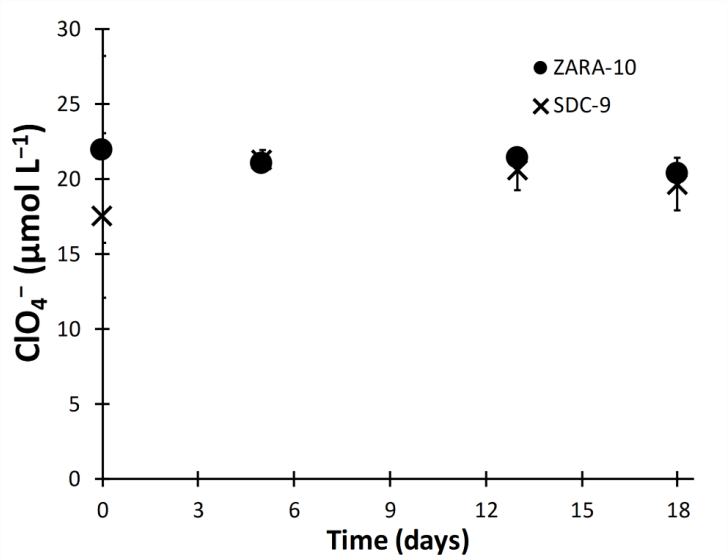

Figure 2.4 Absence of perchlorate reduction in SDC-9 and ZARA-10 cultures used in this study. The data are averages of duplicate cultures and the error bars represent standard deviation of the mean.

This was evident from the "No Fe/cultures" microcosms where ClO_4^- was reduced to below detection limit from the first semi-batch cycle onwards (Figure 2.5A). While no fermentable substrates were added to these microcosms (Table 2.2), ~ 0.3 mM H_2 was introduced from the anaerobic glove chamber and likely served as the electron donor for the indigenous perchlorate-reducing bacteria.

In the non-bioaugmented "High Fe^0" and "High Fe^0 & ZARA-10" microcosms, residual ClO_4^- concentrations were detected at the end of all semi-batch cycles, indicating inhibition of microbiological ClO_4^- reduction by the high concentration of Fe^0 (Figure 2.5A). Microbial inhibition was also observed in (Shrout et al., 2005) when 20 g L^{-1} Fe^0 were added to an enrichment culture with an initial ClO_4^- concentration of 50 µmol L^{-1}. The inhibitory effect on ClO_4^- reduction was mitigated in the "High Fe^0 & SDC-9" microcosms and significantly faster ($p < 0.05$) rates of ClO_4^- reduction were

observed by the end of the second semi-batch cycle (day 28) compared to "High Fe^0" and "High Fe^0 & ZARA-10" (Figure 2.5A).

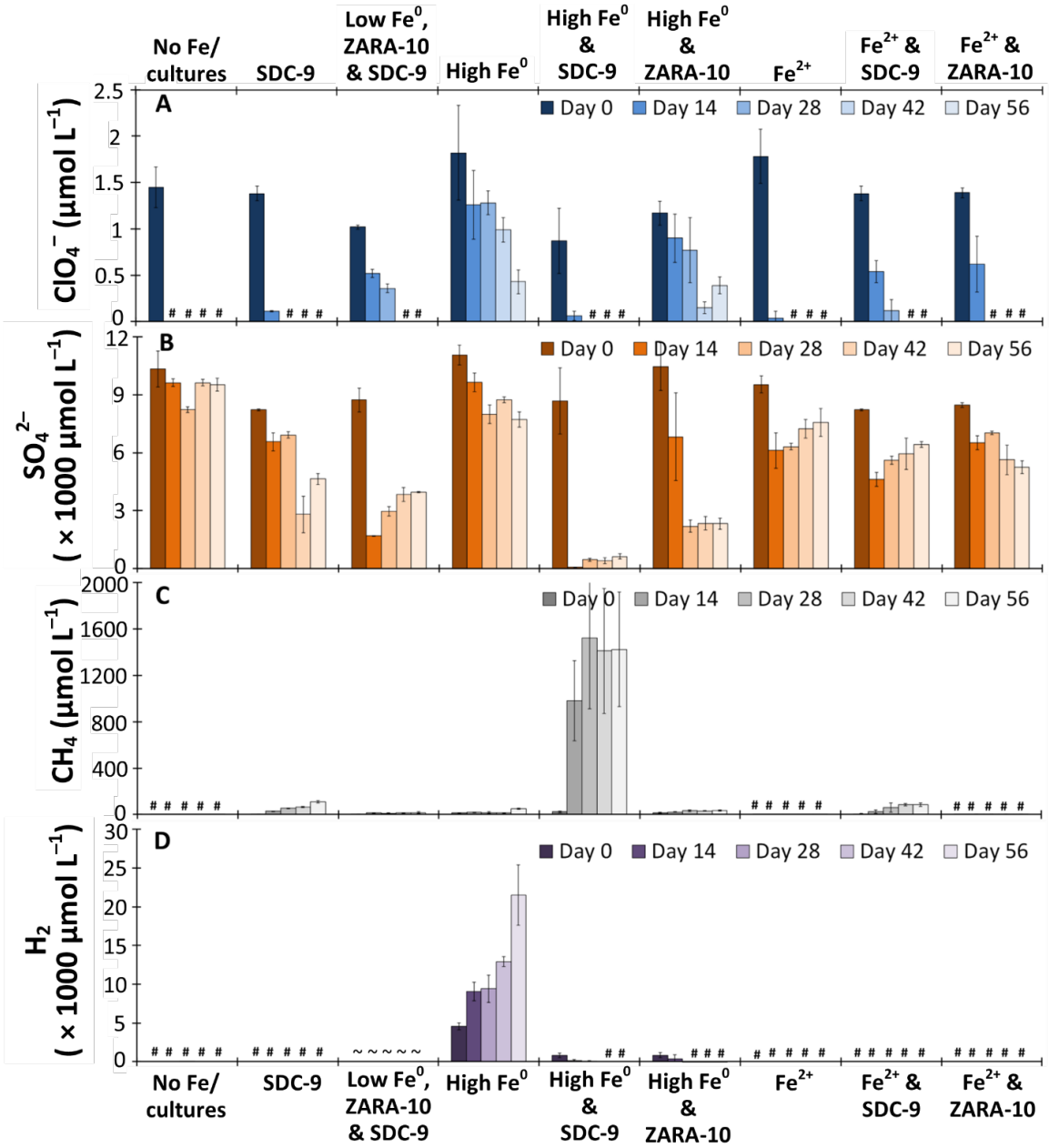

Figure 2.5 Concentrations of (A) ClO_4^-, (B) SO_4^{2-}, (C) CH_4, and (D) H_2 in semi-batch microcosms with aquifer soil and groundwater at time 0 and at the end of each 14-day semi-batch cycle. The data are averages of triplicate microcosms and the error bars indicate the standard deviation of the mean. Symbols: #, not detected; ~, not measured.

It is possible that Fe^0 cytotoxic effects were lessened in "High Fe^0 & SDC-9" microcosms due to a higher cell density of SDC-9 culture than ZARA-10. qPCR targeting the 16S rRNA genes of Bacteria and Archaea in the inocula cultures indicated that the combined concentration of 16S rRNA genes in SDC-9 was ~2 orders of magnitude higher than in ZARA-10 (Figure 2.6).

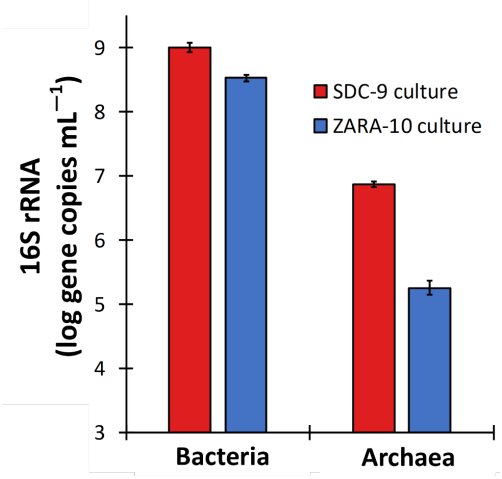

Figure 2.6. Concentrations of the 16S rRNA gene of Bacteria and Archaea in SDC-9 and ZARA-10 inocula. The data are averages of duplicate cultures and the error bars indicate the standard deviation of the mean.

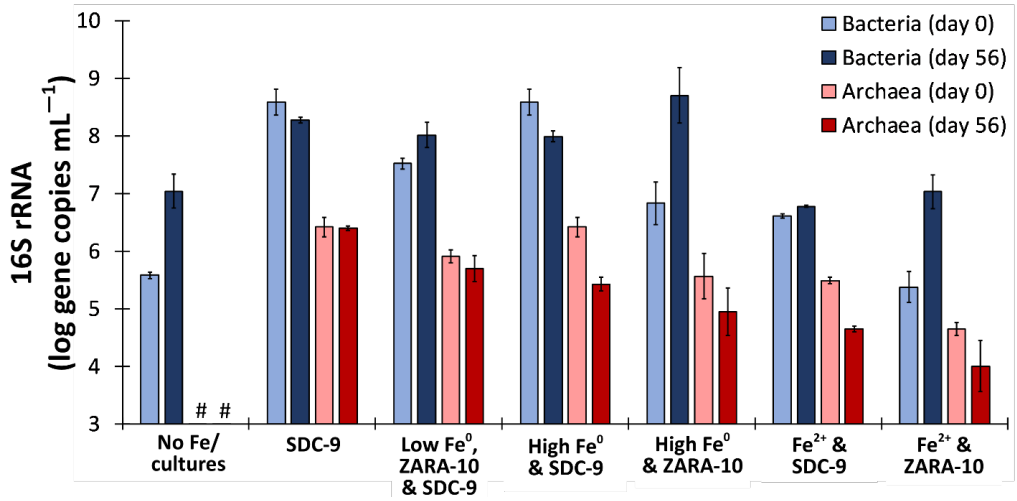

Figure 2.7 Concentrations of the 16S rRNA gene of Bacteria and Archaea in semi-batch microcosms with aquifer soil and groundwater. Day 0 represents the beginning of the first semi-batch cycle, while day 56 represents the end of the fourth semi-batch cycle. The data are averages of duplicate microcosms and the error bars indicate the standard deviation of the mean.

The combined concentration of bacterial and archaeal 16S rRNA genes in "High Fe^0 & SDC-9" microcosms at time 0 was also ~2 orders of magnitude higher than in "High Fe^0 & ZARA-10" microcosms (Figure 2.7).

2.4.2 Synergistic abiotic and microbiological TCE and ClO_4^- reduction was achieved at low Fe^0 concentrations

High Fe^0 concentration obscured microbiological TCE dechlorination and impeded microbiological ClO_4^- reduction in the microcosms. However, in the "Low Fe^0" microcosms, TCE was reduced to ethene with transient accumulation and reduction of *cis*-DCE and VC (Figure 2.2C). Ethane, a product observed in the microcosms amended with 16.5 g L^{-1} Fe^0, was not detected in "Low Fe^0" microcosms containing 2.5 mL of spent slurry collected from the "High Fe^0" microcosms after 56 days (four semi-batch cycles) (Figure 2.2C). These results support a substantial contribution of the bioaugmented microorganisms to TCE complete dechlorination to ethene. "SDC-9" microcosms without added Fe also effectively dechlorinated TCE (Figure 2.2B). However, the production of ethene in the "Low Fe^0, ZARA-10 & SDC-9" microcosms started earlier at day 7 (Figure 2.2C), compared to day 13 in "SDC-9" microcosms (Figure 2.2B). The TCE dechlorination data highlight the potential benefits of a low concentration of Fe^0 at increasing the rate of ethene production and minimizing the accumulation of DCE and VC. "Low Fe^0, SDC-9 & ZARA-10" microcosms also showed complete ClO_4^- reduction at the end of the third and fourth semi-batch cycle (Figure 2.5A). These results indicate that a low concentration of Fe^0 is amenable for synergistic

abiotic and microbiological TCE reductive dechlorination and simultaneous microbial ClO_4^- reduction.

2.4.3 Soluble Fe^{2+} partially antagonized TCE reductive dechlorination

Oxidation of Fe^0 yields water-soluble Fe^{2+} ions (Equation 2.1) that can travel downstream with the flow of groundwater in the subsurface and can reduce available dissolved O_2 producing Fe^{3+} (Keenan et al., 2009; Xie et al., 2017). Production of Fe^{3+} *via* Equation 2.2 in our microcosms with 0.25 g L^{-1} Fe^{2+} was inferred from the resulting groundwater ORP of –160 ± 9 to –174 ± 5 mV upon addition of Fe^{2+} at time 0 in the microcosms (Table 2.3, "Fe^{2+}", "Fe^{2+} & ZARA-10", and "Fe^{2+} & SDC-9"). Note that groundwater containing dissolved O_2 was resupplied in the beginning of the second, third, and fourth semi-batch cycle. Contrary to previous studies that used Fe^{2+} in the form of soil FeS (Jeong and Hayes, 2007; He et al., 2010b), we did not observe abiotic TCE reduction by Fe^{2+} added as $FeCl_2$ (Figure 2.2G). However, TCE was microbially reduced in the microcosms with SDC-9 and ZARA-10 with accumulation of *cis*-DCE and VC (Figure 2.2H-I). Ethene production started in the third semi-batch cycle with culture SDC-9 and fourth cycle with ZARA-10 (Figure 2.2H-I). However, significant concentrations of *cis*-DCE (17 ± 37-169 ± 114 µmol L^{-1}) and VC (114 ± 89-352 ± 62 µmol L^{-1}) were still present in "Fe^{2+} & ZARA-10" and "Fe^{2+} & SDC-9" at the end the fourth semi-batch cycle (Figures 2.2H-I). The diminished dechlorination rates in bioaugmented Fe^{2+} microcosms could be a result of cytotoxicity from ROS generated due to Fe^{2+} reaction with O_2 (Reinke et al., 1994; Davies, 2000; Keenan and Sedlak, 2008; Ševců et al., 2009), and/or competition for H_2 and nutrients between reductive

dechlorinators and iron-reducing bacteria (Evans and Koenigsberg, 2001; Zaa et al., 2010). In all the microcosms with Fe^{2+}, ClO_4^- was completely reduced within the second or third semi-batch cycle (Figure 2.5A), suggesting less prominent inhibitory effects of Fe^{2+} compared to Fe^0 on perchlorate-reducing bacteria.

2.4.4 The availability of electron acceptors and the initial microbial community in Fe-containing microcosms determined the major electron sinks

The concentration of natural constituents serving as terminal electron acceptors in groundwater, such as SO_4^{2-} and HCO_3^-, and the flow of electrons from H_2 or fermentable substrates to SO_4^{2-} reduction and methanogenesis are major determinants of success in bioremediation. The groundwater from PGAN Superfund site contained 11 ± 0.5 mM or 1060 ± 50 mg L^{-1} SO_4^{2-}, a concentration in the high range for groundwater (Hem, 1985). The concentration of HCO_3^-, the electron acceptor for hydrogenotrophic methanogens, was 4.1 ± 0.1 mM (based on alkalinity measurements) (Wolf-Gladrow et al., 2007). In all microcosms biostimulated with lactate and EVO (Table 2.2), fermentation proceeded to mainly acetate and propionate (Figure 2.8). In the microcosms without Fe^0, H_2 generated from fermentation of the added substrates remained below detection limit throughout the experiments (Figure 2.5D). The microcosms with high Fe^0 accumulated H_2 concentrations as high as 22 ± 4 mmol L^{-1} (Figure 2.5D). SO_4^{2-} reduction was a major microbiological process in the microcosms and was particularly stimulated in the bioaugmented "High Fe^0" microcosms (Figure 2.5B), where microbial TCE reductive dechlorination was primarily absent. These data showed that H_2 generated by Fe^0 and

acetate produced by fermentation and H_2-dependant homoacetogenesis (Delgado et al., 2012) were primarily channeled to SO_4^{2-} reduction (Figure 2.5B).

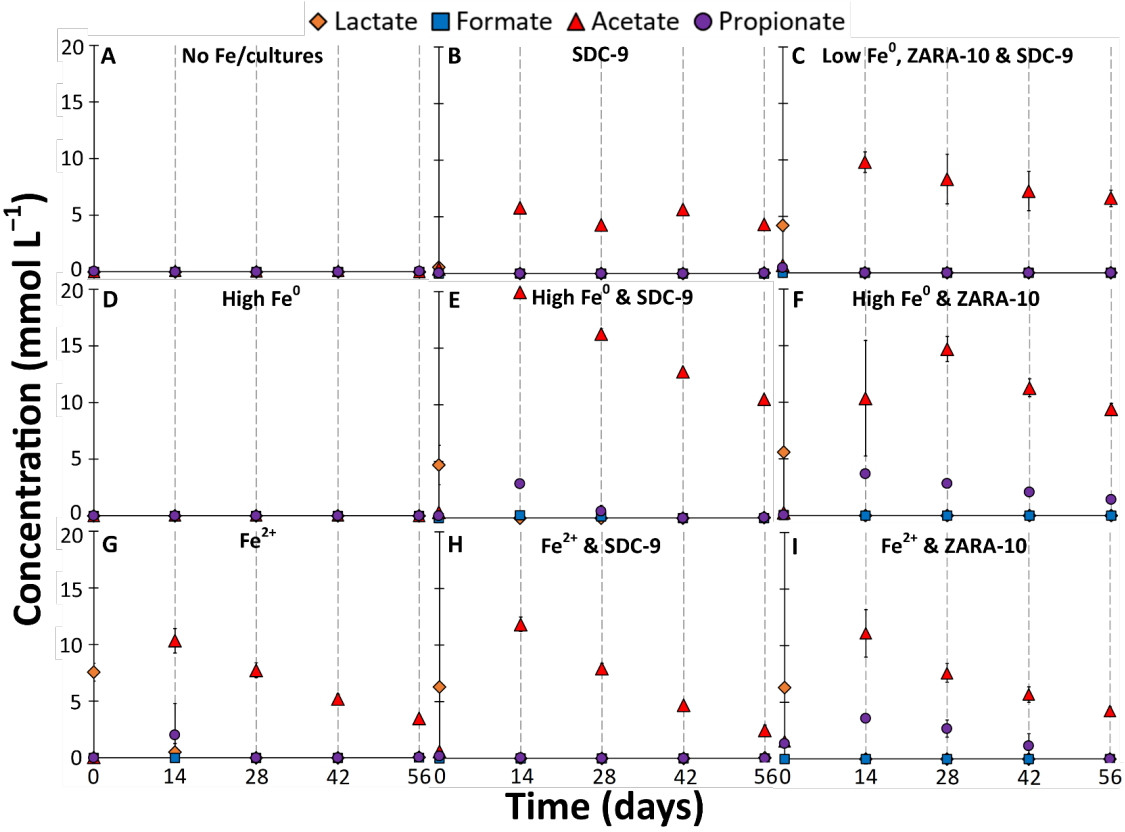

Figure 2.8. Fermentation of lactate and emulsified vegetable oil product (EOS Pro) in the semi-batch microcosms with aquifer soil and groundwater. The dashed lines denote end/beginning of a 14-day semi-batch cycle. Data from days 14, 28, and 42 show the concentrations of products at the end of the respective semi-batch cycle (before re-adding amendments). The data are averages of triplicate microcosms and the error bars indicate the standard deviation of the mean.

Methanogenesis also contributed to H_2 consumption in the high Fe^0 microcosms (Figure 2.5C). "High Fe^0 & SDC-9" microcosms produced significantly more CH_4 per semi-batch cycle and cumulatively (40 ± 17 times higher cumulative concentration, $p < 0.05$, Figure 2.5C) than ZARA-10 counterparts. The difference in methanogenic activity at high Fe^0 concentrations is at least partially explained by the significantly higher ($p < 0.05$) initial concentration of 16S rRNA archaeal genes in SDC-9 inoculum and at time 0

in the microcosms (Figure 2.6 and 2.7). Previous work showed that addition of Fe^0 can enrich methanogens but also sulfate-reducing bacteria (Kirschling et al., 2010; Liu et al., 2015a; Liu et al., 2015b). In our study, "High Fe^0 & SDC-9" and "High Fe^0 & ZARA-10" microcosms reduced between 15 ± 0.5 and 19 ± 1.9 mM SO_4^{2-} in four semi-batch cycles (Figure 2.5B). In "Fe^{2+} & SDC-9", "Fe^{2+} & ZARA-10", and "SDC-9" microcosms, only a total of 7.4 ± 0.0 to 9.2 ± 0.0 mM SO_4^{2-} was reduced during four semi-batch cycles (Figure 2.5B). These data highlight a significant enhancement of SO_4^{2-} reducing activity by the high Fe^0 concentration. Our results point out that at high Fe^0 concentrations, the presence of alternate electron acceptors and the microbial composition of the indigenous or bioaugmented communities play a major role in diverting the electron donors generated by Fe^0 and fermentation reactions.

2.4.5 Fe speciation influenced the microbial community structure and the relative abundance of D. mccartyi

Addition of Fe^0 and Fe^{2+} showed diverse effects on microbiological TCE dechlorination and ClO_4^- reduction. Substantial changes were noted in the microbial community composition from time 0 to the end of the fourth semi-batch cycle in the microcosm conditions tested (Figure 2.9). In all microcosms with Fe^0, sequences most similar to *Dehalococcoidaceae* were at ≤ 0.7 % after 4 semi-batch cycles while the "SDC-9" microcosms (without Fe) contained ~2% *Dehalococcoidaceae* sequences (Figure 2.9B). *D. mccartyi* cell concentration assessed by qPCR increased by two orders of magnitude in the "SDC-9" microcosms over the four semi-batch cycles (Figure 2.10). In "High Fe^0 & SDC-9" and "High Fe^0 & ZARA-10" microcosms, the changes in *D.*

mccartyi cell concentration inferred from qPCR data were within the same order of magnitude over four semi-batch cycles (Figure 2.10).

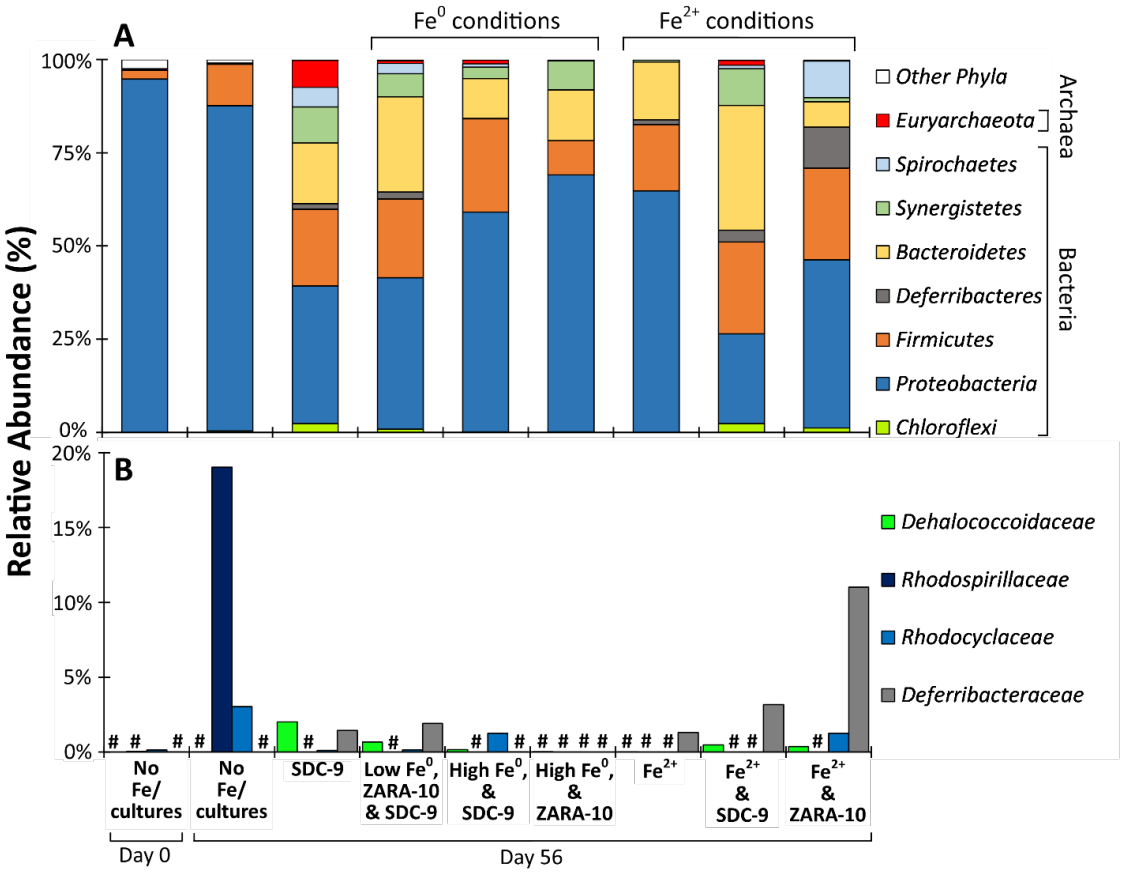

Figure 2.9 Relative abundance of (A) microbial phylotypes at the phylum level and (B) select phylotypes at the family level in semi-batch microcosms with aquifer soil and groundwater at time 0 and at the end of the fourth semi-batch cycle (day 56). The data are averages of sequences from duplicate microcosms. # = relative abundance below 0.01%.

These results concur with a limitation in *D. mccartyi* cell growth in microcosms that are dominated by Fe^0 abiotic TCE dechlorination (Figure 2.2E-F and 2.3 B-C). In an *ex situ* case study of bioremediation of chlorinated ethenes-contaminated soil *via* 2% Fe^0 and organic substrate mix, *D. mccartyi* 16S rRNA gene concentration was also lower by one order of magnitude in monitoring wells inside the Fe^0-treatment zone compared to control wells (outside of the treatment zone) (Stevenson and Herrera, 2018). While *D.*

mccartyi reductive dehalogenase gene concentrations were not measured in this study, (Xiu et al., 2010a) reported a 97- and 137-fold down-regulation in *tceA* and *vcrA* gene expression, respectively, when exposed to bare/non-coated nano-scale Fe^0 (as used in our study), inferring a limitation of electron acceptor for *D. mccartyi* due to Fe^0 abiotic TCE reduction (Xiu et al., 2010a).

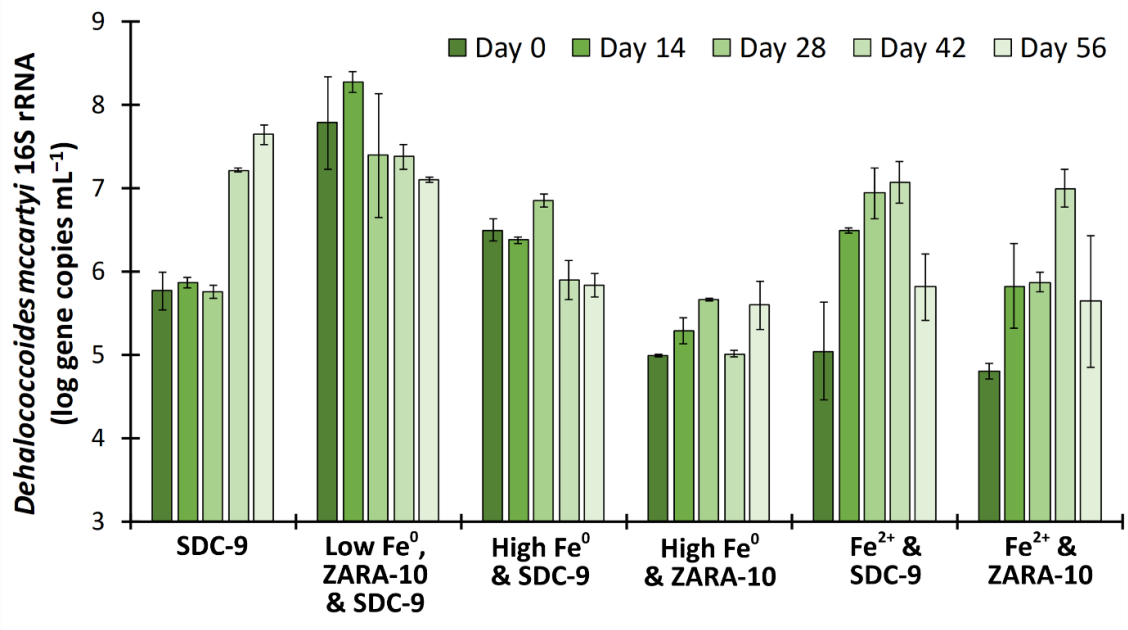

Figure 2.10 Quantification of *Dehalococcoides mccartyi* 16S rRNA gene copies in the slurry of semi-batch microcosms with aquifer soil and groundwater. Day 0 represents the beginning of the first semi-batch cycle. Days 14, 28, 42, and 56 represent the end of the first, second, third, and fourth semi-batch cycle, respectively. The data are averages of duplicate microcosms and the error bars indicate the standard deviation of the mean.

In the presence of 0.25 g L^{-1} Fe^{2+} and enrichment cultures, phylotypes most similar to *Dehalococcoidaceae* accounted for 0.3-0.5 % of the microbial communities at the end of the fourth semi-batch cycle (Figure 2.9B). In "Fe^{2+} & SDC-9" and "Fe^{2+} & ZARA-10" microcosms, *D. mccartyi* 16S rRNA gene concentrations increased ~2 orders of magnitude from the beginning until the end of third semi batch cycle (Figure 2.10; day 42). However, in the fourth semi-batch cycle, we observed a significant decrease ($p <$

0.05) in *D. mccartyi* 16S rRNA gene concentration in both sets of microcosms by 1-2 orders of magnitude (Figure 2.10). The decrease in *D. mccartyi* concentrations in "Fe^{2+} & SDC-9" and "Fe^{2+} & ZARA-10" in the fourth semi-batch cycle can possibly be attributed to competition from H_2-utilizing iron-reducing bacteria. H_2 was non-detectable in all Fe^{2+}-amended microcosms throughout the experiment (Figure 2.5D). Illumina Miseq high-throughput sequencing showed that phylotypes most similar to the iron-reducing bacteria from the family *Deferribacteraceae* accounted for 3-11% of the sequences analyzed in "Fe^{2+} & SDC-9" and "Fe^{2+} & ZARA-10" at the end of the experiments (Figure 2.9B). In microcosms with Fe^0 or without Fe ("SDC-9"), the relative abundance of phylotypes most similar to *Deferribacteraceae* was 1.5-6 times less (Figure 2.9B), suggesting a more prominent enrichment of iron-reducers in Fe^{2+}-amended microcosms. Phylotypes most similar to perchlorate-reducing bacteria from *Rhodocyclaceae* (Coates et al., 1999; Melnyk et al., 2011; Ontiveros-Valencia et al., 2014; Melnyk and Coates, 2015) were detected at 0.1-3% relative abundance in most of the microcosm conditions tested at the end of the experiment but were highest (3%) in the "No Fe/cultures" (Figure 2.9B).

In conclusion, our study evaluated the effects of Fe^0 and Fe^{2+} on microbiological TCE and ClO_4^- reduction in the presence of soil and groundwater from a co-contaminated Superfund site. Our results point out that the concentration and speciation of Fe, the availability of electron acceptors, and the initial microbial community play major roles in achieving synergistic abiotic and microbiological TCE and ClO_4^- reduction. These factors are likely to determine remediation success in subsurface

environments. Our work showed that high Fe^0 concentration (16.5 g L^{-1}) inhibited microbiological TCE and ClO_4^- reduction, while enhancing competing processes such as methanogenesis and SO_4^{2-} reduction. These results strongly suggest that simultaneous injection of Fe^0 and *D. mccartyi*-containing bioaugmentation cultures in the field could be detrimental for microbiological TCE and ClO_4^- reduction. Furthermore, when abundant Fe^{2+} concentrations were present, our results documented slower TCE dechlorination to ethene compared to no-Fe controls. These results imply a possible accumulation of *cis*-DCE and VC downgradient of the Fe^0 injection zones. However, a low concentration of aged-Fe^0 synergistically promoted TCE abiotic and biotic dechlorination while simultaneously achieving complete ClO_4^- reduction. Hence, bioaugmentation with enrichment cultures downstream of Fe^0 injection zones could bring about synergistic effects to support microbiological TCE and ClO_4^- reduction. Research on sequential application of Fe^0 and bioaugmentation cultures could help leverage Fe^0-based schemes for enhanced bioremediation in contaminated subsurface environments.

4.5 References

Amos, B.K., Christ, J.A., Abriola, L.M., Pennell, K.D., Löffler, F.E., 2007. Experimental evaluation and mathematical modeling of microbially enhanced tetrachloroethene (PCE) dissolution. Environmental Science & Technology 41, 963-970.

Arizona Department of Environmental Quality, 2017. , Phoenix-Goodyear Airport North | Site History.

Arnold, W.A., Roberts, A.L., 2000. Pathways and kinetics of chlorinated ethylene and chlorinated acetylene reaction with Fe (0) particles. Environmental Science & Technology 34, 1794-1805.

Auffan, M., Achouak, W., Rose, J., Roncato, M.-A., Chaneac, C., Waite, D.T., Masion, A., Woicik, J.C., Wiesner, M.R., Bottero, J.-Y., 2008. Relation between the redox state of iron-based nanoparticles and their cytotoxicity toward *Escherichia coli*. Environmental science & technology 42, 6730-6735.

Bardiya, N., Bae, J.-H., 2011. Dissimilatory perchlorate reduction: a review. Microbiological research 166, 237-254.

Bokulich, N.A., Kaehler Benjamin, D., Rideout Jai, R., Dillon, M., Bolyen, E., Knight, R., Huttley Gavin, A.a., 2018. Optimizing taxonomic classification of marker-gene amplicon sequences with QIIME 2's q2-feature-classifier plugin. Microbiome.

Bolyen, E., Rideout Jai, R., Dillon Matthew, R., Bokulich Nicholas, A., Abnet Christian, C., Al-Ghalith Gabriel, A., Alexander, H., Alm Eric, J., Arumugam, M., Asnicar, F., Bai, Y., Bisanz Jordan, E., Bittinger, K., Brejnrod, A., Brislawn Colin, J., Brown, C.T., Callahan Benjamin, J., Caraballo-Rodrguez Andrs, M., Chase, J., Cope Emily, K.a., 2019. Reproducible, interactive, scalable and extensible microbiome data science using QIIME 2. Nature Biotechnology.

Borden, R.C., 2007. Concurrent bioremediation of perchlorate and 1,1,1-trichloroethane in an emulsified oil barrier. Journal of Contaminant Hydrology 94, 13--33.

Callahan, B.J., McMurdie, P.J., Rosen, M.J., Han, A.W., Johnson, A.J.A., Holmes, S.P., 2016. DADA2: high-resolution sample inference from Illumina amplicon data. Nature methods 13, 581-583.

Caporaso, J.G., Lauber Christian, L., Walters William, A., Berg-Lyons, D., Huntley, J., Fierer, N., Owens Sarah, M., Betley, J., Fraser, L., Bauer, M., Gormley, N., Gilbert Jack, A., Smith, G., Knight, R., 2012. Ultra-high-throughput microbial community analysis on the Illumina HiSeq and MiSeq platforms. The ISME Journal 6, 1621--1624.

Chowdhury, A.I., Krol, M.M., Kocur, C.M., Boparai, H.K., Weber, K.P., Sleep, B.E., O'Carroll, D.M., 2015. nZVI injection into variably saturated soils: Field and modeling study. Journal of contaminant hydrology 183, 16-28.

Coates, J.D., Michaelidou, U., Bruce Royce, A., Oapos, Connor, S.M., Crespi Jill, N., Achenbach Laurie, A., 1999. Ubiquity and diversity of dissimilatory (per)chlorate-reducing bacteria. Applied and Environmental Microbiology 65, 5234-5241.

Dang, H., Kanitkar, Y.H., Stedtfeld, R.D., Hatzinger, P.B., Hashsham, S.A., Cupples, A.M., 2018. Abundance of chlorinated solvent and 1, 4-dioxane degrading microorganisms at five chlorinated solvent contaminated sites determined via shotgun sequencing. Environmental science & technology 52, 13914-13924.

Davies, K.J., 2000. Oxidative stress, antioxidant defenses, and damage removal, repair, and replacement systems. IUBMB life 50, 279-289.

Delgado, A.G., Fajardo-Williams, D., Bondank, E., Esquivel-Elizondo, S., Krajmalnik-Brown, R., 2017. Coupling bioflocculation of *Dehalococcoides mccartyi* to high-rate reductive dehalogenation of chlorinated ethenes. Environmental science & technology 51, 11297-11307.

Delgado, A.G., Fajardo-Williams, D., Kegerreis, K.L., Parameswaran, P., Krajmalnik-Brown, R., 2016. Impact of ammonium on syntrophic organohalide-respiring and fermenting microbial communities. Msphere 1, e00053-00016.

Delgado, A.G., Fajardo-Williams, D., Popat, S.C., Torres, C.I., Krajmalnik-Brown, R., 2014a. Successful operation of continuous reactors at short retention times results in high-density, fast-rate *Dehalococcoides* dechlorinating cultures. Applied microbiology and biotechnology 98, 2729-2737.

Delgado, A.G., Kang, D.-W., Nelson, K.G., Fajardo-Williams, D., Miceli III, J.F., Done, H.Y., Popat, S.C., Krajmalnik-Brown, R., 2014b. Selective enrichment yields robust ethene-producing dechlorinating cultures from microcosms stalled at *cis*-dichloroethene. PloS one 9.

Delgado, A.G., Parameswaran, P., Fajardo-Williams, D., Halden, R.U., Krajmalnik-Brown, R., 2012. Role of bicarbonate as a pH buffer and electron sink in microbial dechlorination of chloroethenes. Microbial cell factories 11, 128.

Dong, H., Li, L., Lu, Y., Cheng, Y., Wang, Y., Ning, Q., Wang, B., Zhang, L., Zeng, G., 2019. Integration of nanoscale zero-valent iron and functional anaerobic bacteria for groundwater remediation: a review. Environment international 124, 265-277.

Evans, P.J., Koenigsberg, S., 2001. A bioavailable ferric iron assay and relevance to reductive dechlorination. Bioaugmentation, biobarriers, and biogeochemistry. Battelle Press, Columbus, Ohio, 209-215.

Hatzinger, P., Diebold, J., 2009. In situ bioremediation of perchlorate in groundwater. Shaw Environmental, Inc., Lawrenceville, NJ.

He, F., Zhao, D., Paul, C., 2010a. Field assessment of carboxymethyl cellulose stabilized iron nanoparticles for in situ destruction of chlorinated solvents in source zones. Water research 44, 2360-2370.

He, Y.T., Wilson, J.T., Wilkin, R.T., 2010b. Impact of iron sulfide transformation on trichloroethylene degradation. Geochimica et Cosmochimica Acta 74, 2025-2039.

Hem, J.D., 1985. Study and interpretation of the chemical characteristics of natural water. Department of the Interior, US Geological Survey.

Jeong, H.Y., Hayes, K.F., 2007. Reductive dechlorination of tetrachloroethylene and trichloroethylene by mackinawite (FeS) in the presence of metals: reaction rates. Environmental science & technology 41, 6390-6396.

Keenan, C.R., Goth-Goldstein, R., Lucas, D., Sedlak, D.L., 2009. Oxidative stress induced by zero-valent iron nanoparticles and Fe (II) in human bronchial epithelial cells. Environmental science & technology 43, 4555-4560.

Keenan, C.R., Sedlak, D.L., 2008. Factors affecting the yield of oxidants from the reaction of nanoparticulate zero-valent iron and oxygen. Environmental Science & Technology 42, 1262-1267.

Kirschling, T.L., Gregory, K.B., Minkley, J., Edwin G, Lowry, G.V., Tilton, R.D., 2010. Impact of nanoscale zero valent iron on geochemistry and microbial populations in trichloroethylene contaminated aquifer materials. Environmental Science & Technology 44, 3474-3480.

Kucharzyk, K.H., Meisel, J.E., Kara-Murdoch, F., Murdoch, R.W., Higgins, S.A., Vainberg, S., Bartling, C.M., Mullins, L., Hatzinger, P.B., Löffler, F.E., 2020. Metagenome-Guided Proteomic Quantification of Reductive Dehalogenases in the Dehalococcoides mccartyi-Containing Consortium SDC-9. Journal of Proteome Research 19, 1812-1823.

Liu, Y., Lowry, G.V., 2006. Effect of particle age (Fe^0 content) and solution pH on NZVI reactivity: H_2 evolution and TCE dechlorination. Environmental science & technology 40, 6085-6090.

Liu, Y., Wang, Q., Zhang, Y., Ni, B.-J., 2015a. Zero valent iron significantly enhances methane production from waste activated sludge by improving biochemical methane potential rather than hydrolysis rate. Scientific reports 5, 1-6.

Liu, Y., Zhang, Y., Ni, B.-J., 2015b. Zero valent iron simultaneously enhances methane production and sulfate reduction in anaerobic granular sludge reactors. Water research 75, 292-300.

Lyon, D.Y., Vogel, T.M., 2013. Bioaugmentation for groundwater remediation: an overview. Bioaugmentation for groundwater remediation. Springer, pp. 1-37.

Löffler, F.E., Sanford, R.A., Ritalahti, K.M., 2005. Enrichment, cultivation, and detection of reductively dechlorinating bacteria. Methods in enzymology 397, 77-111.

Mao, X., Polasko, A., Alvarez-Cohen, L., 2017. Effects of sulfate reduction on trichloroethene dechlorination by *Dehalococcoides*-containing microbial communities. Applied and environmental microbiology 83.

McDonald, D., Price, M.N., Goodrich, J., Nawrocki, E.P., DeSantis, T.Z., Probst, A., Andersen, G.L., Knight, R., Hugenholtz, P., 2012. An improved Greengenes taxonomy with explicit ranks for ecological and evolutionary analyses of bacteria and archaea. The ISME journal 6, 610-618.

Melnyk, R.A., Coates, J.D., 2015. The perchlorate reduction genomic island: mechanisms and pathways of evolution by horizontal gene transfer. BMC genomics 16, 862.

Melnyk, R.A., Engelbrektson, A., Clark, I.C., Carlson, H.K., Byrne-Bailey, K., Coates, J.D., 2011. Identification of a perchlorate reduction genomic island with novel regulatory and metabolic genes. Appl. Environ. Microbiol. 77, 7401-7404.

Miao, Z., Carroll, K.C., Brusseau, M.L., 2013. Characterization and quantification of groundwater sulfate sources at a mining site in an arid climate: The Monument Valley site in Arizona, USA. Journal of hydrology 504, 207-215.

Moore, A.M., De Leon, C.H., Young, T.M., 2003. Rate and extent of aqueous perchlorate removal by iron surfaces. Environmental science & technology 37, 3189-3198.

Naftz, D., Morrison, S.J., Fuller, C.C., Davis, J.A., 2002. Handbook of groundwater remediation using permeable reactive barriers: applications to radionuclides, trace metals, and nutrients. Academic Press.

Ontiveros-Valencia, A., Tang, Y., Krajmalnik-Brown, R., Rittmann, B.E., 2014. Managing the interactions between sulfate-and perchlorate-reducing bacteria when using hydrogen-fed biofilms to treat a groundwater with a high perchlorate concentration. Water research 55, 215-224.

O'Carroll, D., Sleep, B., Krol, M., Boparai, H., Kocur, C., 2013. Nanoscale zero valent iron and bimetallic particles for contaminated site remediation. Advances in Water Resources 51, 104-122.

Pantazidou, M., Panagiotakis, I., Mamais, D., Zikidi, V., 2012. Chloroethene biotransformation in the presence of different sulfate concentrations. Groundwater Monitoring & Remediation 32, 106-119.

Pawlett, M., Ritz, K., Dorey Robert, A., Rocks, S., Ramsden, J., Harris Jim, A., 2013. The impact of zero-valent iron nanoparticles upon soil microbial communities is context dependent. Environmental Science and Pollution Research 20, 1041-1049.

Rangan, S.M., 2017. Trade-offs in Utilizing of Zero-Valent Iron for Synergistic Biotic and Abiotic Reduction of Trichloroethene and Perchlorate in Soil and Groundwater. Arizona State University.

Reinke, L.A., Rau James, M., McCay Paul, B., 1994. Characteristics of an oxidant formed during iron (II) autoxidation. Free Radical Biology and Medicine 16, 485-492.

Robles, A., 2019. Reductive Dechlorination Sustained by Microbial Chain Elongation. Arizona State University.

Rosenthal, H., Adrian, L., Steiof, M., 2004. Dechlorination of PCE in the presence of Fe^0 enhanced by a mixed culture containing two Dehalococcoides strains. Chemosphere 55, 661-669.

Russell, H.H., Matthews, J.E., Guy, W.S., 1992. TCE removal from contaminated soil and groundwater. EPA Environmental Engineering Sourcebook, 87-100.

Shrout, J.D., Williams, A.G., Scherer, M.M., Parkin, G.F., 2005. Inhibition of bacterial perchlorate reduction by zero-valent iron. Biodegradation 16, 23-32.

Son, A., Lee, J., Chiu Pei, C., Kim Byung, J., Cha Daniel, K., 2006. Microbial reduction of perchlorate with zero-valent iron. Water Research 40, 2027-2032.

Srinivasan, A., Viraraghavan, T., 2009. Perchlorate: health effects and technologies for its removal from water resources. International Journal of Environmental Research and Public Health 6, 1418-1442.

Stephenson, J.B., 2007. Department of Defense Activities Related to Trichloroethylene, Perchlorate, and Other Emerging Contaminants. United States Government Accountability Office.

Stevenson, A., Herrera, J., 2018. Role of Zero Valent Iron and Organic Substrates in Chlorinated Solvent Degradation: An Ex-Situ Remediation Case Study. The University of Western Ontario.

Stroo, H.F., West, M.R., Kueper, B.H., Borden, R.C., Major, D.W., Ward, C.H., 2014. In situ bioremediation of chlorinated ethene source zones. Chlorinated solvent source zone remediation. Springer, pp. 395-457.

U.S. Department of Defense, 2005. Perchlorate in the Southwestern United States. DOD Environment, Safety and Occupational Health Network and Information Exchange.

U.S. EPA, 2003. Drinking Water Advisory: Consumer Acceptability Advice and

Health Effects Analysis on Sulfate. U.S. Environmental Protection Agency.

Urbansky, E.T., 2002. Perchlorate as an environmental contaminant. Environmental Science and Pollution Research 9, 187-192.

US EPA, 2017. , Search superfund site information.

Vainberg, S., Condee Charles, W., Steffan Robert, J., 2009. Large-scale production of bacterial consortia for remediation of chlorinated solvent-contaminated groundwater. Journal of Industrial Microbiology and Biotechnology 36, 1189-1197.

Velimirovic, M., Simons, Q., Bastiaens, L., 2015. Use of CAH-degrading bacteria as test-organisms for evaluating the impact of fine zerovalent iron particles on the anaerobic subsurface environment. Chemosphere 134, 338-345.

Vogel, T.M., Criddle, C.S., McCarty, P.L., 1987. ES&T critical reviews: transformations of halogenated aliphatic compounds. Environmental science & technology 21, 722-736.

Warren, L.A., Ferris, F.G., 1998. Continuum between sorption and precipitation of Fe (III) on microbial surfaces. Environmental Science & Technology 32, 2331-2337.

WHO, 2004. Sulfate in Drinking-water. World Health Organization.

Wolf-Gladrow, D.A., Zeebe, R.E., Klaas, C., Körtzinger, A., Dickson, A.G., 2007. Total alkalinity: The explicit conservative expression and its application to biogeochemical processes. Marine Chemistry 106, 287-300.

Xie, Y., Dong, H., Zeng, G., Tang, L., Jiang, Z., Zhang, C., Deng, J., Zhang, L., Zhang, Y., 2017. The interactions between nanoscale zero-valent iron and microbes in the subsurface environment: a review. Journal of hazardous materials 321, 390-407.

Xiu, Z.-m., Gregory, K.B., Lowry, G.V., Alvarez, P.J., 2010a. Effect of bare and coated nanoscale zerovalent iron on *tceA* and *vcrA* gene expression in *Dehalococcoides* spp. Environmental science & technology 44, 7647-7651.

Xiu, Z.-m., Jin, Z.-h., Li, T.-l., Mahendra, S., Lowry, G.V., Alvarez, P.J., 2010b. Effects of nano-scale zero-valent iron particles on a mixed culture dechlorinating trichloroethylene. Bioresource Technology 101, 1141-1146.

Yang, Y., Guo, J., Hu, Z., 2013. Impact of nano zero valent iron (NZVI) on methanogenic activity and population dynamics in anaerobic digestion. Water research 47, 6790-6800.

Yu, X., Amrhein, C., Deshusses, M.A., Matsumoto, M.R., 2006. Perchlorate reduction by autotrophic bacteria in the presence of zero-valent iron. Environmental science & technology 40, 1328-1334.

Zaa, C.L.Y., McLean Joan, E., Dupont, R.R., Norton Jeanette, M., Sorensen Darwin, L., 2010. Dechlorinating and iron reducing bacteria distribution in a TCE-contaminated aquifer. Ground Water Monitoring and Remediation 30, 46-57.

Zhao, S., He, J., 2019. Reductive dechlorination of high concentrations of chloroethenes by a Dehalococcoides mccartyi strain 11G. FEMS microbiology ecology 95, fiy209.

Ziv-El, M., Delgado, A.G., Yao, Y., Kang, D.-W., Nelson, K.G., Halden, R.U., Krajmalnik-Brown, R., 2011a. Development and characterization of DehaloR^2, a novel anaerobic microbial consortium performing rapid dechlorination of TCE to ethene. Applied microbiology and biotechnology 92, 1063-1071.

Ziv-El, M., Delgado Anca, G., Yao, Y., Kang Dae, W., Nelson Katherine, G., Halden Rolf, U., Krajmalnik-Brown, R., 2011b. Development and characterization of DehaloR 2, a novel anaerobic microbial consortium performing rapid dechlorination of TCE to ethene. Applied Microbiology and Biotechnology 92, 1063--1071.

Ziv-El, M., Kalinowski, T., Krajmalnik-Brown, R., Halden, R.U., 2014. Simultaneous determination of chlorinated ethenes and ethene in groundwater using headspace solid-phase microextraction with gas chromatography. Journal of chromatographic science 52, 137-142.

Ziv-El, M., Popat Sudeep, C., Parameswaran, P., Kang Dae, W., Polasko, A., Halden Rolf, U., Rittmann Bruce, E., Krajmalnik-Brown, R., 2012. Using electron balances and molecular techniques to assess trichoroethene-induced shifts to a dechlorinating microbial community. Biotechnology and Bioengineering 109, 2230--2239.

Ševců, A., El-Temsah, Y.S., Joner, E.J., Černík, M., 2009. Oxidative stress induced in microorganisms by zero-valent iron nanoparticles. Microbes and Environments, 1107220320-1107220320.

CHAPTER 3

DECOUPLING Fe^0 APPLICATION AND BIOAUGMENTATION IN SPACE AND TIME ENABLES MICROBIAL REDUCTIVE DECHLORINATION OF TRICHLOROETHENE TO ETHENE[b]

3.1 Introduction

Fe^0 is a powerful reductant with applications for remediation of an array of soil and groundwater contaminants, (Phillips et al., 2010; Mueller et al., 2012; Singh et al., 2012; Su et al., 2012; Statham et al., 2016; Han et al., 2021) including the chlorinated organic solvents, tetrachloroethene (PCE) and trichloroethene (TCE). The reduction of PCE and TCE by Fe^0 involves a β-elimination reaction which yields chloroacetylene and is followed by hydrogenolysis to produce acetylene and ethene/ethane as end products (Arnold and Roberts, 2000; Liu et al., 2007; Brown et al., 2009; Moratalla et al., 2022). When applied *in situ*, Fe^0 particles rapidly oxidize to form oxide shells such as Fe_3O_4 and $Fe(OH)_3$ (Kanel et al., 2007; Guan et al., 2015; Zhang et al., 2019). Fe^{3+} aggregates passivate the surface of Fe^0 and limit the rate of abiotic chlorinated ethene reduction (Farrell et al., 2000a; Parbs et al., 2007; Olson and Sale, 2015; Gong et al., 2020). Phosphate (PO_4^{3-}) and bicarbonate (HCO_3^-) ions, common groundwater constituents, accelerate Fe^0 oxidation (Parbs et al., 2007; Gong et al., 2020). Overall, Fe^0 offers a low electron transfer efficiency to target contaminants (Guan et al., 2015; Wang et al., 2016).

---

[b]This chapter will soon be submitted in an altered format to *Environmental Science & Technology* with co-authors Rao, S., Robles, A., Mouti, A., LaPat-Polasko, L., Lowry, G. V., Krajmalnik-Brown, R., & Delgado, A. G.

Instead, more than 80% of the electrons from Fe^0 oxidation are channeled to the production of H_2 from H_2O (Farrell et al., 2000b; Wang et al., 2016). The H_2 evolved from Fe^0 oxidation can be used as an electron donor for the reductive dechlorination of chlorinated ethenes to ethene by the organohalide-respiring bacteria, *Dehalococcoides mccartyi* and *Dehalogenimonas* sp. (Lampron et al., 1998; Rosenthal et al., 2004; Xiu et al., 2010b; Koenig et al., 2016; Rangan et al., 2020).

Microbial reductive dechlorination supported by Fe^0 has been documented in soil-free cultures (Lampron et al., 1998; Rosenthal et al., 2004) and soil and groundwater microcosms (Kirschling et al., 2010; Rangan et al., 2020) and, to a lesser extent, in flow-through soil columns (Lorah et al., 2008). Pertinent factors affecting reductive dechlorination in the presence of Fe^0 include the size (Summer et al., 2020), concentration (Velimirovic et al., 2015), and properties of Fe^0 (Xiu et al., 2010a; Rangan et al., 2020), the initial concentration of microorganisms and microbial community composition (Kirschling et al., 2010; Yang et al., 2013; Rangan et al., 2020), and the clay and organic matter contents of soil and groundwater (Li et al., 2010; Chen et al., 2011; Pawlett et al., 2013). To date, laboratory testing in microcosm (Rosenthal et al., 2004; Xiu et al., 2010b; de Guzmán et al., 2018; Summer et al., 2020) and soil column (Gregory et al., 2000; Lorah et al., 2008; Baric et al., 2012; Velimirovic et al., 2014; de Guzmán et al., 2018) has been performed with a common feature in the experimental design: the simultaneous addition in space and time of Fe^0, organic substrate (biostimulation), and microbial culture containing *D. mccartyi* (bioaugmentation). When added together with the microbial culture, Fe^0 can disrupt cell membranes of the bioaugmented

microorganisms and damage proteins/DNA due to reactive oxygen species generated by Fe^0 (Lee et al., 2008a; Ševců et al., 2009; Barnes et al., 2010; Kim et al., 2010; Marsalek et al., 2012). Fe^0 can also create a chlorinated ethene limitation to the organohalide-respiring bacteria (from abiotic dichlorination) (Xiu et al., 2010a; Rangan et al., 2020) and enhance the consumption of H_2 by sulfate (SO_4^{2-})-reducing bacteria (Xin et al., 2008; Kirschling et al., 2010) and methanogens (Yang et al., 2018b; Zhou et al., 2020).

Typical concentrations of Fe^0 applied at contaminates sites are on the order of 0.2 to 10 g L^{-1} of porewater (Henn and Waddill, 2006; Bennett et al., 2010; He et al., 2010a; Kocur et al., 2014; Chowdhury et al., 2015). At these concentrations, abiotic dechlorination is typically the main chlorinated ethene removal mechanism in the first three weeks post Fe^0 injection (Kocur et al., 2015; Czinnerová et al., 2020). The addition of Fe^0 is often accompanied by an immediate decrease in *D. mccartyi* concentrations in groundwater (e.g., by ~ 0.5-1 log (Kocur et al., 2015; Czinnerová et al., 2020)). Concentrations of nano-scale Fe^0 greater than 0.05 g L^{-1} exacerbate cell damage and inhibitory effects (Auffan et al., 2008; Lee et al., 2008a; Velimirovic et al., 2015). While coupling Fe^0 with the metabolism of H_2-utilizing organohalide-respiring bacteria could maximize Fe^0 utilization efficiency at contaminated sites, knowledge from laboratory and field applications suggests that *in situ* biostimulation and bioaugmentation should occur at a downstream location from Fe^0 to minimize undesired effects. Yet, neither laboratory nor field investigations exist in peer-reviewed literature where such an approach was evaluated for bioremediation of chlorinated ethenes. In this study, we tackled this knowledge gap and experimentally evaluated a disjoint Fe^0 application and

biostimulation/bioaugmentation in space and time (Figure 3.1). A column containing Fe^0 and soil was used as a proxy for an upstream injection zone where Fe^0 would be applied. Fe^0-reduced groundwater was flown into soil packed columns with added organic substrates and a *D. mccartyi* mixed culture; these Bio-columns were a proxy for a downstream zone of biostimulation and bioaugmentation. To increase environmental relevance, we used soil and groundwater collected from a Superfund site in Arizona, USA, and field-pertinent concentrations of TCE and Fe^0.

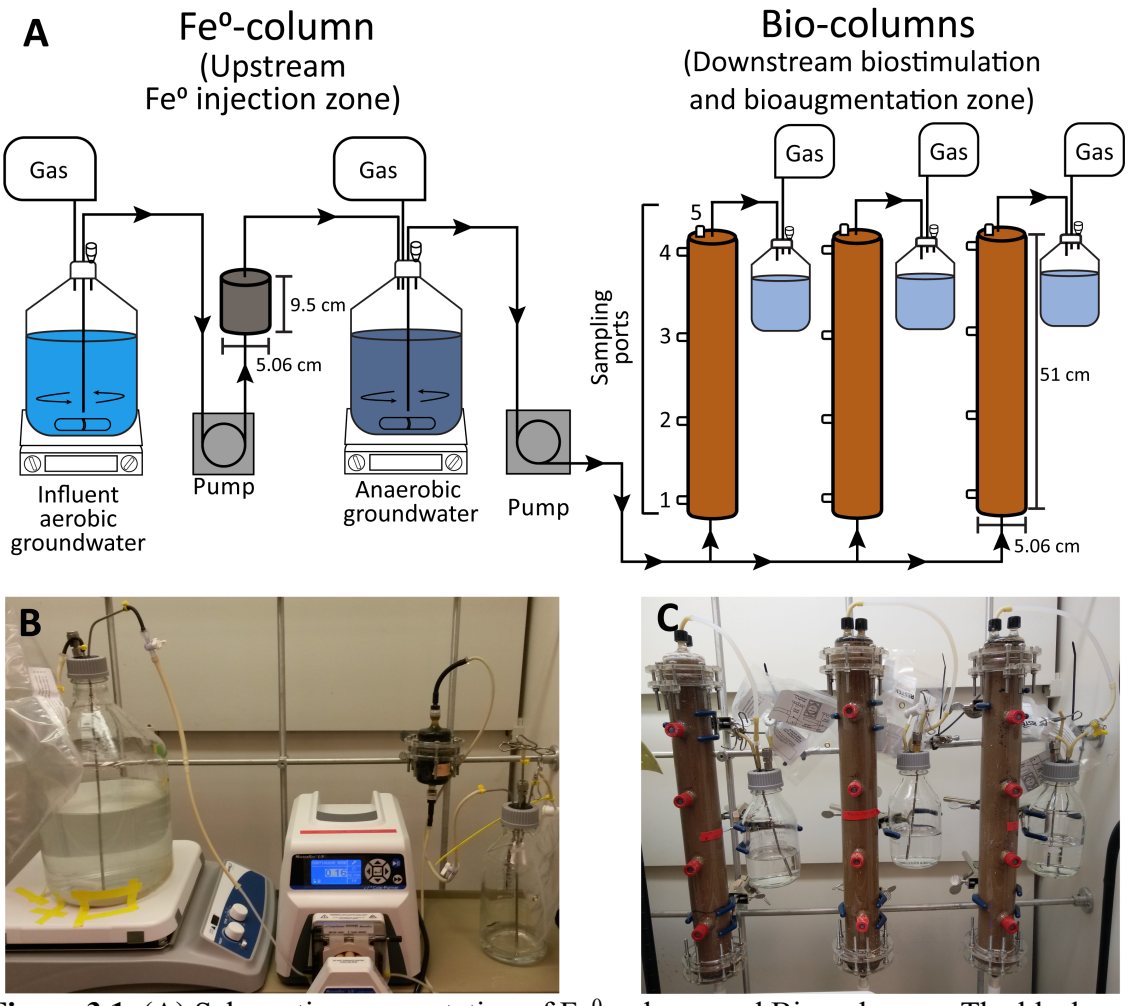

Figure 3.1. (A) Schematic representation of Fe^0-column and Bio-columns. The black arrows indicate the flow of groundwater through the system. Photographs of (B) Fe^0 column and (C) Bio-columns during operation in the study.

3.2 Materials and Methods

3.2.1 Aquifer materials, Fe^0 products, and microbial inocula

Soil and groundwater from the Phoenix-Goodyear Airport-North (PGAN) Superfund site were used in this study. The site was a former manufacturing facility for defense and aerospace equipment. TCE and perchlorate are the main contaminants of concern at this site (Arizona Department of Environmental Quality, 2017). The soil was sampled from 25-52 m below ground surface and it was homogenized in the laboratory before use in the experiments (Rangan et al., 2020). The resulting soil was a mix of silty sand, well graded sand and poorly graded sand (Rangan et al., 2020). The groundwater was sampled from a depth of 34-46 m (upper aquifer) (Rangan et al., 2020). The groundwater contained 8 ± 1.2 μmol L^{-1} TCE, 1.6 ± 0.2 μmol L^{-1} perchlorate, 11.9 ± 1.6 mmol L^{-1} SO_4^{2-}, and 1.0 ± 0.3 mmol L^{-1} nitrate. The pH and oxidation reduction potential (ORP) of the groundwater were 6.4 ± 0.2 and 213 ± 62 mV, respectively. Other PGAN groundwater characteristics were previously reported (Rangan et al., 2020).

The Fe^0 products used in this study were carbonyl iron powder OM ($d_{particle}$ = 4-7 μm) from BASF (Florham Park, NJ) and Z-loy MicroMetal ($d_{particle}$ = 2-3 μm) from OnMaterials (Escondido, CA). The reductive dechlorinating cultures were ZARA-10 (Delgado et al., 2014b; Delgado et al., 2016; Delgado et al., 2017) and BAC-9 (EOS remediation LLC, Research Triangle Park, NC). BAC-9 culture is also marketed and distributed as SDC-9 (Vainberg et al., 2009). ZARA-10 and BAC-9 cultures contain *D. mccartyi* strains capable of dechlorinating PCE and TCE to ethene, other organohalide-

respiring bacteria (e.g., *Geobacter* and *Desulfitobacterium*), fermenters, methanogens, and acetogens (Robles et al., 2021).

3.2.2 Preparation of soil columns

Experiments were performed in glass columns packed with soil (Figure 3.1). The experimental setup consisted of a soil column amended with Fe^0 (Fe^0-column, Figure 3.1A) and three soil columns for biostimulation/bioaugmentation (Bio-columns A, B, and C, Figure 3.1A). The Fe^0-column had a length of 9.5 cm and an inner diameter of 5.06 cm. Stainless steel meshes with a 1.7 mm^2 pore size were installed at the influent and effluent sides of the column. The Fe^0-column was packed inside an anaerobic glove chamber by adding 280 g of soil in increments of ~30 g and manually compacting the soil after each addition. Then, the packed soil was saturated with 40 mL of a Fe^0 solution containing 15 g L^{-1} Fe^0 (7.5 g L^{-1} carbonyl iron powder OM and 7.5 g L^{-1} Z-loy MicroMetal). The rationale for combining the two Fe^0 products was based on their reactivity characteristics. Specifically, Z-loy MicroMetal has a higher reactivity (by ~30 times) than carbonyl iron powder (Freim) while carbonyl iron powder has a longer reactivity (Islam et al., 2020). The overall concentration of Fe^0 in the soil was ~ 2 g Fe^0 kg^{-1} soil. The porosity of the Fe^0-column was 0.22 and the pore volume was 40 mL.

The Bio-columns had stainless steel meshes at both the ends and the same inner diameter as the Fe^0-column, but their length was 51 cm. The Bio-columns were packed in a chemical fume hood with a continuous stream of N_2 gas in the column headspace. Packing consisted of adding soil in increments of ~ 30 g, compacting the soil manually, and saturating with groundwater. The influent and effluent containers of the columns

were Pyrex bottles (Cole-Parmer, Vernon Hills, IL) with butyl rubber stoppers and screw caps with aperture modified as in our previous works with bioreactors for reductive dechlorination (Delgado et al., 2014a; Delgado et al., 2017). Specifically, the butyl rubber stoppers were perforated and equipped with an influent or effluent line, a Tedlar bag (Restek, Bellefonte, PA) for sampling, and a gas sampling port with a removable septum (Figure 3.1A). The influent container (5 L) and effluent container (100 mL) were setup similar to those of the Fe^0-column (Figure 3.1A). Prior to the introduction of TCE, the columns used Norprene tubing. To minimize TCE adsorption, the tubing was replaced with stainless steel, viton, or polytetrafluoroethylene (Cole Palmer) before TCE was introduced into the columns.

3.2.3 Experimental design and operation of columns

Fe^0-column. Several Fe^0-columns were packed and operated during the study. Groundwater was pumped from bottom-to-top using a peristaltic pump (Cole-Parmer) and collected in an effluent container. Each Fe^0-column was operated at a flow rate of 100 mL day^{-1}, corresponding to a hydraulic retention time (HRT) of 0.4 d. Approximately 75 HRTs were completed per Fe^0-column before repacking with a fresh batch of soil and Fe^0 as described in section "Preparation of soil columns". TCE was added to the collected effluent from the Fe^0-column (referred to as anaerobic groundwater in Figure 3.1A) before it was flown into the Bio-columns (Figure 3.1A).

Bio-columns. A conservative tracer test was performed to determine the effective porosity of each Bio-column (denoted A, B, and C). N_2-sparged groundwater amended with 10 g L^{-1} NaCl was pumped at a flow rate of 124 mL day^{-1} and conductivity was

measured. The background conductivity of the groundwater was subtracted from the influent and effluent conductivity. C/C_0 was calculated, where C_0 is influent groundwater conductivity and C is effluent groundwater conductivity in units of mS cm^{-1}. Based on the calculated C/C_0, breakthrough curves were plotted for the Bio-columns (Figure 3.2). Assuming the soil was fully saturated in the columns, one pore volume was considered the volume of influent groundwater required for the effluent conductivity to reach 50% of the influent conductivity ($C/C_0 = 0.5$). The effective porosities and effective pore volumes of each Bio-column are presented in Table 3.1.

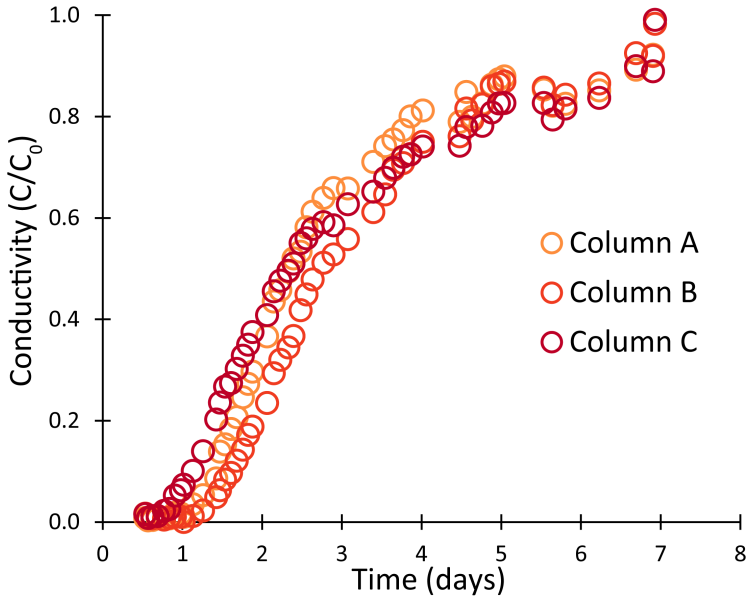

Figure 3.2. Breakthrough curves from conservative tracer (NaCl) tests in the Bio-columns.

Table 3.1. Effective porosities, effective pore volumes, and resulting HRT at a flow rate of 17 mL day^{-1} in the Bio-columns.

Bio-column	Effective porosity	Effective pore volume (mL)	HRT (d)
A	0.28	250	14
B	0.33	290	17
C	0.29	225	13

The experimental phases in the Bio-columns are shown in Table 3.2. In Phase I (column conditioning, days 0-80), anaerobic groundwater collected from the Fe^0-column was continuously flown into the Bio-columns at 17 mL d^{-1} for six pore volumes to ensure saturation of the soil with TCE (Table 3.2). Saturation was observed by day 80, after which Phase II began. In Phase II (days 81-180), the flow rate was 17 mL d^{-1}, corresponding to an HRT of 14 d for Bio-column A, 17 d for Bio-column B, and 13 d for Bio-column C (Table 3.2). The aqueous TCE concentration in the influent of the Bio-columns was maintained between 150 and 220 μM by adding neat TCE every 2-3 days. The influent was agitated on a magnetic stir plate to promote equilibration of TCE between the liquid and gas phases.

Table 3.2. Experimental phases for Bio-columns.

Experimental phase	Time (days)	Influent	Influent TCE (μM)
I (conditioning)	0-80	Anaerobic groundwater collected from the Fe^0-column	150-200
II[a, b]	81-180	Anaerobic groundwater collected from the Fe^0-column	150-220
Batch mode	180-240	None	None
III[c]	240-290	Aerobic groundwater (no Fe^0)	160-210

[a]Biostimulation with lactate, emulsified vegetable oil, yeast extract, and phosphate buffer performed on days 81 and 154.
[b]Bioaugmentation with ZARA-10 and BAC-9 cultures performed on day 85.
[c]Biostimulation with lactate and emulsified vegetable oil performed every 13-20 days.

The Bio-columns received organic substrates and buffer (biostimulation) on days 81 (beginning of Phase II) and 154. Biostimulation consisted of injecting 5 mL of stock solutions containing 140 mg lactate (sodium lactate 60% syrup, Sigma-Aldrich, St. Louis, MO), 42.5 mg emulsified vegetable oil (EOS Pro, EOS Remediation LLC, Raleigh, NC), 50 mg yeast extract, and 240 mg (2.5 mmol) potassium phosphate into each column. The

biostimulation stock solutions were equally divided between ports 1-5 (Figure 3.1A). Bioaugmentation was performed on day 85 by injecting 0.2 mL ZARA-10 and 0.5 mL BAC-9 into each of the five column ports (Figure 3.1A). ZARA-10 culture contained 1.9×10^7 *D. mccartyi* cells mL^{-1} and BAC-9 culture contained 8.8×10^7 *D. mccartyi* cells mL^{-1}.

In Phase III (days 240-290), aerobic groundwater (without Fe^0 pre-treatment) was flown directly into the Bio-columns to evaluate a condition after Fe^0 exhaustion in the subsurface (Table 3.2). The columns were biostimulated with 140 mg lactate, 42.5 mg emulsified vegetable oil, and 240 mg potassium phosphate buffer every 13-20 days (Table 3.2). The flow rate was constant at 17 mL d^{-1} and the influent aqueous TCE concentration was maintained between 160 and 210 µM.

3.2.4 Chemical analyses

Gas samples were collected from the headspace of the influent and effluent glass containers using a 500 µL gas-tight syringe (Hamilton Company, Reno, NV). Chlorinated ethenes, ethene, and methane were quantified by injecting 200 µL gas samples into a gas chromatograph (GC, Shimadzu GC-2010; Columbia, MD) equipped with a flame ionization detector (FID) and a Rt-QS-BOND capillary column (Restek, Bellefonte, PA). Details on the chromatography method and calibrations were previously published (Ziv-El et al., 2011a; Delgado et al., 2012; Delgado et al., 2014a; Rangan et al., 2020). The detection limits for chlorinated ethenes and ethene were in the range of 0.2-0.6 µmol L^{-1} gas concentration. The detection limit for methane was 12 µmol L^{-1} gas concentration (Rangan et al., 2020). H_2 was measured using a GC (Shimadzu GC-2010)

with a thermal conductivity detector and a fused silica capillary column (Carboxen 1010 PLOT, Supelco, Bellefonte, PA). The detailed method for H_2 measurements was previously published (Delgado et al., 2014a; Delgado et al., 2017). Aqueous TCE concentrations were calculated using Henry's constants assuming a gas-liquid equilibrium (Ziv-El et al., 2011a). The influent TCE concentration in Figure 3.3 is reported as the aqueous concentration because only dissolved TCE was fed to the Bio-columns. The concentrations of chlorinated ethenes, ethene, methane, and H_2 in the effluent containers are reported as nominal concentrations (Rangan et al., 2020; Robles et al., 2021) in the effluent recipient due to partitioning of these compounds between the gas phase and liquid phases. The recovery of chlorinated ethenes and ethene during the experimental phases was calculated as described in section 3.2.6 and tabulated in Table 3.3.

Table 3.3. Recovery of chlorinated ethenes and ethene in the effluent of the Bio-columns during the experimental phases. Recovery calculations (%) were performed under two scenarios: 1) relative to the average influent TCE concentration in each phase and 2) relative to the average effluent TCE concentration in each Bio-column during Phase I (conditioning). The second scenario was used to account for TCE sorption to soil and losses due to volatilization in the experimental setup. N/A = not applicable.

Phase	Average influent [TCE] (μM)	Effluent recovery relative to influent [TCE] (%)[a]	Average effluent [TCE] (μM)[b]	Effluent recovery relative to effluent [TCE] in Phase I (%)[a]
I (days 0-80)	167.5	23.6, 28.7, 22.7	38.1, 48.0, 38.0	N/A
II (days 81-180)	180.6	29.6, 28.8, 29.5	N/A	140.4, 108.4, 140.3
III (days 240-290)	188.6	16.9, 24.1, 16.4	N/A	83.7, 94.5, 81.4

[a]The three values are average recoveries calculated for Bio-column A, B, and C, respectively.
[b]The three values are average TCE concentration in effluents of Bio-column A, B, and C, respectively during phase I, where TCE was the only compound detected in the effluent.

Liquid samples were collected from the influent and effluent containers periodically throughout the study. The pH was measured using Orion 2-Star Pro benchtop pH meter (Thermo Scientific, Waltham, MA) and ORP was measured using an

ORP110-GS standard ORP probe (Hach, Loveland, CO). Liquid samples were filtered through a 0.22 μm polyvinylidene fluoride filter (MDI membrane technologies, Harrisburg, PA). The concentration of SO_4^{2-} was measured using an ion chromatograph (Metrohm 930 Compact Flex, Riverview, FL, USA) equipped with a conductivity detector, a 20 μL sample injection loop, a Metrosep A Supp 5 Guard column (5 × 4 mm; Metrohm), and a Metrosep A Supp 5 analytical column (150 × 4 mm; Metrohm). The ion chromatography method was based on EPA Method 9056A. The method details and calibration were described previously (Miranda et al., 2021). SO_4^{2-} detection limit was 0.3 μM (0.03 mg L^{-1}). Lactate, formate, acetate, and propionate were measured using a high-performance liquid chromatograph (HPLC, Shimadzu LC-20AT) equipped with an Aminex HPX-87H column (Biorad, Hercules, CA) as previously described (Delgado et al., 2016; Delgado et al., 2017; Meinel et al., 2022). The detection limit for the HPLC analytes was 20-50 μM (Robles et al., 2021). Electron balances were performed for Phases II (days 89, 159 and 172) and III (days 242 and 290). Details of these calculations are provided in section 3.2.6.

Total Fe concentration (HCl-extractable) was measured using a TNT 858 kit (Hach, Loveland, CO) in the influent and effluent samples of a representative Fe^0-column and in soil samples before use in Bio-columns and at the end of the experiment. Liquid (5 mL) and soil (2 g) were mixed with with 10 mL of 2 M HCl at 37 °C for 24 h (Sutherland, 2002; Boutry et al., 2009). The acidified samples were then centrifuged (Eppendorf 5810 R, Framingham, MA) at 4000 × g for 15 min. The supernatant was collected and the pH of the acid digestate was adjusted to be in the range of 4-5 using 5

M NaOH before measuring Fe concentration. The dry weight of the soil was determined by drying in an over overnight at 105 °C and the Fe concentrations were normalized to the dry weight of the soil. Details on calculations for total Fe concentrations are presented in section 3.2.6.

3.2.5 Microbiological analyses

Soil slurry samples were collected from ports 1-4 of the Bio-columns on days 80 (Phase I, before biostimulation), 83 (Phase II, after the first biostimulation event), 190 (end of Phase II), and 326 (end of Phase III and experiment). Genomic DNA was extracted from 100-180 mg soil using a Qiagen DNeasy Blood & Tissue Kit (MOBIO Laboratories Inc., Carlsbad, CA) and was used for quantitative real-time PCR (qPCR) and high throughput amplicon sequencing. Quantitative real-time PCR (qPCR) targeting the 16S rRNA gene of *D. mccartyi* was performed using a QuantStudio 3 Real-Time PCR System (Applied Biosystems, Foster City, CA). The primers, probes, reagent concentrations, and PCR conditions were those published (Ziv-El et al., 2011b; Delgado et al., 2016; Delgado et al., 2017). The DNA was diluted 1:10 and 4 µL of the diluted DNA was used as the template in a 10 µL reaction volume. All qPCR reactions including samples, six-point calibration standards, and negative controls (no-template) were run in triplicates. An automated epMotion 5070 liquid handling system (Eppendorf, Hauppauge, NY) was used for dilution of the standards and aliquoting liquid into the qPCR 96-well plates. The concentration of gene copies was converted to the concentration of cells (1:1 conversion factor) as each *D. mccartyi* chromosome contains only one copy of the 16S rRNA gene (Holmes et al., 2006). Log_2 fold change of *D.*

mccartyi cell concentrations during Phase III was calculated from the concentrations of *D. mccartyi* at the end of Phases II and III as described in section 3.2.6.

DNA amplicon sequencing was performed at the ASU Genomics Facility, The Biodesign Institute, Tempe, AZ (https://cores.research.asu.edu/genomics/capabilities) using a Miseq sequencer (Illumina, San Diego, CA). The V4 hyper-variable region of the bacterial and archaeal 16S rRNA gene was amplified using the 515F/806R primer set (Caporaso et al., 2012b). QIIME 2 pipeline was used to process the sequences (Bolyen et al., 2019b). DADA2 package was used to quality filter the raw sequences and the reads were truncated using dada2 denoise-single method to generate amplicon sequence variants (ASVs) (Callahan et al., 2016). Taxonomy was assigned to the ASVs by referencing SILVA database (v.138) (Quast et al., 2012) using the q2-feature-classifier plug in (Bokulich et al., 2018a). The raw sequences were submitted to NCBI under the project number PRJNA681587 and accession numbers SRX9612410–SRX9612451.

3.2.6 Analyses and calculations

Electron balance analyses were performed to evaluate the distribution of electrons from electron donor substrates to end-products in the Bio-columns. Electron balances were performed as previously done (Delgado et al., 2012; Joshi et al., 2021; Robles et al., 2021) using the data from Phase II on days 89 (after first biostimulation), 159 (after second biostimulation), 172 (end of Phase II) and Phase III on days 242 (beginning of Phase III) and 290 (end of experiment). Concentrations of added electron donors (lactate and emulsified vegetable oil) and end products of fermentation, reductive dechlorination, methanogenesis, and sulfate reduction were converted to millielectron equivalents. The

number of millielectron equivalents per mmol were as follows: lactate, 12; emulsified vegetable oil, 102 (assuming 100% oleic acid); formate, 2; acetate, 8; propionate, 14; *cis*-DCE, 2; VC, 4; ethene, 6; methane, 8; and sulfate, 8.

The recovery of chlorinated ethenes and ethene in the Bio-column effluents was calculated using Equation 3.1 and 3.2.

$$\text{Recovery relative to influent [TCE] (\%)} = \frac{\text{Y}}{\text{X}} \times 100 \qquad \text{(Equation 3.1)}$$

$$\text{Recovery relative to Phase I effluent [TCE] (\%)} = \frac{\text{Y}}{\text{Z}} \times 100 \qquad \text{(Equation 3.2)}$$

where *Y* is the sum of chlorinated ethenes and ethene concentrations (μM) in the Bio-column effluent, *X* is the average influent TCE concentration (μM) in each experimental Phase, and *Z* is the average effluent TCE concentration (μM) in Phase I (conditioning).

Total Fe concentration in the soil was calculated using Equation 3.3.

$$\text{Total Fe concentration (mg kg}^{-1}) = \left(\frac{C \times V \times D}{\text{ww}}\right) \qquad \text{(Equation 3.3)}$$

where *C* is the measured Fe concentration in the extract (mg L^{-1}), *V* is the volume of extract (L), *D* is the dilution factor, and *ww* is the wet-weight of sample (kg).

Fe concentration in the soil were normalized to the percentage of solids in the soil samples. Percentage of solids were calculated using Equation 3.4.

$$\text{Solids (\%)} = \left(\frac{dw}{\text{ww}}\right) \times 100 \qquad \text{(Equation 3.4)}$$

where, *dw* is the dry weight of the sample, and *ww* is the wet weight of the sample.

Log_2 fold change of *Dehalococcoides mccartyi* cells during Phase III were calculated by using Equation 3.5.

$$\text{Log}_2 \text{ fold change} = \text{Log}_2 \left(\frac{\text{B}}{\text{A}}\right) \qquad \text{(Equation 3.5)}$$

where A is the cell concentration (cells g^{-1} soil) at the end of Phase II (day 190) and B in the cell concentration (cells g^{-1} soil) at the end of Phase III (day 326).

3.3 Results and Discussion

3.3.1 Bio-columns receiving Fe^0-reduced groundwater can achieve reductive dechlorination to ethene when Fe^0 and bioaugmentation are decoupled in space and time

Anaerobic groundwater from the Fe^0-column was flown through the Bio-columns during Phases I and II of the study (Figure 3.3). The groundwater reduced by Fe^0 had an average ORP of –127 ± 67 mV and a pH of 7.1 ± 0.9 (Table 3.4). Conditioning of Bio-columns with Fe^0-reduced groundwater TCE was achieved in Phase I but microbial reductive dechlorination was absent during this time (Figure 3.3B-D). This result concurs with the lack of *D. mccartyi* populations and low organic carbon concentrations in the PGAN aquifer materials (Rangan et al., 2020; Robles et al., 2021). We hypothesized that the decoupling of Fe^0 application and biostimulation/bioaugmentation in space and time could mitigate the typically observed oxidative stress/damage to organohalide-respiring bacteria while inducing the required anoxic conditions for reductive dechlorination. Starting in Phase II, microbial TCE reductive dechlorination was observed after the biostimulation and bioaugmentation events (Figure 3.3B-D and 3.3F-H, days 81-85). *cis*-DCE and VC became detectable in the effluents within two days of bioaugmentation (Figure 3.3B-D). Ethene reached 15-30% of the total effluent composition between days 133 and 138 (Figure 3.4) but conversion to ethene declined between days 138 and 152 (Figure 3.3B-D, Phase II). We rationalized that a limitation in

organic substrate was the main cause for this decline as fermentation products were not detected in the Bio-column effluents after day 95 (Figure 3.3I-K). Indeed, re-addition of organic substrates on day 154 restored TCE reductive dechlorination to ethene (Figure 3.3B-D) and decreased the effluent pH from 8.5 to ~7.5 (Table 3.5). Ethene remained the major product of reductive dechlorination until the end of Phase II at 42-98% of the total effluent composition (Figure 3.4).

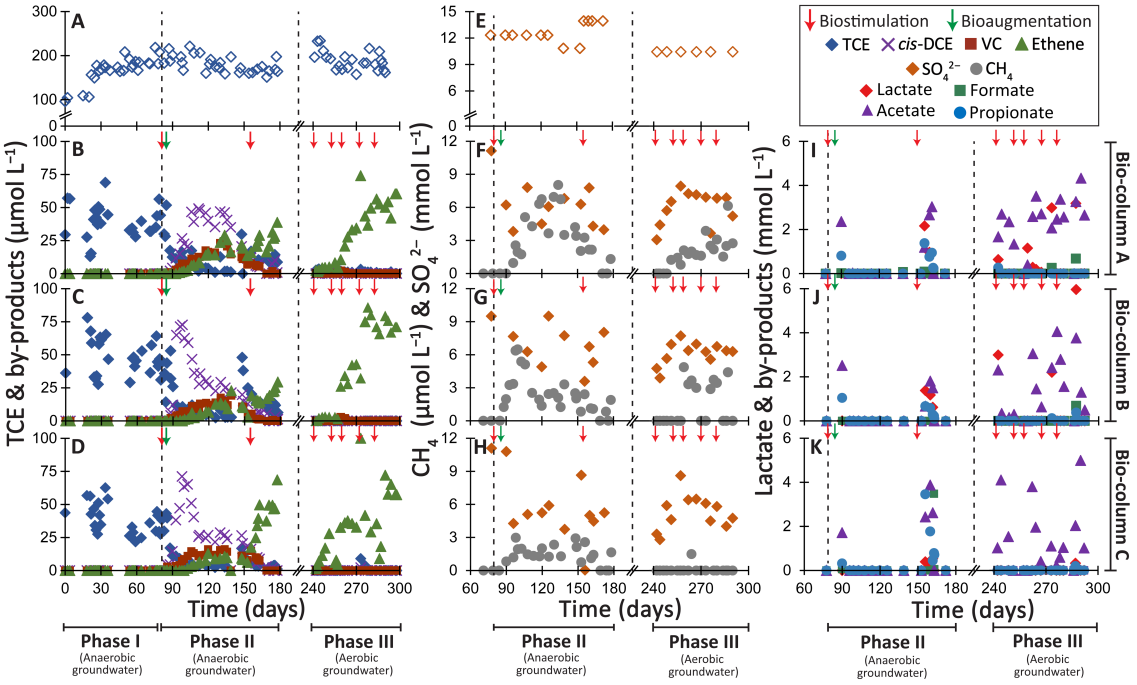

Figure 3.3. TCE reductive dechlorination (left panels), sulfate reduction and methanogenesis (middle panels), and fermentation (right panels) in Bio-columns (A, B, and C) during the experimental stages.

Table 3.4. pH and ORP, and concentrations of TCE, H_2 and CH_4 in the influent and effluent groundwater in a representative Fe^0-column operated during the study at a flow rate of 100 mL d^{-1} (0.4 d HRT). H_2 and CH_4 were not detected in the influent and hence not shown in the table. ND = not detected.

# of 0.4 d HRT completed	Influent		Effluent		Influent	Effluent		
	pH	ORP (mV)	pH	ORP (mV)	TCE (µM)	TCE (µM)	H_2 (mM)	CH_4 (µM)
2.5	6.36	141.4	6.42	–178.1	110.8	0.5	5.9	59.4
5	6.36	186.3	6.41	–219.6	145.1	1.5	7.3	111.5
7.5	6.34	175.8	6.38	–175.6	130.3	ND	6.3	178.7
10	6.48	176.1	6.49	–98.5	130.7	0.5	2.0	162.3
20	6.65	320.9	6.67	–98.6	92.5	ND	ND	16.6
25	7.65	285.6	8.14	–25.2	119.4	1.9	0.2	7.6
37.5	7.72	185.6	8.23	–57.4	110.0	0.6	ND	8.7
42.5	7.56	235.7	8.21	–162.2	99.7	0.3	0.1	4.8

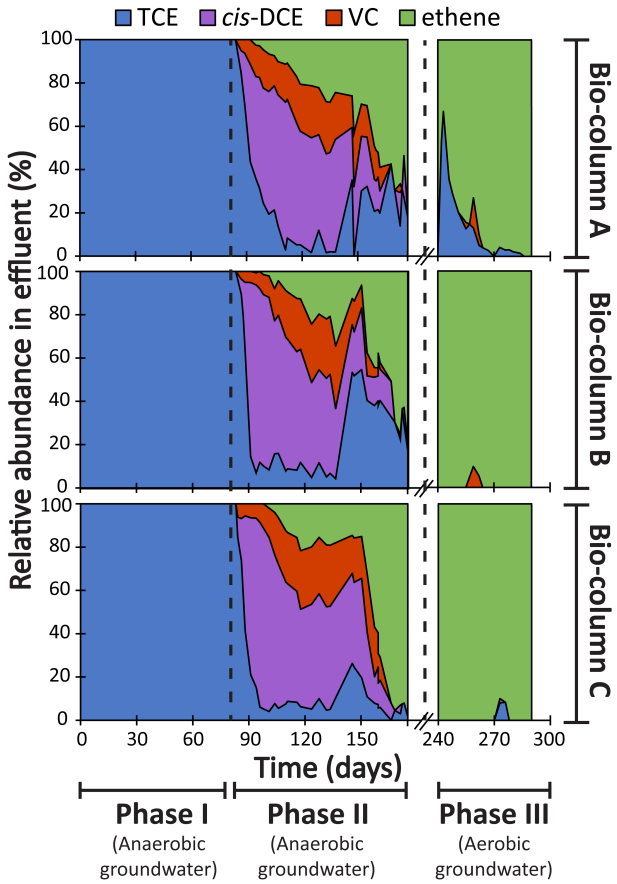

Figure 3.4. Relative abundance of chlorinated ethenes and ethene in the Bio-column effluents during the experimental phases.

Table 3.5. Influent and effluent groundwater pH in Bio-columns receiving Fe^0-reduced groundwater (Phase I and II).

Time (days)	Influent	Bio-column effluent		
		A	B	C
75	7.78	-	-	-
89	-	7.65	7.59	7.82
95	-	8.65	8.22	8.85
102	-	7.78	8.77	8.65
103	7.98	-	-	-
119	-	8.31	8.39	8.75
125	-	9.31	8.64	8.47
138	-	8.70	8.94	8.94
142	8.02	-	-	-
152	-	8.49	-	8.32
161	-	7.43	7.35	7.52
163	-	7.27	8.00	-
172	-	8.16	8.46	7.91
174	8.11	-	-	-
183	-	-	9.10	9.01
188	-	7.95	8.15	8.16

Fe^0 can enhance SO_4^{2-} reduction (Karri et al., 2005; Rangan et al., 2020) and methanogenesis (Kirschling et al., 2010; Liu et al., 2015a; Liu et al., 2015b), especially when Fe^0 and biostimulation/bioaugmentation are applied simultaneously. In a previous study employing columns with 2 g kg^{-1} Fe^0, the concentration of SO_4^{2-} (1 mM) was completely reduced but TCE dechlorination stalled at *cis*-DCE after bioaugmentation with *D. mccartyi* (Ruhl et al., 2008). In our study, SO_4^{2-} reduction in the Bio-columns did not show an obvious negative effect on the extent of reductive dechlorination in the experimental phases. SO_4^{2-} reduction accounted for 22-49% of the electrons supplied *via* biostimulation during Phase II (Figure 3.5). The prevalence of SO_4^{2-} reduction was expected given the particularly high concentration of SO_4^{2-} in the PGAN groundwater (≥

11 mM, Figure 3.3E). CH_4 production accounted for less than 0.1% of electrons supplied (Figure 3.5).

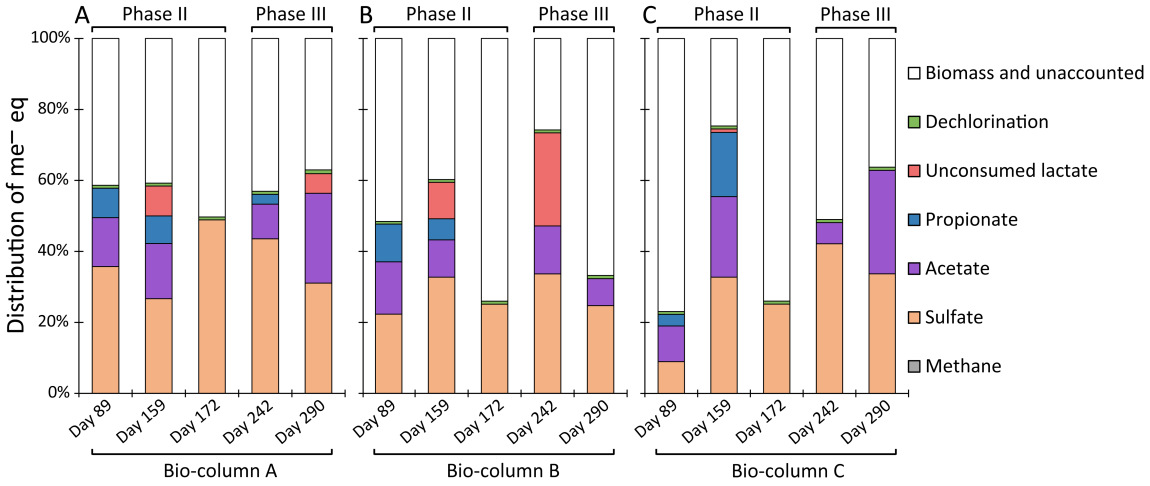

Figure 3.5. Distribution of millielectron equivalents (me^- eq) from lactate and emulsified vegetable oil to measured end products in the Bio-column effluents. Methane production accounted up to 0.02% of me^- eq supplied and thus not visible in the bar graphs.

High throughput DNA sequencing revealed that phylotypes most similar to *Dehalococcoides* accounted for up to 0.54% of the total sequences in the Bio-columns at the end of Phase II (Figure 3.6). Other organohalide-respiring phylotypes, *Geobacteraceae* and *Sulfurospirillum* (Sung et al., 2006; Goris and Diekert, 2016), were at abundances of up to 1.85% and 0.7%, respectively (Figure 3.6). *D. mccartyi* concentrations quantified at the end of Phase II were in the range of $9.3 \pm 2.8 \times 10^2$ to $7.7 \pm 1.4 \times 10^5$ cells g^{-1} soil (Figure 3.6; Day 190). In general, concentrations of *D. mccartyi* were higher in the sampling ports further away from the columns' influent. Results from Phase II showed that the decoupling Fe^0 and biostimulation/bioaugmentation in space and time can achieve microbial reductive dechlorination of chlorinated ethenes to ethene by providing the required anoxic conditions, and potentially mitigating Fe^0-oxidative stress to organohalide-respiring bacteria.

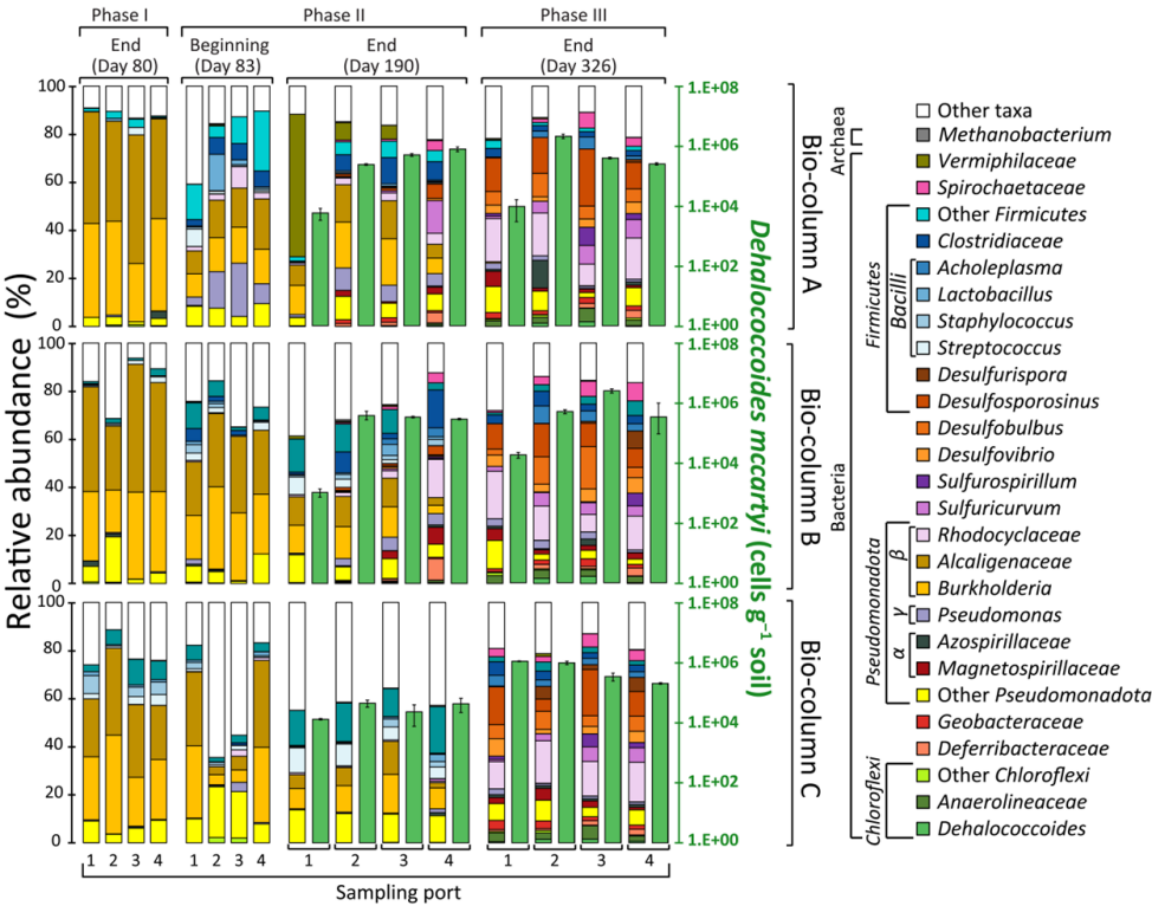

Figure 3.6. Microbial community composition and quantification of *Dehalococcoides mccartyi* (secondary y axis) in Bio-columns A, B, and C during the experimental phases. In Phase I and II, the Bio-columns received Fe^0-reduced anaerobic groundwater. In Phase III, the Bio-columns received aerobic groundwater (no Fe^0). Port 1 was closest to the influent while port 4 was closest to the effluent. *D. mccartyi* cell concentrations were calculated from qPCR data tracking the 16S rRNA gene. The data are averages with standard deviation of triplicate qPCR reactions. *D. mccartyi* 16S rRNA genes were not detected at the end of Phase I (day 80) and beginning of Phase II (day 83, before bioaugmentation) and thus not shown in the figure.

3.3.2 The microbial community established with Fe^0-reduced groundwater can maintain ethene production when challenged with aerobic groundwater

Fe^0 application in the subsurface is restricted by the low mobility and the short reactive lifetime of particles (Wang et al., 2016). For example, a nano-scale Fe^0 stabilized with a carboxymethyl cellulose polymer lost mobility in 13 h and reactivity in 2-3 weeks after *in situ* injection (Bennett et al., 2010; He et al., 2010a; Kocur et al.,

2015). A remedial approach combining Fe^0 and organohalide-respiring bacteria is expected to rely heavily on the microorganisms' metabolic activity to sustain conversion of chlorinated ethenes to ethene in the long-term (Wang et al., 2016; Yang et al., 2018a). In Phase III, we envisioned a scenario where Fe^0 was exhausted. We switched the influent to aerobic groundwater "as collected" from the PGAN site (ORP = 213 ± 62 mV) and thus tested the resilience of the Bio-columns microbial communities enriched during operation with Fe^0-reduced groundwater. We hypothesized that the dissolved O_2 in the groundwater would initially perturb TCE to ethene conversion as O_2 is inhibitory to *D. mccartyi* (Amos et al., 2008b). Contrary to expectations, TCE reductive dechlorination was not perturbed by flowing aerobic groundwater in the Bio-columns (Figure 3.3B-D; Phase III). Throughout Phase III, *cis*-DCE and VC were sparingly detected in the effluents (Figures 3.3B-D; Figure 3.4) with ethene accounting for 33-100% of the effluent composition (Figure 3.4). The concentration of *D. mccartyi* in the Bio-columns at the end Phase III was generally higher by 0.2-5.4 fold (log_2) than in Phase II (Figure 3.6). Further, the relative abundance of phylotypes most similar to *Dehalococcoides* increased up to 2.93% (Figure 3.6; day 326, Phase III). The augmented abundance of *D. mccartyi* in Phase III supports non-limiting conditions of electron donor and carbon source from the more frequent biostimulation regimen (every 13-20 d).

3.3.3 The profiles of the microbial communities in the Bio-columns support multiple mechanisms for O_2 scavenging during Phase III

Dissolved O_2 concentrations ≥ 4 mg L^{-1} irreversibly inhibit reductive dechlorination of VC to ethene by *D. mccartyi*-containing mixed cultures (Amos et al.,

2008b). In Phase III, multiple O_2-scavenging mechanisms likely contributed to allow for complete and sustained reductive dechlorination (Figure 3.3B-D). The first mechanism is consumption of dissolved O_2 and organic substrates by facultative anaerobic microorganisms. Phylotypes of facultative anaerobic bacteria from *Rhodocyclaceae* (Oren, 2014), *Sulfuricurvum* (Kodama and Watanabe, 2004), and *Sulfurospirillum* (Goris and Diekert, 2016) were in high abundance in the Bio-columns during Phase III. Within *Rhodocyclaceae* (7.3-19.7% of the total sequences in Figure 3.6), *Azoarcus*, *Denitratisoma*, and *Thauera* were the most abundant genera (data not shown). *Azoarcus*, *Denitratisoma*, and *Thauera* species have a strict respiratory metabolism and utilize O_2 as an electron acceptor (Oren, 2014). *Sulfuricurvum* (up to 7.8% of the total sequences, day 326, Figure 3.6) can oxidize sulfide, elemental sulfur, and/or H_2 in the presence of dissolved O_2 (Kodama and Watanabe, 2004). The relative abundance of phylotypes most similar to *Sulfurospirillum* in Bio-columns increased from < 1% (end of Phase II) to 5.5-7.6% (end of Phase III) (Figure 3.6). Species of *Sulfurospirillum* have been regarded as obligate anaerobes (Scholz-Muramatsu et al., 1995) but were recently shown to respire O_2 at low concentrations (Goris et al., 2014; Gadkari et al., 2018). Some species of *Sulfurospirillum* are also capable of reductive dechlorination of PCE and TCE to *cis*-DCE under oxic conditions (Goris and Diekert, 2016; Gadkari et al., 2018).

The second potential mechanism for dissolved O_2 removal was Fe^{2+}-mediated reduction. Fe^0 oxidation yields dissolved Fe^{2+} in the aqueous medium (Noubactep, 2013; Li et al., 2021b). Fe^{2+} at an average concentration of 2.8 ± 0.3 mg L^{-1} in the groundwater was introduced into the Bio-columns during Phases I and II (Figure 3.7A). Black

precipitates typical of FeS (Csákberényi-Malasics et al., 2012) or FeO (Kiyama, 1974) were visually obvious along the length of the Bio-columns (Figure 3.7C). Overall, the total Fe concentration in the soil of Bio-columns increased by 24% at the end of the experiment (Figure 3.7B). FeS and/or FeO can scavenge O_2, producing Fe^{3+} oxides (Stumm and Lee, 1961; Davison and Seed, 1983). Dissimilatory iron-reducing bacteria can reduce Fe^{3+} (oxides) and regenerate Fe^{2+}, thus propagating the removal of O_2. The phylotypes of dissimilatory iron-reducing bacteria, *Geobacteraceae*, *Deferribacteraceae*, and *Magnetospirillaceae*, became substantially enriched during Phases II and III (Figure 3.6; days 190 and 326), suggesting the possibility of such Fe^{2+}/Fe^{3+} cycling.

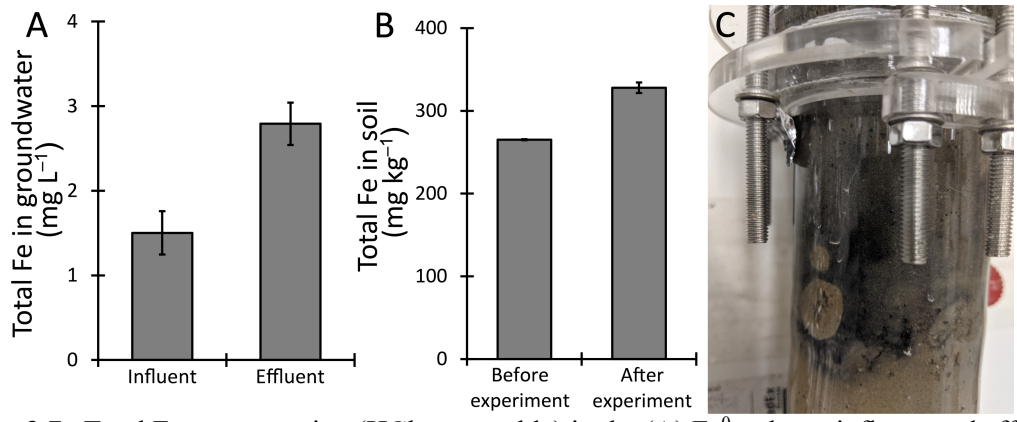

Figure 3.7. Total Fe concentration (HCl-extractable) in the (A) Fe^0-column influent and effluent, and in the Bio-columns before and after the experiment. (C) Photograph of black precipitates formed in the Bio-columns during Phase II.

One of the most striking changes between Phases II and III occurred in the fermenting microbial community. At the end of Phase II, fermenting phylotypes most similar to *Lactobacillus*, *Streptococcus*, and *Staphylococcus* were present at abundances of up to 4.6%, 10.4%, and 3.3%, respectively (Figure 3.6; day 190). None of these phylotypes were detected at the end of Phase III. Instead, *Acholeplasma* (up to 7.2% of total sequences) and *Spirochaetaceae* (up to 7.6% of the total sequences) were enriched

in Phase III (Figure 3.6; day 326). *Acholeplasma* are saprotrophic bacteria with the ability to oxidize complex organic substrates (Abu-Amero et al., 2000) and dead biomass using O_2 (Lazarev et al., 2011; Hanajima et al., 2015). *Spirochaetaceae* are obligate fermenters of complex organic substrates producing lactate, acetate, formate, H_2 and CO_2 (Caro-Quintero et al., 2012; Koelschbach et al., 2017). Members of *Spirochaetaceae* contain genes related to oxidative stress defense from reactive oxygen species and O_2, and are frequently detected with *D. mccartyi* in environments with oxidative stress fluctuations (Caro-Quintero et al., 2012).

3.3.4 Lessons gained from column studies and potential implications for Fe^0-mediated microbial reductive dechlorination in the field

Soil columns are a means to obtain meaningful insights into environmental contaminant fate and transport processes (Magga et al., 2008; Biel-Maeso et al., 2021). The combination of continuous-flow of groundwater and contaminants through a soil matrix, the development of a soil biofilm, and the activity of microorganisms under plug-flow conditions, goes beyond the typical batch microcosms testing. Based on my review of the literature, Table 3.6 is an exhaustive list of column studies where Fe^0 and microbial cultures capable of reductive dechlorination of chlorinated solvents were combined (Gregory et al., 2000; Lorah et al., 2008; Ruhl et al., 2008; Baric et al., 2012; Velimirovic et al., 2014; Patterson et al., 2016; Schiwy et al., 2016; de Guzmán et al., 2018). Table 3.6 highlights that in a scenario of simultaneous addition of Fe^0, organic substrates, and microbial cultures, Fe^0 rarely enhances microbial reductive dechlorination to ethene (Lorah et al., 2008; Patterson et al., 2016). In the few studies where conversion of

contaminants to mainly ethene/ethane was achieved, the benefits of Fe^0 to the microbial processes were neither obvious nor always straight forward (Lorah et al., 2008; Patterson et al., 2016). A more common outcome of column studies with Fe^0 and microbial cultures has been the incomplete reductive dechlorination of the target contaminants (Ruhl et al., 2008; Velimirovic et al., 2014; Patterson et al., 2016; Schiwy et al., 2016).

Fe^0 has been applied to remediate chlorinated ethenes at contaminated sites for about two decades (Xie et al., 2017). Despite its high reducing potency, Fe^0 is short-lived in the subsurface. Concentrations of chlorinated ethenes can rebound post Fe^0 application in just a matter of weeks (Kocur et al., 2015; Czinnerová et al., 2020). The benefit of bioaugmentation with *D. mccartyi*-containing cultures at chlorinated ethene-contaminated sites undergoing *in situ* anaerobic bioremediation is well documented for enhancing the rates and extent of reductive dechlorination (Ritalahti et al., 2005; Schaefer et al., 2010; Lyon and Vogel, 2013). Yet, to date, peer-reviewed publications on Fe^0 and microbial dechlorination have only concerned the biostimulation of native *D. mccartyi* in the groundwater either through the injection of Fe^0 slurries modified with organic polymer coatings (He et al., 2010a; Kocur et al., 2015) or emulsions of Fe^0 and organic substrates (Su et al., 2012; Sheu et al., 2016; Yang et al., 2018a).

The results from this study support a conceptual model where decoupling the application of Fe^0 and biostimulation/bioaugmentation in space and/or time could enhance microbial TCE reductive dechlorination, particularly in aerobic aquifers. Our study indicates that microbial TCE reductive dechlorination to ethene can be sustained by the addition of organic substrates once Fe^0 is exhausted in the subsurface. Decoupling

Fe^0 application and biostimulation/bioaugmentation benefits reductive dechlorination in two major ways: i) induces anoxic conditions and ii) minimizes Fe^0-induced oxidative stress and damage to bioaugmented microbial cells. A bioremediation approach based on H_2 evolved from Fe^0 may also decrease the requirement for an organic substrate (e.g., lactate, emulsified vegetable oil), which is typically provided as a H_2-precursor for the organohalide-respiring bacteria.

Table 3.6. Column studies which employed Fe^0 and biostimulation/bioaugmentation for reduction of chlorinated solvents. Abbreviations: TCE = trichloroethene; PCE = tertrachloroethene; CT = tetrachloromethane (or carbon tetrachloride); 1,1,1-TCA = 1,1,1-trichloroethane; TeCA =1,1,2,2-tetrachloroethane; CF = trichloromethane (or chloroform); 1,1-DCE = 1,1-dichloroethene; 1,1-DCA = 1,1-dichlorothane; 1,2-DCA = 1,2-dichloroethane; *cis*-DCE = *cis*-1,2-dichloroethene; VC = chloroethene (or vinyl chloride); 1,1,2-TCA = 1,1,2-trichloroethane.

Reference	Contaminant	Packing material	Aqueous medium	HRT (d)	Fe^0 material	$[Fe^0]$
Gregory et al. 2000	PCE; CT; 1,1,1-TCA	None	Reduced mineral medium	7	Steel wool (52% Fe^0 by weight)	20 g L^{-1}
Lorah et al. 2008	TeCA; PCE; TCE; CT; CF	Compost/peat and sand	Groundwater	4.1	Fe^0 fillings ($d_{particle}$ = 0.15-2.36 mm)	453 g kg^{-1}
Ruhl et al. 2008	TCE	None[a] or pea gravel[b]	Groundwater	2.9[c]	Iron wool ($d_{particle}$ = 8-60 μm) or ReSponge ($d_{particle}$ = 12-15 mm)	[a]227 g L^{-1} or [b]2 g kg^{-1}
Baric et al. 2012	TeCA	Sand	Reduced mineral medium	0.96 ± 0.13	Granular Fe^0 ($d_{particle}$ = 0.6-4.75 mm)	50 g kg^{-1}
Velimirovic et al. 2014	TCE; *cis*-DCE; 1,1-DCE; 1,1-DCA	Aquifer material mixed with 25% sand	Groundwater	13 ± 5	Micro-Fe^0 ($d_{particle}$ = 25-70 μm)	25 g kg^{-1}
Patterson et al. 2016	1,1,2-TCA	Sand	Groundwater	20.4 and 40.7	Micro-Fe^0 ($d_{particle}$ = 50-150 μm)	100 g kg^{-1}
Schiwy et al. 2016	PCE	Aquifer material mixed with 50% sand	Groundwater	0.92	Nano-Fe^0 ($d_{particle}$ < 0.1 μm)	Not disclosed
de Guzmán et al. 2018	TCE	Mulch/compost	Groundwater	0.19-0.32	Fe^0 shavings ($d_{particle}$ = 150-4700 μm)	29 g kg^{-1}
This study	TCE	Aquifer material	Groundwater	15 ± 2	Micro-Fe^0 ($d_{particle}$ 2-7 μm)	2 g kg^{-1}

Columns with [a]iron wool and [b]ReSponge.

[c]Calculations assuming 100% porosity in the columns with iron wool and 30% porosity in the columns with ReSponge

Reference	Organic substrate and microbial inoculum	Experimental setup	Maximum contaminant removal and conversion to end-products (%); benefits or challenges to microbial reductive dechlorination
Gregory et al. 2000	Acetate/lactate; mixed cultures	Fe^0, organic substrate, and culture added simultaneously	91% PCE removal; ethene/ethane not measured; addition of cultures accelerated Fe^0 corrosion; PCE removal was not enhanced after culture addition
Lorah et al. 2008	Ethanol/Lactate; mixed *D. mccartyi* culture	Fe^0, organic substrate, and culture added simultaneously	100% conversion to ethene/ethane in columns with Fe^0 and without Fe^0
Ruhl et al. 2008	None; mixed culture containing *D. mccartyi*	Culture added after 100 days of operation with Fe^0	80% conversion to *cis*-DCE; ethene/ethane not measured or reported; bioaugmentation did not improve TCE reduction extent
Baric et al. 2012	Polyhydroxybutyrate; none	Fe^0 and organic substrate added simultaneously	100% TeCA removal; ethene/ethane not measured/reported; addition of Fe^0 enhanced fermentation of polyhydroxybutyrate
Velimirovic et al. 2014	Guar gum; none	Fe^0 and organic substrate added simultaneously	100% TCE removal and ~50 % 1,1-DCE removal; no removal of *cis*-DCE and 1,1-DCA; ethene/ethane not measured or reported; addition of Fe^0 did not significantly change the concentration of *D. mccartyi*
Patterson et al. 2016	Not specified organic substrate; mixed cultures containing *D. mccartyi* and *Dehalobacter*	Culture and organic substrate added after 432 days of operation with Fe^0	> 80% conversion to VC (mainly abiotic) at 1.27 ± 0.15 mM TCA; 30-60% conversion to ethene at 0.29 ± 0.08 mM TCA; benefits of Fe^0 to reductive dechlorination were unclear
Schiwy et al. 2016	Not specified organic substrate; none	Fe^0 added on days 82, 110, and 236 during operation	> 95% conversion to *cis*-DCE; Fe^0 enhanced microbial PCE dechlorination to *cis*-DCE
de Guzmán et al. 2018	Lactate; SDC-9 (BAC-9) culture	Fe^0, organic substrate, and culture added simultaneously	Not measured or reported; Fe^0 decreased the concentration of *D. mccartyi* cells in the columns by ~1.3 $\log_2$ (relative to columns without Fe^0)
This study	Lactate and emulsified vegetable oil; SDC-9 (BAC-9) and ZARA-10 cultures	Fe^0 was added in a column upstream of organic substrates and culture; reduced groundwater from Fe^0 column was flown into biostimulated and bioaugmented column	100% conversion to ethene; Fe^0 supported microbial reductive dechlorination

CHAPTER 4

ENRICHMENT OF POTENTIAL Cr (VI)-RESPIRING *Morganella* Sp. ENHANCED RATE AND EXTENT OF Cr (VI) REDUCTION IN MIXED MICROBIAL COMMUNITIES[c]

4.1 Introduction

Chromium-containing compounds are commonly used in a wide range of industrial processes such as electroplating, leather tanning, manufacture of alloys, pigments, and dye production (Zhitkovich, 2011; Karthik et al., 2017). Consequently, more than 170000 tons of chromium per year are discharged globally (Gadd and White, 1993; Lytras et al., 2017). The most stable oxidation states of chromium in the aqueous phase are hexavalent (Cr (VI)) and trivalent (Cr (III)) (Joutey et al., 2015). While the highly water-soluble Cr (VI) (typically as CrO_4^{2-} at neutral pH) is carcinogenic and mutagenic, Cr (III) is readily precipitated as $Cr(OH)_3$ and is at least 1000 times less mutagenic than Cr (VI) (Biedermann and Landolph, 1990; Zhitkovich, 2011; Qian et al., 2016; Lytras et al., 2017). Anthropogenic discharge of chromium surface water and groundwater is mainly in the form of Cr (VI) (Blowes et al., 1997; Ludwig et al., 2007; Lytras et al., 2017). Cr (VI) can also naturally occur in groundwater due to oxidation of Cr (III) bearing minerals, particularly chromite (Robles-Camacho and Armienta, 2000; Oze et al., 2007; Mills et al., 2011). The World Health Organization (WHO) set a maximum allowable limit of 50 $\mu g\ L^{-1}$ for Cr (VI) in groundwater and drinking water (WHO, 2003a; El-Shahawi et al., 2011).

---

[c]This chapter will soon be submitted in an altered format to *Chemosphere* with co-authors Ibrahim, I., Sachs, S., Delgado, A. G., & Krajmalnik-Brown, R.

In the United States, Cr (VI) is present at more than 170 Superfund sites and has been in the top 20 priority pollutants across Superfund sites for two decades (Dhal et al., 2013; US EPA, 2017; ATSDR, 2019).

Certain microorganisms have shown to mediate Cr (VI) reduction to Cr (III), which can be applied for bioremediation of Cr (VI) (Chen and Hao, 1998). *In situ* bioremediation approaches relying on Cr (VI)-reducing microorganisms provide advantages over chemical treatment such as cost-effectiveness, efficiency, specificity, and environmental compatibility in soil and groundwater (He et al., 2009; Xia et al., 2019; Pushkar et al., 2021). Over the last two decades, several laboratory studies have shown the ability of various microbial isolates to tolerate and reduce Cr (VI) to Cr (III). Strains of *Pseudomonas* (Huang et al., 2016; Sathishkumar et al., 2017), *Desulfovibrio* (Lovley and Phillips, 1994), *Shewanella* (Guha et al., 2001), *Acinetobacter* (Ahmad et al., 2013), *Bacillus* (Zhao et al., 2012; Mala et al., 2015), and *Ochrobactrum* (Hora and Shetty, 2015) are able to tolerate and reduce Cr (VI) at rates up to 16 μmol L^{-1} d^{-1}. Some species of *Pseudomonas* and *Acinetobacter* have shown to tolerate and partially reduce Cr (VI) up to 1000 mg L^{-1} (Sathishkumar et al., 2017). An extensive list of Cr (VI)-resistant and/or Cr (VI)-reducing microorganisms was published (Huang et al., 2017). Reducing equivalents produced *via* NADH during fermentation can also be directly transferred to Cr (VI), converting it to Cr (III) within the microbial cells (Bai et al., 2018). However, these processes lead to accumulation of Cr (III) inside the microbial cells (Barak et al., 2006; Ontañon et al., 2015) and to gradual inhibition of microbial Cr (VI) reduction (Bencheikh-Latmani et al., 2007; Han et al., 2016). Thus, metal-

microorganism interactions and extracellular precipitation of Cr (III) have recently become of significant interest (Gutiérrez-Corona et al., 2016; Fernández et al., 2018; Ma et al., 2019).

In the 1990s, (Chen and Hao, 1998) stressed the need for microbial mixed culture studies to achieve successful Cr (VI) bioremediation in the field, yet, knowledge on Cr (VI)-respiring microorganisms as members of mixed microbial communities is limited (Ma et al., 2019). Bioaugmentation with mixed cultures enriched in Cr (VI)-reducing microorganisms may enhance the rate of microbial Cr (VI) reduction (Ibarrolaza et al., 2009; Hassan et al., 2022). However, *in situ* bioremediation of Cr (VI) is usually performed by biostimulation of native Cr (VI)-reducing microbial communities using fermentable organic substrates (Jobby et al., 2018; Nazarova et al., 2020; Song et al., 2021). However, Cr (VI) at concentrations above 2.5 mg L^{-1} can inhibit microbial metabolic pathways, leading to a decrease in overall microbial abundance and diversity (Sandrin and Maier, 2003; Zheng et al., 2019). To date, the effect of bioaugmentation with mixed cultures for enhanced microbial Cr (VI) reduction remains poorly understood, in part for the lack of laboratory and field studies. Assessing the contribution of metabolic Cr (VI)-respiring microorganisms and fermentation-mediated Cr (VI) reduction (direct NADH-mediated reduction) in microbial mixed cultures would help assess the benefits of bioaugmentation for Cr (VI) bioremediation. The major goals of this work were (i) to selectively enrich a Cr (VI)-resistant and Cr (VI)-respiring microbial culture from soil, and (ii) to assess the rate and extent of Cr (VI) reduction by the culture enriched with Cr (VI)-respiring microorganisms relative to fermentation-mediated Cr

(VI)-reduction (in the absence of Cr (VI)-respiring microorganisms). To achieve these goals, we pre-exposed soil microorganisms to a high Cr (VI)-concentration to aid in the selective enrichment of Cr (VI)-resistant/respiring microorganisms. The developed microbial mixed culture exhibited sustained Cr (VI) reduction compared to a subculture in the absence of Cr (VI)-respiring microorganisms.

4.2 Materials and Methods

4.2.1 Enrichment of a Cr (VI)-respiring mixed culture and conditions tested

Soil and groundwater were obtained from a Superfund site in Arizona, USA. The details on soil and groundwater sampling and characteristics were previously described (Rangan et al., 2020; Robles et al., 2021). Equal parts of soil from various depths between 25 and 52 m below the surface were homogenized in the anaerobic glove chamber (Coy laboratory products Inc., Grass Lake, MI) under 3.5% H_2 and 96.5% N_2 atmosphere prior to use.

All experiments were performed triplicate in 160 mL serum bottles sealed with butyl rubber stoppers and aluminum crimps (Table 4.1). "Soil microcosms w/o inoculum" were established with 25 g of soil, 5 mL of groundwater, and 95 mL of reduced anaerobic mineral medium with the composition described previously (Robles et al., 2021). The enrichment process for Cr (VI) respiring microorganisms is illustrated in Figure 4.1. "Enrichment-1" microcosms were established similar to "Soil microcosms w/o inoculum", but amended with 0.1 mL of soil slurry that was pre-exposed to 3.85 mM Cr (VI) (200 mg L^{-1}) for 50 days. For both "Soil microcosms w/o inoculum" and "Enrichment-1" microcosms, 0.1 mM Cr (VI), 500 mg L^{-1} yeast extract, and 0.6 mM

lactate were added initially. On day 10 of incubation, Cr (VI) and lactate were re-added to achieve a concentration of 0.6 mM Cr (VI) and 3 mM lactate. 0.6 mM Cr (VI) was re-added when complete Cr (VI) reduction was observed in the microcosms. Serial transfers were performed by adding 1 mL soil slurry/inoculum to 99 mL fresh anaerobic medium after two doses of 0.6 mM Cr (VI) were reduced. The third transfer yielded a microbial mixed culture free of sediments referred to as "Soil-free culture" (Figure 4.1). The Soil-free culture was initially amended with 0.3 mM Cr (VI) and 8 mM lactate. 0.35 mM Cr (VI) was re-added (twice) when Cr (VI) was completely reduced. "Formate-amended subculture" was established by transferring 4 % (vv^{-1}) of the "Soil-free culture" anaerobic mineral medium, amended with 2.5 mM formate and 0.5 mg L^{-1} yeast extract.

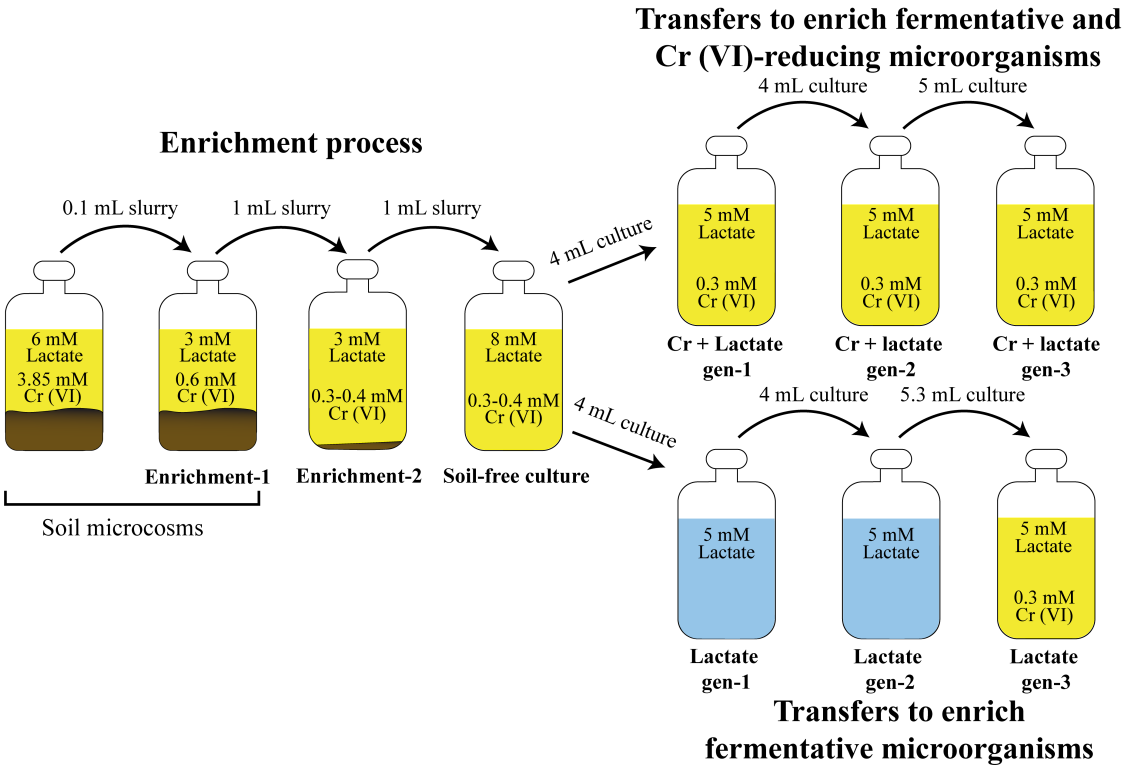

Figure 4.1. Enrichment of a Cr (VI)-reducing mixed culture in this study.

Table 4.1. Conditions established in this study. All microcosms and transfers were established in 160 mL serum bottles with 100 mL liquid volume containing anaerobic mineral medium, in triplicates.

Label	Soil (g)	Groundwater (mL)	Cr (VI) (mM)	SO_4^{2-} (mM)	Yeast extract (g L^{-1})	Lactate (mM)	Formate (mM)	Inocula (mL)
Abiotic control (Lactate)	0	0	0.3	0	0.5	3	0	0
Soil microcosms w/o inoculum	25	5	0.15[a]	1	0.5	0.5[b]	0	0
Enrichment-1	25	5	0.15[a]	1	0.5	0.5[b]	0	0.1[c]
Soil-free culture	0	0	0.3	0	0.5	7.5	0	1
Abiotic control (Formate)	0	0	0.4	0	0.5	0	2.5	0
Formate-amended subculture	0	0	0.4	0	0.5	0	2.5	4
Cr + lactate gen-3	0	0	0.3	0	0.5	5	0	5[d]
Lactate gen-3	0	0	0.3	0	0.5	5	0	5.3[d]

[a]Cr (VI) was re-added to achieve a concentration of 0.6 mM on day 10.
[b]Lactate was re-added to achieve a concentration of 3 mM on day 10.
[c]Soil slurry pre-exposed to 3.85 mM (200 mg L^{-1}) Cr (VI).
[d]Volume of the inoculum was normalized to achieve 15 mg L^{-1} initial protein concentration.

From the soil-free culture, serial transfers were performed with lactate and Cr (VI) to enrich fermentative and Cr (VI)-respiring microorganisms ("Cr + lactate gen-1" and "Cr + lactate gen-2"). 4 % (vv^{-1}) culture was transferred to 96 mL of anaerobic mineral medium with 5 mM lactate and 0.3 mM Cr (VI) as shown in Figure 4.1, after two additions of Cr (VI) was completely reduced in each transfer. A third transfer was performed similarly with 5 mM lactate and 0.3 mM Cr (VI), referred to as "Cr + lactate gen-3" (Figure 4.1). To enrich fermentative microorganisms and remove Cr (VI)-respiring microorganisms from the culture, serial transfers were performed with 5 mM lactate, but without Cr (VI) ("Lactate gen-1" and "Lactate gen-2"). A third transfer was performed with 5 mM lactate and 0.3 mM Cr (VI), referred to as "Lactate gen-3" (Figure 4.1). The "Cr + lactate gen-3" and "Lactate gen-3" were established by transferring 5 mL

and 5.3 mL inoculum, respectively, to achieve 15 mg L^{-1} initial protein concentration in each condition (Table 4.1). All conditions were established in triplicate, incubated in the dark at 30°C, and shaken horizontally on a platform shaker at 125 rpm.

4.2.2 Microbiological analyses

Microbial biomass samples were collected from the beginning and the end of "Enrichment-1", and the end of "Enrichment-2", "Soil-free culture", "Cr + lactate gen-3", and "Lactate gen-3" conditions. 1 mL of soil slurry sample or liquid sample were pelleted in an Eppendorf microcentrifuge 5415R at 13200 rpm for 7 min. Genomic DNA was extracted from the pellets using the MOBIO PowerSoil DNA extraction kit (Carlsbad, CA). DNA amplicon sequencing was performed on the extracted DNA using the Illumina Miseq platform at the Microbiome Facility at the Biodesign Institute (https://cores.research.asu.edu/genomics/capabilities), Arizona State University, as previously described (Joshi et al., 2021). Briefly, the 515F and 806R primers were used to amplify the V4 hyper-variable region of the 16S rRNA genes of Bacteria and Archaea (Caporaso et al., 2012). QIIME 2 (v2022.2) software package was used to process the sequences (Bolyen et al., 2019). The raw sequences were quality filtered by removing phiX, chimeric, and erroneous reads using DADA2 software package (Callahan et al., 2016). Before processing, the reads were truncated at 141 bases with the dada2 denoise-single method. Default settings were used for all other DADA2 parameters (Callahan et al., 2016). The q2-feature-classifier (Bokulich et al., 2018) and SILVA database (v.138) was used to assign taxonomy to amplicon sequence variants (ASVs) (Quast et al., 2012). The study sequences were compared against the National Center for Biotechnology

(NCBI) database using BLAST + consensus taxonomy classifier (Camacho et al., 2009). Dissimilarity between microbial communities in "Cr + lactate gen-3" and "Lactate gen-3" were assessed using beta diversity analyses. Beta diversity calculations were performed using weighted UniFrac distance metrics in QIIME 2 (Lozupone et al., 2006). Principal Coordinate Analyses (PCoA) was performed using Dokdo (v1.15.0-dev) application programming interface with Jupyter notebook (Park et al., 2021). The raw sequences were submitted to the NCBI database and are available under the BioProject accession number PRJNA756407 and BioSample accession numbers SAMN20865384–5410.

4.2.3 Chemical Analyses

1 mL Liquid samples were collected and centrifuged in an Eppendorf microcentrifuge 5415R (Hauppauge, NY) at 13200 rpm for 7 min. The supernatant was filtered through 0.2 μm membrane filters (PVDF membrane, mdi Membrane Technologies, Harrisburg, PA) for downstream chemical analyses. Cr (VI) concentrations were measured using a calorimetry method based on EPA Method 7196A. 0.1 mL of filtered sample was added to a 10 mL test tube followed by addition of 1 mL each of 10% (vv^{-1}) H_2SO_4 (95-98% solution; VWR™, Randor, PA) and 10% (vv^{-1}) H_3PO_4 (85 % solution; Alfa Aesar™, Haverhill, MA). Then, 0.1 mL complexing reagent that contained 5 g L^{-1} 1,5-diphenylcarbazide (ACS reagent, Sigma-Aldrich, St. Louis, MO) in acetone (≥ 99.5%, Chem Impex, Wood Dale, IL) was added to the acidified sample. After mixing and incubating the contents for 5 mins at room temperature (25 °C), the absorbance of the magenta color was measured at 540 nm using a Varian Cary 50 UV-Vis spectrophotometer (Agilent, Santa Clare, CA). Cr (VI) concentrations in

samples were evaluated using a calibration curve generated with the absorbance values of standard Cr (VI) concentrations. The calibration range for Cr (VI) was from 0.5 to 75 mg L^{-1} Cr (VI) and the detection limit was 0.25 mg L^{-1} Cr (VI). Confirmatory analyses for Cr (VI) concentrations below the 0.5 mg L^{-1} was performed using Ion chromatography (IC) and suppressed conductivity detection as described previously (Mohana Rangan et al., 2021).

SO_4^{2-} was analyzed using EPA Method 9056A. A Dionex ICS 3000 IC equipped with a Dionex IonPac AG18 pre-column and a Dionex IonPac AS18 column was used with KOH as eluent. The method used an injection volume of 40 µL and employed an eluent gradient from 15 mM KOH to 40 mM KOH, a flow rate of 1 mL min^{-1} and 30 °C column temperature. The detection limit for SO_4^{2-} was 1.0 µmol L^{-1} (100 µg L^{-1}). Lactate, formate, acetate, and propionate were measured using a high-performance liquid chromatograph (HPLC, Shimadzu LC-20AT) as described previously (Rangan et al., 2020; Miranda et al., 2021; Robles et al., 2021). The detection limits were in the range of 0.02-0.08 mmol L^{-1}. The pH was measured using Orion 2-Star bench top pH meter (Thermo Scientific, Waltham, MA) with an Orion economy series pH electrode, calibrated with 4.01, 7.00 and 10.01 Orion pH standard solutions. A student's *t*-test was used to determine statistically significant difference with 95% confidence interval in chemical data between experimental conditions.

Homogenized liquid samples were collected at the end of "Cr + lactate gen-2" and "Lactate gen-2" conditions. Protein concentration was measured using the Pierce BCA Protein Assay Kit (Thermo Scientific) to determine the volume of inoculum needed to

achieve 15 mg L^{-1} protein concentration in the "Cr + lactate gen-3" and "Lactate gen-3" conditions.

4.2.4 Scanning Electron Microscopy (SEM), Energy-dispersive X-ray Spectroscopy (EDX) and X-ray photoelectron spectroscopy (XPS)

Liquid samples were removed from the "Soil-free culture" after reduction of three concentration spikes of ~0.4 mM Cr (VI) for SEM and XPS analyses. Samples for SEM analyses were prepared based on the methods previously published (Ziv-El et al., 2012; Delgado et al., 2017). Specifically, samples were fixed in a suspension overnight at 4 °C with Dulbecco's phosphate buffered saline (DBPS) containing 2.5% glutaraldehyde. This solution was centrifuged with an Eppendorf microcentrifuge 5415R at 13200 rpm for 5 mins. The supernatant was removed, and the samples were resuspended in 50 µL DBPS. The resuspended samples were applied to poly-L-lysine coated coverslips and rested for 10 mins. The coverslips were placed in DBPS containing 1% OsO_4 (ReagentPlus, Sigma-Aldrich) for 1 hr, followed by washing with deionized water (≥18.2 MΩ-cm). Samples were dehydrated in a graded ethanol series (20%, 40%, 60%, 75%, 90% and 100 %) and critical point dried using CPD-020 (Balzers-Union, Liechtensein) using CO_2 as the transition fluid. After mounting on aluminum stubs and sputter-coating with gold-palladium using Technics Hummer II unit (Anatech, Hayward, CA) micrographs were captured using a Philips/FEI XL-30 Environmental Scanning Electron Microscope (Thermo Fisher Scientific, Waltham, MA), and Energy-dispersive X-ray Spectroscopy was performed using a with a Schottky field emission gun.

All X-ray Photoelectron Spectra were collected and processed at the Laboratory for Electron Spectroscopy and Surface Analysis (LESSA) in the Department of Chemistry and Biochemistry at the University of Arizona using a Kratos Axis 165 Ultra DLD Hybrid Ultrahigh Vacuum Photoelectron Spectrometer. Samples (30 mL) were removed from the reactors and centrifuged with an Eppendorf microcentrifuge 5415R at 13200 rpm for 15 mins. The supernatant was removed and the precipitates were dried in an oven at 90°C for 75 min under vacuum.

4.3 Results and Discussion

4.3.1 Soil inoculum pre-exposed to high Cr (VI) concentration supported selective enrichment of Cr (VI)-resistant and potential Cr (VI)-respiring microorganisms.

To develop a microbial mixed culture enriched with Cr (VI) resistant and Cr (VI) respiring microorganisms, we established microcosms and performed serial transfers as shown in Figure 4.1. In the "Soil microcosms w/o inoculum", the rate of decrease in aqueous Cr (VI) concentration was similar to the microcosms without soil/microbial inoculum denoted as "Abiotic control (Lactate)" (Figure 4.2A & 4.2C; $p > 0.05$), indicating that Cr (VI) reduction was not due to soil microorganisms or soil minerals. The observed Cr (VI) reduction in these microcosms can be attributed to the reducing agents added to the anaerobic medium: 0.2 mM Na_2S and 0.4 mM L-cysteine. Decrease in aqueous Cr (VI) concentration was negligible in deionized water without any reducing agents (Figure 4.3).

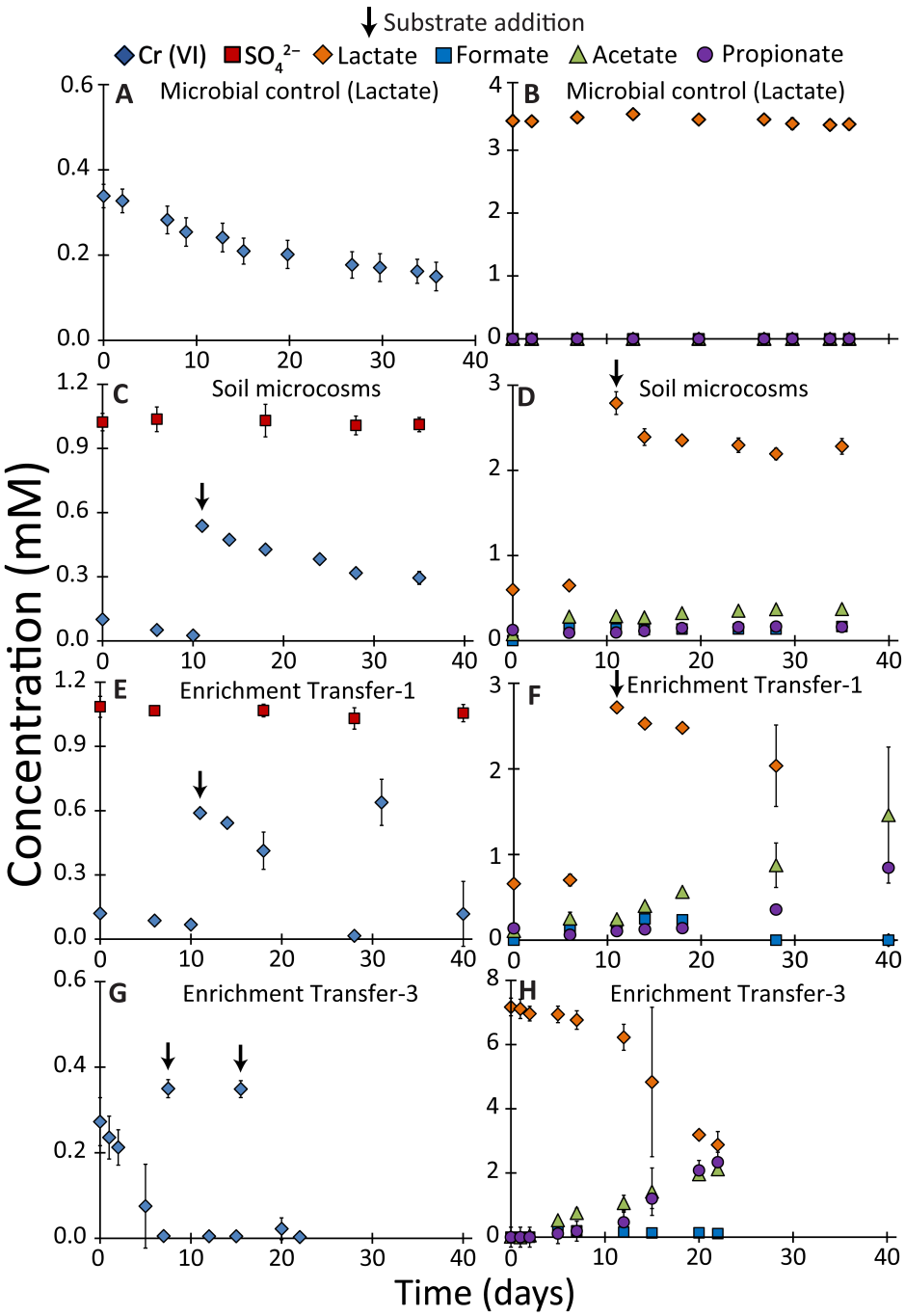

Figure 4.2. Time course concentrations of Cr (VI) and SO_4^{2-} (left panels) and organic acids (right panels) in lactate-amended sterile medium "Microbial control (Lactate)", "Soil microcosms", soil amended with pre-exposed inoculum "Enrichment Transfer-1" and sediment free culture "Enrichment transfer-3". The data are averages of triplicate microcosms and the error bars indicate the standard deviation of the mean.

In contrast, when a 0.1 mL soil slurry that was pre-exposed to a high Cr (VI) concentration (3.85 ± 0.1 mM) was added, 0.6 ± 0.00 mM Cr (VI) was completely removed from the solution in less than 28 days (Figure 4.2E; Enrichment-1). Higher anaerobic microbial activity in the "Enrichment-1" compared to "Soil microcosms w/o inoculum" was evident from higher rates of lactate fermentation to formate, acetate and propionate in the "Enrichment-1" microcosms (Figures 4.2D & 4.2F). Overall, these data show that the addition of an inoculum pre-exposed to high Cr (VI) concentration enhanced the microbial activity, and indicate that microbial Cr (VI) reduction and/or microbial-mediated chemical reduction were possible mechanisms of Cr (VI) removal from solution in the "Enrichment-1".

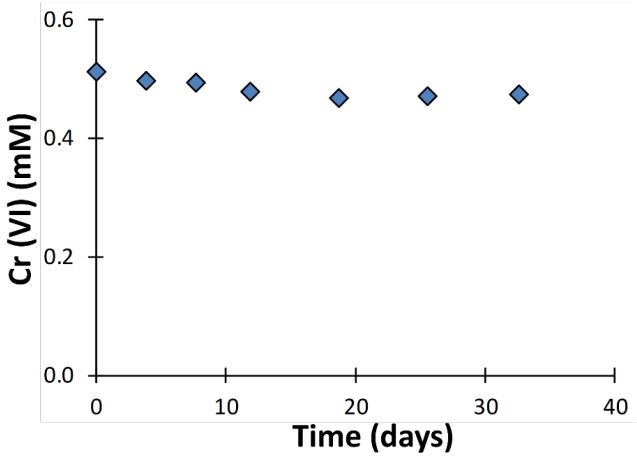

Figure 4.3. Cr (VI) concentrations in controls with sterile deionized water without reducing agents.

The "Soil microcosms w/o inoculum" and "Enrichment-1" microcosms received 5 mL groundwater that contained 11 ± 0.5 mM SO_4^{2-} (Rangan et al., 2020). Additional SO_4^{2-} was supplied to achieve a final concentration of 1.1 ± 0.1 mM in the microcosms. As shown in Figures 4.2C & 4.2E, SO_4^{2-} reduction was absent in both microcosm

conditions during the incubation time. Sulfate-reducing bacteria such as *Desulfovibrio* spp. co-metabolically reduce Cr (VI) due to structural similarity between SO_4^{2-} and CrO_4^{2-} (Cr (VI) anion at pH > 6.5) (Michel et al., 2001; Heidelberg et al., 2004; Franco et al., 2018). Microbial sulfidogenesis-induced Cr (VI) reduction is also possible (Chang and Kim, 2007; Qian et al., 2016). However, absence of SO_4^{2-} reduction in our microcosms eliminates the possibility of co-metabolic Cr (VI) reduction by sulfate-reducing bacteria and/or sulfidogenesis-induced Cr (VI) reduction. The observed Cr (VI) reduction in the "Enrichment-1" is likely an enzyme-mediated microbial process by Cr (VI)-reducing microorganisms.

To address if the observed Cr (VI) reduction was associated to microbial growth (metabolic respiration), and to develop a soil-free culture enriched with Cr (VI)-respiring microorganisms, serial transfers were performed from "Enrichment-1" (Figure 4.1). "Soil-free culture" was obtained after two serial transfers of 1 mL slurry from "Enrichment-1" to fresh anaerobic mineral medium (Figure 4.1). Figure 4.2G shows Cr (VI) reduction in the "Soil-free culture". 0.27 ± 0.06 mM Cr (VI) was completely reduced within 7 days and the two subsequent Cr (VI) additions of 0.3 mM Cr (VI), were each completely reduced within 5 days. The rate of Cr (VI) reduction increased between the serial transfers that involved dilution of the microbial cells indicating enrichment and growth of metabolic Cr (VI)-respiring microorganisms.

Fermentation of lactate produced formate, acetate, and propionate in "Enrichment-1" and "Soil-free culture". While acetate and propionate accumulated, formate was produced and consumed during Cr (VI) reduction in "Enrichment-1" and

"Soil-free culture" (Figures 4.2F & 4.2H). This suggests that formate was used as the electron donor for the microbiological Cr (VI) reduction observed. To study the effect of direct addition of formate on microbiological Cr (VI) reduction by the culture, we established "Formate-amended subculture" using inoculum from the "Soil-free culture" (Table 4.1). In the presence of formate, Cr (VI) reduction was slower, where 0.4 mM Cr (VI) was not completely reduced until 32 days (Figure 4.4C).

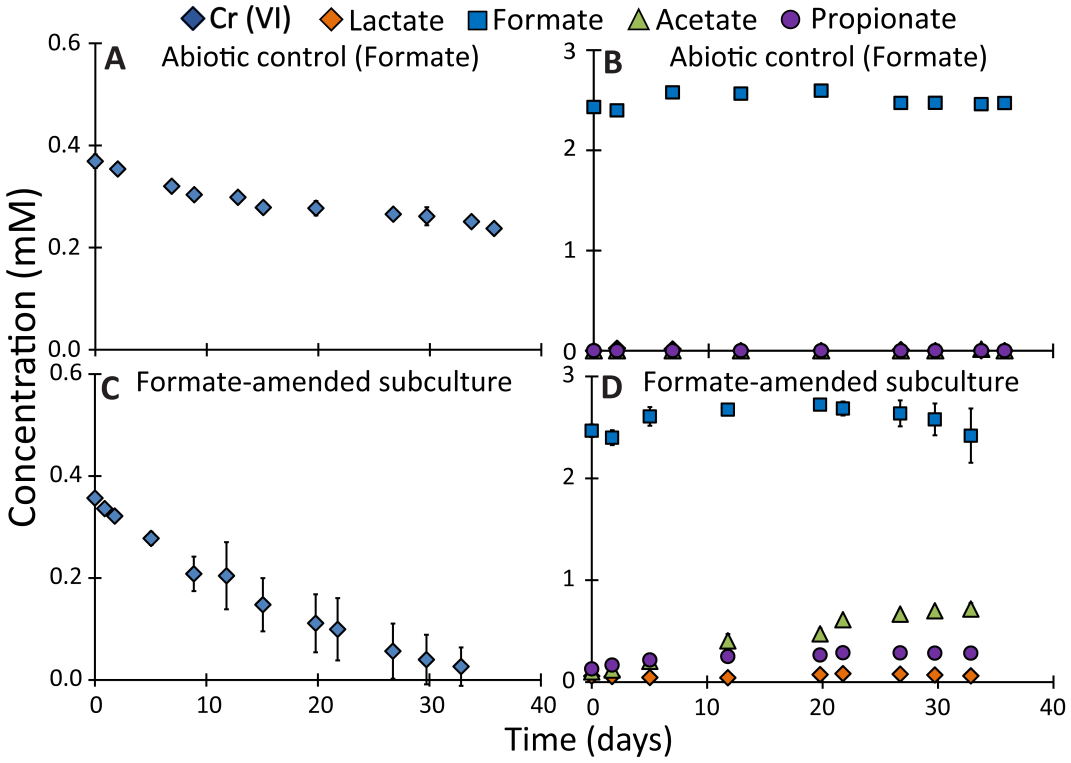

Figure 4.4. Time course concentrations of Cr (VI) (left panels) and organic acids (right panels) in (A) and (B) formate-amended sterile medium "Abiotic control (Formate), and (C) and (D) in "Formate-amended subculture". Data are averages of triplicate microcosms and error bars indicate standard deviation of the mean.

In the "Abiotic control (Formate)", no change in formate concentration was observed (Figure 4.4B), indicating absence of direct Cr (VI) reduction by formate. (Ancona et al., 2020) showed that lactate played a key role in enhancing microbiological Cr (VI) reduction in laboratory-scale microcosms. In contrast to other microbial metal-

redox reactions, microbiological Cr (VI) reduction using sludge microorganisms and mixed culture was shown to be faster in the presence a complex carbon substrate compared to non-fermentable substrates, H_2 and acetate (Liu et al., 2002; Tekerlekopoulou et al., 2010). Fermentation of organic substrates generates coenzymes and cofactors such as NADH and NAD(P)H (Garrigues et al., 1997; Michel et al., 2015), which are essential for enzyme-mediated microbial Cr (VI) reduction (Bae et al., 2005; Elangovan et al., 2006). These coenzymes and cofactors can also directly reduce Cr (VI) (Bai et al., 2018). Limitation of such coenzymes and cofactors is likely the reason for the observed low Cr (VI) reduction rate in the "Formate-amended subculture".

4.3.2. Microbial mixed culture grown with Cr (VI) and lactate showed sustained Cr (VI) reduction compared to a subculture grown with lactate only

To evaluate the effect of enriched potential Cr (VI) respiring microorganisms grown with Cr (VI) and lactate (Cr + lactate gen-3), and fermentative microorganisms grown with lactate only (Lactate gen-3) on the rate and extent of Cr (VI) reduction, we performed serial transfers from "Soil-free culture" (Figure 4.1). We hypothesized that the "Cr + lactate gen-3" containing enriched metabolic Cr (VI)-respiring microorganisms would exhibit enhanced rate and extent of Cr (VI) reduction, while the "Lactate gen-3" enriched with fermentative microorganisms would be inhibited from Cr (VI) toxicity. Contrary to the expectations, initial Cr (VI) reduction was faster in "Lactate gen-3" than in "Cr + lactate gen-3" (Figure 4.5C & 4.5E), with Cr (VI) reduction rates of 0.32 mmol L^{-1} d^{-1} and 0.11 mmol L^{-1} d^{-1}, respectively (Figure 4.6). However, Cr (VI) reduction rate declined in "Lactate gen-3" after the second and third addition of Cr (VI), to 0.23 mmol

L^{-1} d^{-1} and 0.1 mmol L^{-1} d^{-1}, respectively (Figure 4.6). In "Cr + lactate gen-3", the Cr (VI) reduction rate increased with the subsequent Cr (VI) additions to 0.4 mmol L^{-1} d^{-1} and 0.52 mmol L^{-1} d^{-1} after the second and third addition, respectively (Figure 4.6).

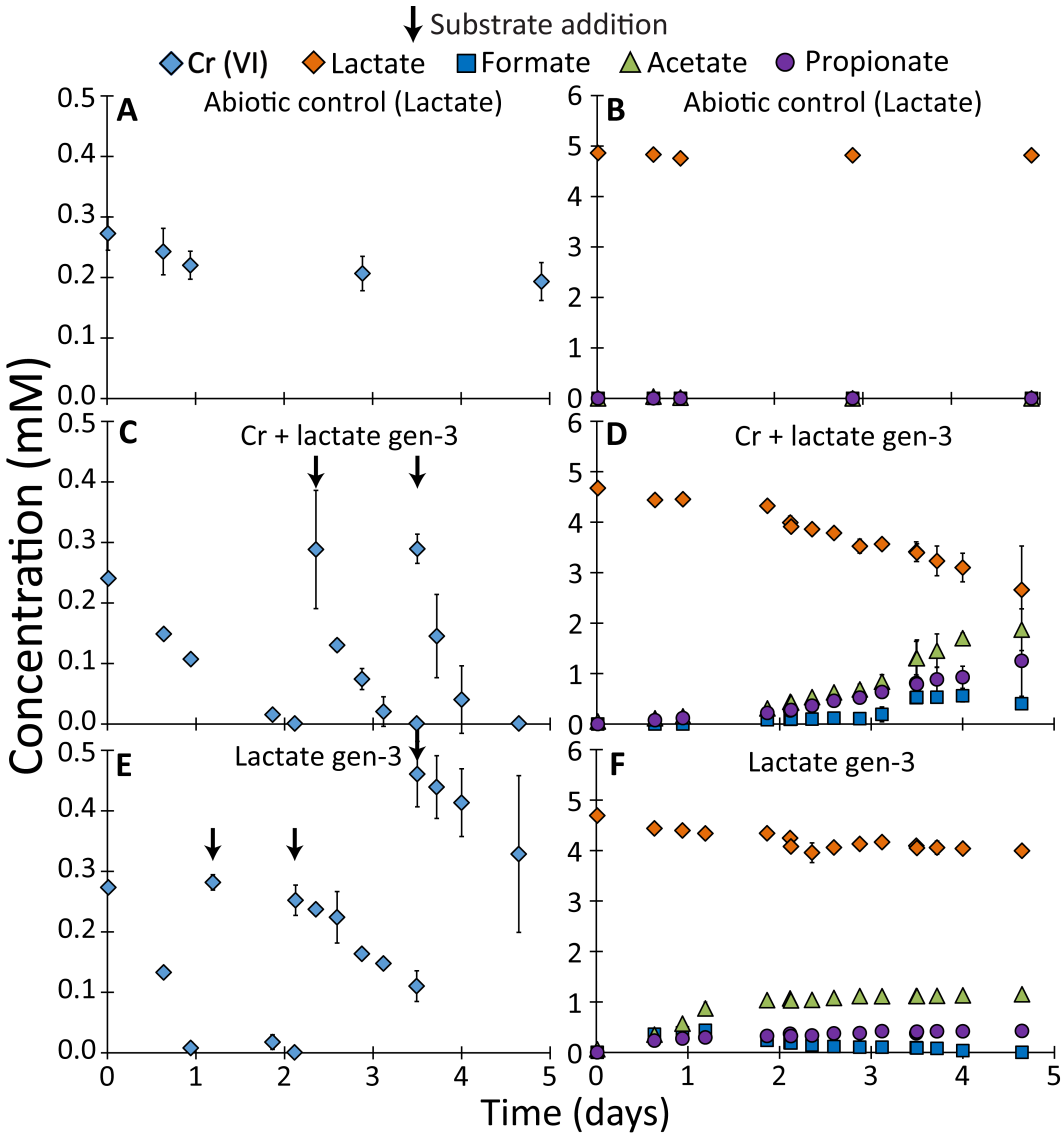

Figure 4.5. Time course concentrations of Cr (VI) (left panels) and organic acids (right panels) in lactate-amended sterile medium "Abiotic control (Lactate)", culture grown with Cr (VI) and lactate "Cr + lactate gen-3", and culture grown with lactate only "Lactate gen-3". The data are averages of triplicate microcosms and error bars indicate standard deviation of the mean.

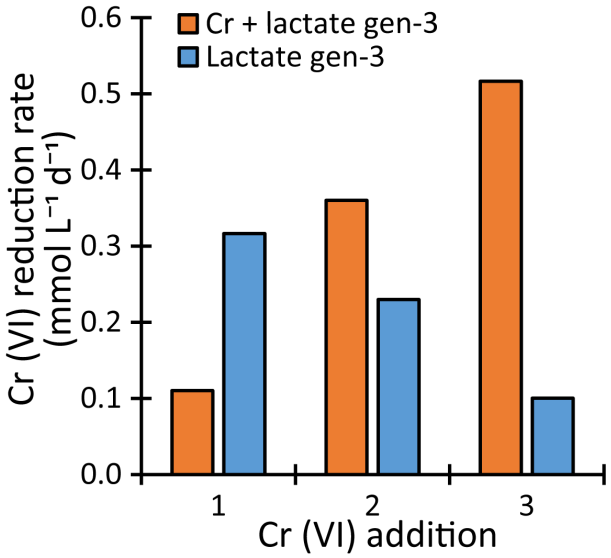

Figure 4.6. Average Cr (VI) reduction rate after each addition of Cr (VI) in "Cr + lactate gen-3" and "Lactate gen-3".

Previous studies with microbial mixed cultures have reported much slower Cr (VI) reduction rates, in the range of 4-16 µmol L^{-1} h^{-1} (Tekerlekopoulou et al., 2010; Ma et al., 2019). The higher Cr (VI) reduction rate by our microbial mixed culture can be attributed to enrichment of possible Cr (VI)-respiring microorganisms present in our culture.

Corresponding to the Cr (VI) reduction rates in our experiments, lactate fermentation to formate, acetate and propionate was more pronounced in "Lactate gen-3" during the first two days compared to "Cr + lactate gen-3" (Figures 4.5D and 4.5F). From day three onwards, lactate fermentation stalled in "Lactate gen-3", indicating inhibition of microbial activity, likely due to toxicity from Cr (VI) or reduced Cr (III) within the microbial cells. The rate of Cr (VI) reduction by both cultures in the absence of lactate was similar to the "Abiotic control (Lactate) ($p > 0.05$; Figures 4.5A, 4.7A & 4.7B), showing that biosorption of Cr (VI) on the microbial cells was negligible. Our

data showed high Cr (VI) reduction rates initially by the lactate grown culture, but the fermentative microorganisms were gradually inhibited, resulting in stalling of Cr (VI) reduction. However, the enriched culture with possible metabolic Cr (VI) respiring microorganisms in the "Cr + lactate gen-3" showed sustained Cr (VI) reduction without inhibition of microbial activity. Overall, these data highlight the potential benefits of bioaugmentation with mixed microbial cultures enriched with microorganism that can stand higher toxic concentration of Cr (VI) during their growth, and that are possible Cr (VI)-respiring microorganisms.

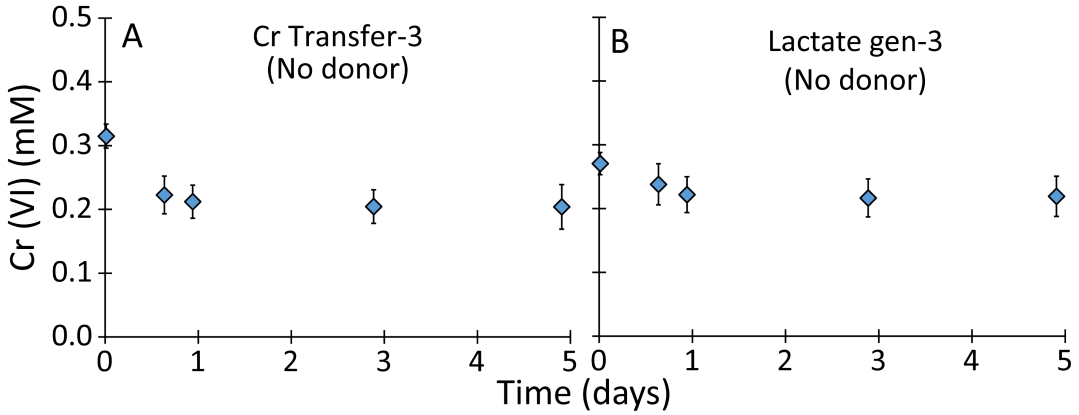

Figure 4.7. Time course Cr (VI) concentrations in the (A) Cr + lactate gen-3 and (B) Lactate gen-3, without electron donor. Data are averages of triplicate microcosms and error bars indicate standard deviation of the mean.

4.3.3 Morganella and Pleomorphomonas were the enriched in the developed Cr (VI)-reducing microbial mixed culture

We performed 16S rRNA gene amplicon sequencing to study the composition of microbial communities during the enrichment process and identified enriched possible Cr (VI)-respiring microorganisms. In the "Enrichment-1" microcosms, phylotypes most similar to previously reported Cr (VI)-reducing bacteria such as *Morganella* (Ergul-Ulger et al., 2014; Princy et al., 2020), *Burkholderia* (Wani et al., 2007), and *Corynebacterium*

(Viti et al., 2003) were < 0.9% at the beginning. At the end of "Enrichment-1", Phylotypes most similar to *Morganella* accounted to 1.5%, *Burkholderia* to 5.9% and *Corynebacterium* to 5.2% of the sequences obtained (Figure 4.8). In the soil-free culture, the phylotypes most similar to potentially Cr (VI)-reducing microorganisms enriched, with *Morganella* (15.5%) and *Corynebacterium* (8.3%), and *Burkholderia* (5.8%) (Figure 4.8; Soil-free culture).

After two subsequent transfers with Cr (VI) and lactate (Figure 4.1), phylotypes most similar to *Morganella* accounted to 66.3% and *Pleomorphomonas* accounted to 25.4% of the microbial communities, dominating the microbial communities (Figure 4.8; Cr + lactate gen-3). Phylotypes most similar to other known Cr (VI)-reducing bacteria such as *Burkholderia* and *Corynebacterium* were present at < 0.1%. *Morganella* has been well established as a Cr (VI)-reducing bacterium (Ergul-Ulger et al., 2014; Huang et al., 2019; Princy et al., 2020), but *Pleomorphomonas* sp. have not been recognized as such. In a recent soil column study using viscous carbon and sulfate-releasing colloidal substrates for Cr (VI) bioremediation, *Pleomorphomonas* was among the phylotypes enriched, but their role in Cr (VI)-reduction was not discussed (Lin et al., 2022). Generally, *Pleomorphomonas* are nitrogen-fixing bacteria with some species capable of metabolizing carbon monoxide (Esquivel-Elizondo et al., 2018). The complete genome of *Pleomorphomonas* has not been sequenced yet, and the role of *Pleomorphomonas* in our enriched Cr (VI)-respiring mixed culture remains unclear. As expected, the microbial community structure of "Lactate gen-3" was distinct from the "Cr + lactate gen-3" (Figure 4.9). In the "Lactate gen-3", phylotypes most similar to *Limnohabitans* were

dominant, constituting to 41% of the sequences. Neither Cr (VI)-reducing bacteria from *Morganella*, *Burkholderia* and *Corynebacterium*, nor *Pleomorphomonas* were detected (Figure 4.8). Absence of sequences most similar to *Morganella* in the "Lactate gen-3" culture and high relative abundance of sequences most similar to *Morganella* in the "Cr + lactate gen-3" suggests that *Morganella* sp. require Cr (VI) for growth, and are potential Cr (VI)-respiring bacteria.

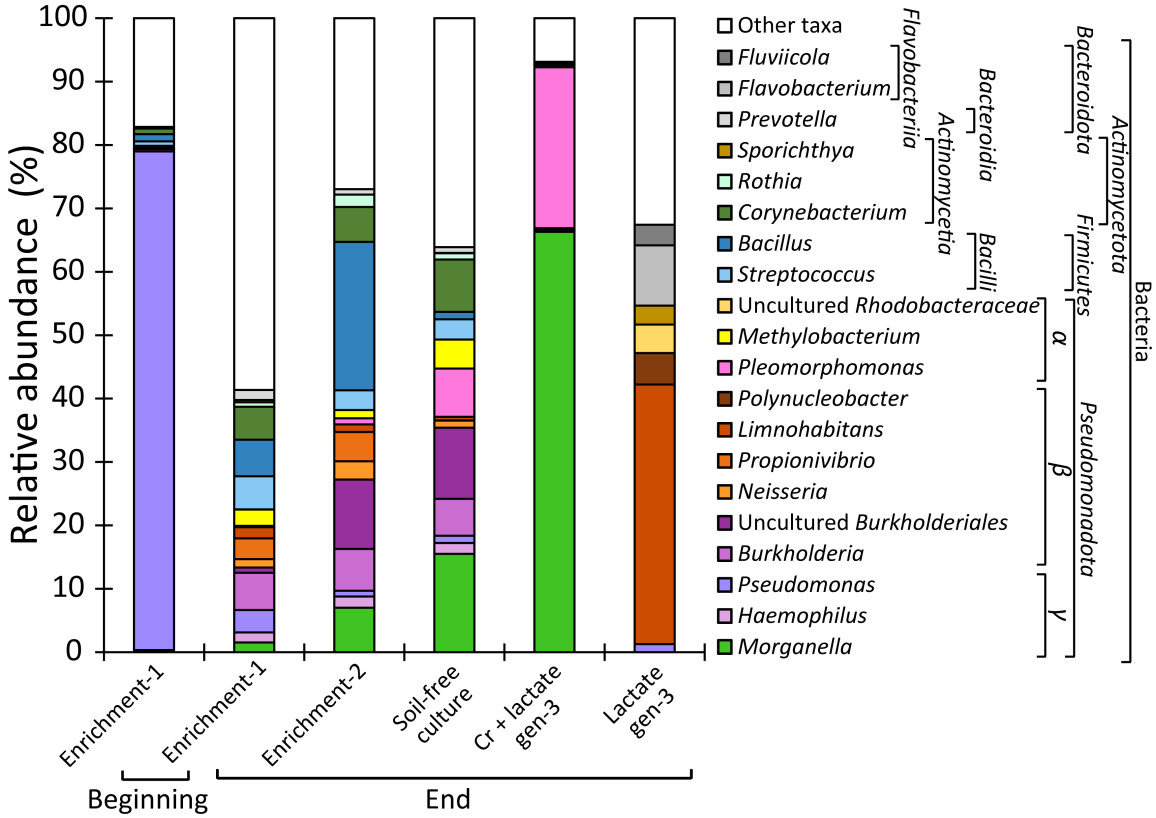

Figure 4.8. Relative abundance of microbial phylotypes (genus level) at the beginning of enrichment "Enrichment-1" and at the end other conditions. Data are averages of sequences from triplicate samples.

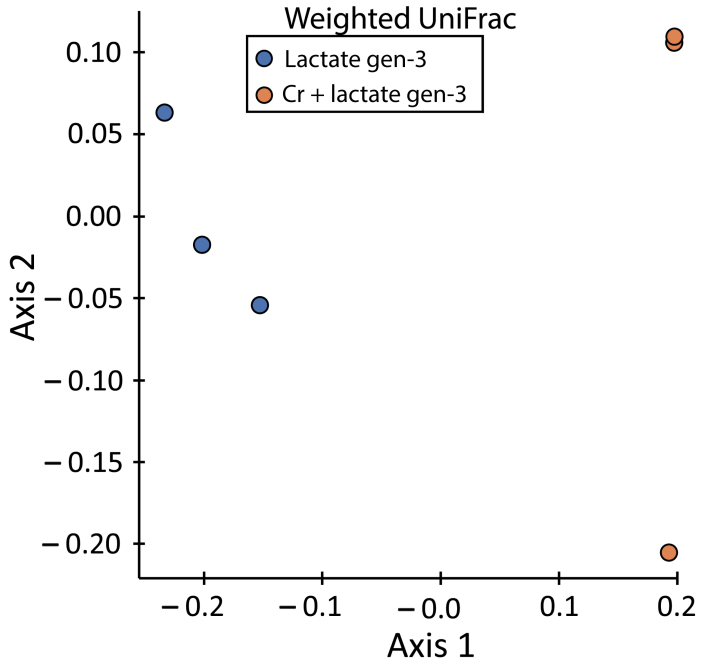

Figure 4.9. PCoA analyses of variation based on weighted UniFrac distance metrics between microbial communities present in culture grown with lactate only (Lactate gen-3) and culture grown with lactate and Cr (VI) (Cr + lactate gen-3).

4.3.4 Microbiological Cr (VI) reduction led to extracellular precipitation of $Cr(OH)_3$ and Cr_2O_3

Cr (VI) reduction by the enriched culture yielded a pale green-colored precipitate in the bioreactors (Figure 4.10). To study the oxidation state and the compound state of Cr in the precipitate, we performed X-ray photoelectron spectroscopy (XPS) and scanning electron microscopy-energy dispersive X-ray spectrometry (SEM-EDS) of the precipitates obtained. Figure 4.11 shows high-resolution Cr 2p XPS spectra of precipitates obtained from Cr (VI) reduction by the enriched Cr (VI)-respiring culture, fitted with Cr 2p3/2 peaks. The binding energy of Cr (III) $2p_{3/2}$ peaks of Cr_2O_3 and $Cr(OH)_3$ compounds have been consistently reported to be between 576 eV and 578.5 eV (Desimoni et al., 1988; Biesinger et al., 2011; Han et al., 2016; Bai et al., 2018; Shi et al.,

2019; Yi et al., 2020). Therefore, peaks at binding energies 577.8 eV and 576.4 eV in our precipitates indicate presence of Cr (III) compounds, most likely Cr_2O_3 and/or $Cr(OH)_3$ (Figures 4.11A & 4.11B). A sharp peak at ~579 eV, characteristic of Cr (VI) was absent indicating absence of Cr (VI) in the precipitates (Aronniemi et al., 2005). Overall, the XPS data revealed the presence of Cr (III)-compounds (as $Cr(OH)_3$ and/or Cr_2O_3) in the precipitate.

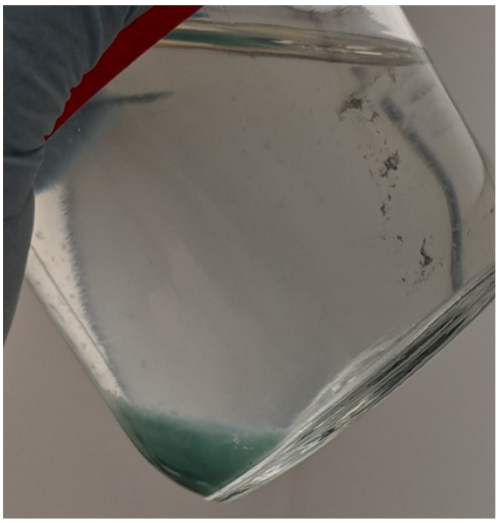

Figure 4.10. Photographic image of precipitate obtained from Cr (VI) reduction by sediment-free Cr (VI)-reducing mixed culture.

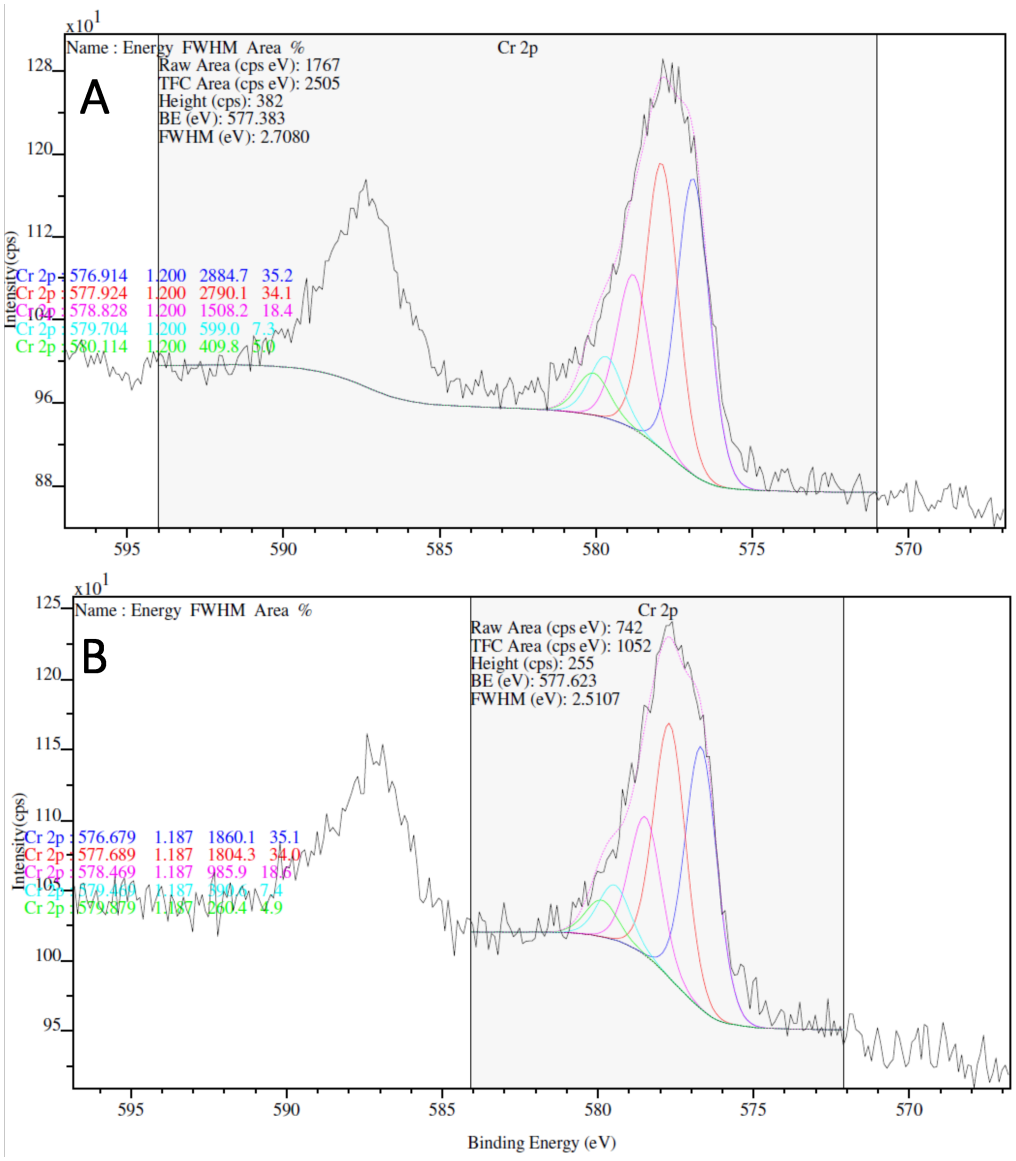

Figure 4.11. High-resolution Cr 2p XPS spectrum of the precipitate obtained from microbial Cr (VI) reduction by the developed microbial mixed culture, fitted with Cr 2p3/2 peaks. (A) and (B) are data from duplicate samples.

To evaluate the fate of Cr (III) precipitate after Cr (VI) reduction by the mixed culture, we performed SEM-EDS analysis of the precipitates obtained. The SEM image in Figure 4.12A reveal that the Cr (III)-compounds were precipitated extracellularly around the microbial cells and the microbial cells were morphologically intact. The precipitation of Cr inside the cells interferes with the phosphate backbone of DNA,

peptides and amino acids, causing dysfunction and death of bacteria (Zhitkovich et al., 1996; Han et al., 2016). For example, *Shewanella* sp. strain MR-4 showed fast rate Cr (VI) reduction initially with 0.1–0.2 mM Cr (VI), but the cells were gradually inhibited as Cr (III) was incorporated into the cells (Bencheikh-Latmani et al., 2007; Han et al., 2016). Therefore, extracellular precipitation of Cr is beneficial for enhanced and sustained Cr (VI) bioremediation (Han et al., 2016). In our study, reduced Cr (III) compounds mostly precipitated outside the microbial cells in the mixed culture enriched with potential Cr (VI)-respiring microorganisms.

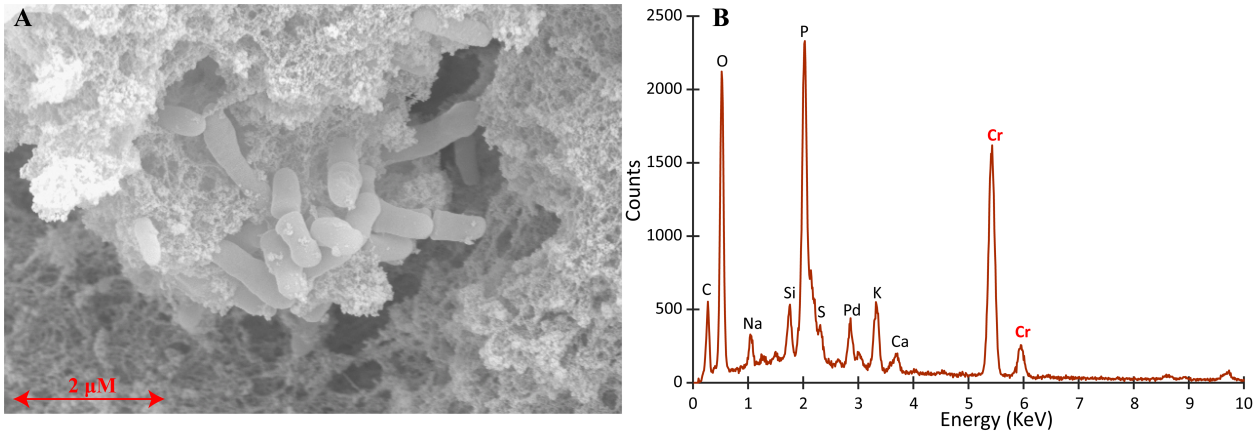

Figure 4.12. (A) SEM image and (B) EDS spectrum showing extracellular precipitation of chromium in the soil-free culture.

4.4. Conclusion

In this study, we developed a microbial mixed culture by selectively enriching Cr (VI)-resistant/respiring microorganisms from soil. The enrichment culture grew and sustained Cr (VI) reduction with Cr (VI) as the sole electron acceptor. The microbial mixed culture enriched in Cr (VI)-respiring bacteria showed sustained Cr (VI) reduction, while Cr (VI) reduction by a subculture grown with lactate only was inhibited after reduction of ~0.6 mM Cr (VI). These data highlight potential benefits of metabolic Cr

(VI)-respiring microorganisms on microbial Cr (VI) reduction. *Morganella* was the dominant and constituted to ~66% of the microbial communities in the mixed culture, indicating that *Morganella* are potentially Cr (VI)-respiring bacteria in our culture. The role of *Pleomorphomonas* in microbial Cr (VI) reduction requires further investigation. The enriched potential Cr (VI)-respiring mixed culture precipitated Cr (III) compounds (Cr_2O_3 and/or $Cr(OH)_3$) extracellularly. The results from this study show how potential Cr (VI)-respiring microorganisms can work in tandem with fermenters to provide long term benefits and imply that bioaugmentation with microbial mixed cultures enriched with these potential Cr (VI)-respiring bacteria can be beneficial for sustained reduction of Cr (VI) in contaminated aquifers. Further studies using Cr (VI)-respiring microorganisms as members of mixed microbial communities in the presence of aquifer materials and other co-occurring electron acceptors can provide useful insights into the benefits of bioaugmentation for Cr (VI) bioremediation in the field.

CHAPTER 5

AN ION CHROMATOGRAPHY METHOD FOR SIMULTANEOUS QUANTIFICATION OF CHROMATE, ARSENATE, SELENATE, PERCHLORATE, AND OTHER INORGANIC ANIONS IN ENVIRONMENTAL MEDIA[d]

5.1 Abstract

Chromium (VI) is a toxic, mutagenic, and carcinogenic water pollutant. The standard ion chromatography (IC) method for quantification of Cr (VI) in water samples is EPA Method 218.7, which requires post column derivatization with 1,5-diphenylcarbazide and UV-Vis spectroscopy detection. Method 218.7 is Cr (VI)-specific; thus, it does not allow detection of co-occurring natural and anthropogenic anions in environmental media. In this study, we developed an isocratic IC method with suppressed conductivity detection, a Metrohm Metrosep A Supp 7 column, and sodium carbonate/acetonitrile as mobile phase for simultaneous quantification of Cr (VI), ClO_4^-, As (V) as arsenate, Se (VI) as selenate, and the common anions F^-, Cl^-, NO_2^-, NO_3^-, and SO_4^{2-}. The determination coefficient for every analyte was > 0.99 and the method showed good accuracy in quantification. Cr (VI), As (V), Se (VI) and ClO_4^- limit of detection (LOD) and limit of quantification (LOQ) were 0.1–0.6 μg L^{-1} and 0.5–2.1 μg L^{-1}, respectively. Recovery of Cr (VI) in various aqueous samples (tap water, surface water, groundwater and wastewater) was between 97.2% and 102.8%.

---

[e] This chapter was published in an altered format as Mohana Rangan, S., Krajmalnik-Brown, R., and Delgado, A.G. (2020) "An Ion Chromatography Method for Simultaneous Quantification of Chromate, Arsenate, Selenate, Perchlorate, and Other Inorganic Anions in Environmental Media." *Environmental Engineering Science, 38*(7), 626-634.

Overall, most analytes showed acceptable recovery (80–120%) in the environmental samples tested. The IC method was applied to track Cr (VI) and other anion concentrations in laboratory batch microcosms experiments with soil, surface water, and anaerobic medium. The IC method developed in this study should prove useful to environmental practitioners, academic and research organizations, and industries for monitoring low concentrations of multiple anions in environmental media, helping to decrease the sample requirement, time, and cost of analysis.

5.2 Introduction

Chromium (VI) is a toxic, mutagenic, and carcinogenic water pollutant (Cohen et al., 1993; Costa, 1997; Salnikow and Zhitkovich, 2008). The World Health Organization set a maximum allowable limit of 50 μg L^{-1} for Cr (VI) in groundwater and drinking water (WHO, 2003b; El-Shahawi et al., 2011). In the United States, the drinking water maximum contaminant level (MCL) set by the Environmental Protection Agency (EPA) is 100 μg L^{-1} total Cr (US EPA, 2010). At the state level, the MCL can be even lower (e.g., 50 μg L^{-1} as total Cr) (California State Water Quality Control Board, 2020). The standard ion chromatography (IC) method for quantification of chromate ion (CrO_4^{2-}), the most common Cr (VI) anion, in water samples is EPA Method 218.7 (Zaffiro et al., 2011). Method 218.7 involves the separation of CrO_4^{2-} (referred henceforth as Cr (VI)) using a high capacity anion exchange separator column, a post-column derivatization with Cr (VI)-specific reagent 1,5-diphenylcarbazide, and a UV-Vis detection of the colored complex at 530 nm (Zaffiro et al., 2011). The Cr (VI)-specific reagent

diphenylcarbazide and UV-Vis detection allow sensitive quantification of Cr (VI) at low μg L^{-1} concentrations by avoiding interference from other anions like sulfate ion (SO_4^{2-}). However, method 218.7 and methods using similar principles are Cr (VI)-specific and do not quantify other analytes present in a given samples (Metrohm USA; Thermo Fisher Scientific; Rakhunde et al., 2012; Onchoke and Sasu, 2016).

Cr (VI) often co-occurs with one or more common inorganic anions such as chloride ion (Cl^-), SO_4^{2-}, and nitrate ion (NO_3^-) in drinking water, industrial wastewater, surface waters, groundwater, acid mine drainage, soils, and sediments (Riley, 1992; Gandhi et al., 2002). In groundwater, acid mine drainage and other process waters, Cr (VI) is often a co-contaminant with other regulated anions such as arsenate ion (AsO_4^{3-}) and selenate ion (SeO_4^{2-}) (referred henceforth as As (V) and Se (VI), respectively) or perchlorate ion (ClO_4^-) (Pyrzyńska, 2002; Urbansky, 2002; Parker et al., 2008; Yoon et al., 2009; Zhitkovich, 2011; Wang et al., 2013; Steinmaus, 2016; Khamkhash et al., 2017; WHO, 2018). ClO_4^- and Cr (VI) are frequently co-detected in drinking water systems across the world (Zhitkovich, 2011; Steinmaus, 2016). Most laboratories use IC with conductivity detection to simultaneously quantify Cl^-, SO_4^{2-} and NO_3^- using EPA Method 9056A (US EPA, 2007; Weiss, 2016). Separate IC methods with conductivity detection have been reported for quantification of ClO_4^- (EPA Method 314.0) (Hautman et al., 1999), As (V) (Lee and Choi, 2002; Ike et al., 2008; Yeo and Choi, 2009; Bhandari et al., 2011), and (Se (VI)) (Karlson and Frankenberger Jr, 1986; Mehra and Frankenberger, 1988; Pyrzyńska, 2002). Thus, analysis of surface water, groundwater, acid mine drainage, and other environmental aqueous samples containing Cr (VI) and co-

occurring anions requires multiple IC analytical methods with different anion exchange columns and eluent compositions. This requirement not only increases the sample volume demand but also the time and overall cost of analysis.

A limited numbers of studies achieved separation and detection of Cr (VI), As (V) and Se (VI) in the presence of common inorganic anions using anion exchange columns and conductivity detection (Bruzzoniti et al., 1999; Kończyk et al., 2018). However, linearity, precision, and accuracy of the co-detected analytes were not reported in these studies (Bruzzoniti et al., 1999; Kończyk et al., 2018), limiting the methods' applicability to environmental samples commonly analyzed in academic or other research-focused laboratories. In this work, we developed an isocratic IC analytical method with suppressed conductivity detection for simultaneous quantification of Cr (VI) and 8 other environmentally-relevant anions: fluoride ion (F^-), Cl^-, nitrite ion (NO_2^-), NO_3^-, SO_4^{2-}, Se (VI), As (V), and ClO_4^-. The method was validated by determining the linearity and accuracy (precision and trueness) for all the anion analytes. I used the method to evaluate recovery of Cr (VI) and the other analytes in tap water, surface water, groundwater and industrial wastewater samples and to analyze Cr (VI), SO_4^{2-}, NO_3^- and Cl^- in laboratory microcosm experiments.

5.3 Materials and Methods

5.3.1 Instrumentation

All analyses were performed using a Metrohm AG 930 compact IC flex system (Herisau, Switzerland). The IC was equipped with a chemical suppressor (Metrohm Suppressor Module (MSM)) and a conductivity detector. An 800 dosino regeneration

system was used to deliver the chemical suppressor solution to the MSM. The Metrohm CO_2 Suppressor (MCS) removed the carbonate (as CO_2) produced during the chemical suppression reaction in the MSM. The anions were separated using a Metrosep A Supp 7 analytical column (250 mm × 4 mm, Metrohm) and a Metrosep A Supp 5 Guard column (5 mm × 4 mm, Metrohm). A Metrohm AG 919 IC autosampler plus was used for sample injection. The volume of the sample injection loop was 1000 µL. The data acquisition and processing were performed with the MagIC Net 3.2 Metrodata software.

5.3.2 Chemicals and reagents

Reagent water, LC-MS Ultra CHROMASOLV (Honeywell, Charlotte, NC), was used to prepare the standards and the sample dilutions. Cr (VI) standards were prepared using K_2CrO_4 (Sigma-Aldrich, St. Louis, MO). As (V) and Se (VI) standards were prepared using $Na_2HAsO_4 \bullet 7H_2O$ (J.T. Baker, Phillipsburg, NJ) and Na_2SeO_4 (ACROS Organics, Geel, Belgium). ClO_4^- standards (Metrohm; Cat. # REAIC1023) and mixed anion standard (Metrohm; Cat. # REAIC1035) were used to generate the calibration curves for ClO_4^-, F^-, Cl^-, NO_2^-, NO_3^-, and SO_4^{2-}.

The eluent and the MSM suppressor solutions were prepared using deionized and purified water using a PURELAB Ultra (ELGA LabWater, United Kingdom) with a specific resistance ≥ 18.2 MΩ-cm. The eluent (mobile phase) contained 10.8 mM Na_2CO_3 (3 % (v v^{-1}) of Metrohm's A Supp 7 eluent 100X concentrate) and 35% (v v^{-1}) gradient grade acetonitrile (Sigma-Aldrich) in deionized water. The pH of the eluent as prepared was 11.9 ± 0.02. The MSM suppressor solution contained 500 mM H_2SO_4 in deionized water.

The 10 % (v v^{-1}) H_2SO_4 and 10 % (v v^{-1}) H_3PO_4 solutions for colorimetric determination of Cr (VI) were prepared from concentrated H_2SO_4 (95-98 % solution; VWR, Randor, PA) and concentrated H_3PO_4 (85 % solution; Alfa Aesar, Haverhill, MA), respectively. The complexing reagent contained 5 g L^{-1} of 1,5-diphenylcarbazide (Sigma-Aldrich) in acetone.

5.3.3 Analytical methods

The IC method used a constant eluent flow rate of 0.8 mL min^{-1} and a constant column/oven temperature of 55 °C. The MSM stepping interval was 10 mins and the conductivity detector was set at 2.3% per °C. At these conditions, the back pressure was 12 ± 0.4 MPa. The pump start-up time was at 45 to 60 min during the equilibration of the instrument. Calibrations for the anion analytes were established by injecting quadruplicates of 1, 5, 10, 25, 50, 100 and 200 µg L^{-1} standard mixture. The upper limit of quantification for Cl^-, NO_3^-, SO_4^{2-}, ClO_4^-, and Cr (VI) was 10000 µg L^{-1} (10 mg L^{-1}). For other analytes, the upper limit of quantification was in the range of 1000 – 9000 µg L^{-1}.

EPA Method 7196A was used to quantify Cr (VI) in a contaminated surface water sample and compare the concentrations obtained by the IC method. Cr (VI) concentration was determined colorimetrically at 540 nm using the diphenylcarbazide method (US EPA, 1992). Briefly, 0.1 mL of sample or standard was added to a 10 mL test tube followed by addition of 1 mL each of 10% H_2SO_4 and 10% H_3PO_4. Then, 0.1 mL of 5 g L^{-1} diphenylcarbazide in acetone was added to the test tube. The mixture was then vortexed and incubated at room temperature for 5 min. Absorbance of the magenta

color was analyzed using a Varian Cary 50 UV-Vis spectrophotometer (Agilent, Santa Clare, CA) at 540 nm. The spectrophotometer was calibrated using the standard Cr (VI) solution. The calibration range for the colorimetry method was 0.5–75 mg L^{-1} Cr (VI) and the detection limit was 0.25 mg L^{-1}.

5.3.4 Resolution, limit of detection, limit of quantification, and accuracy

Resolution of two peaks (R), defined as the ratio of the difference in retention times between two peaks and the average baseline width of two peaks (Harris, 2010), was determined using Equation 5.1:

$$R = \frac{T_{R2} - T_{R1}}{(w_{b1} + w_{b2})/2} \quad \text{(Equation 5.1)}$$

where T_{R1} and T_{R2} are the retention times of adjacent peaks (analyte 1 elutes before analyte 2) and w_{b1} and w_{b2} are the widths of the peaks at baseline.

The limit of detection (LOD), defined as the lowest concentration of analyte in a sample that can be readily distinguished from the absence of that analyte (a blank value) (McNaught and Wilkinson, 1997; Inczedy et al., 1998; Allegrini and Olivieri, 2014), was determined using Equation 5.2:

$$LOD = \frac{3S_a}{b} \quad \text{(Equation 5.2)}$$

The limit of quantification (LOQ), defined as the smallest concentration of analyte in a sample that can be quantitatively determined with suitable precision and accuracy, was determined using Equation 5.3:

$$LOQ = \frac{10S_a}{b} \quad \text{(Equation 5.3)}$$

In Equations 2 and 3, S_a is the standard deviation of the response estimated by the standard error of y-intercepts of the regression lines and b is the slope of the calibration

curve (Shrivastava and Gupta, 2011). A calibration curve with concentrations between 0.3 and 25 μg L^{-1} was used to obtain LOD and LOQ of all analytes.

Accuracy, defined as the closeness between a measured value and either a true or accepted value, was evaluated from precision and trueness values of each analyte (Munch et al., 2005). The precision was determined by calculating the relative standard deviation (RSD) using Equation 5.4. Trueness was determined by calculating the recovery using Equation 5.5.

$$RSD\ (\%) = \frac{\text{Standard deviation of measured concentrations}}{\text{Average of measured concentrations } (\mu g\ L^{-1})} \times 100 \qquad \text{(Equation 5.4)}$$

$$Recovery\ (\%) = \frac{\text{Average of measured concentrations } (\mu g\ L^{-1})}{\text{Spiked concentration } (\mu g\ L^{-1})} \times 100 \qquad \text{(Equation 5.5)}$$

5.3.5 Environmental samples

Tap water from the city of Tempe and reverse osmosis (RO) grade water (US Water Systems, Indianapolis, IN) were collected at the Biodesign Institute, Arizona State University, Tempe, AZ. Tap water from the City of Mesa was collected from a domicile in Mesa, AZ. Three groundwater samples were obtained for testing. One groundwater sample was from Phoenix Goodyear Airport-North Superfund site, Arizona, USA (Rangan et al., 2020). The other samples were collected from two confidential sites in the Southwestern United States. Cr (VI) contaminated surface water was collected from Tamilnadu Chromates and Chemicals Ltd. (TCCL), an abandoned chromate manufacturing facility in Ranipet, Tamil Nadu, India. The wastewater samples used in this study were received from a power station in the Eastern United States and from the Northwest Water Reclamation Plant, Mesa, AZ, USA.

5.3.6 Laboratory microcosm experiments

The developed IC method was applied to monitor anions in soil and culture-only batch microcosms. Soil laboratory microcosms (Ziv-El et al., 2011a; Rangan et al., 2020; Joshi et al., 2021) focused on abiotic and microbiological Cr (VI) reduction were established in 160 mL glass serum bottles with 25 g of Cr (VI)-contaminated soil and 100 mL anaerobic mineral medium as described elsewhere (Delgado et al., 2012; Delgado et al., 2017). The soil was collected from 0-0.25 m depth at the TCCL site, India, and was homogenized in the anaerobic glove chamber (Coy Laboratory Products Inc., Grass Lake, MI) under 3.5% H_2 and 96.5% N_2 atmosphere. 2 g L^{-1} yeast extract and 10 mM lactate (870 mg L^{-1}) were added to the microcosms as electrons and carbon sources for the microorganisms. The initial Cr (VI) concentration in the soil microcosms was ~ 90 mg L^{-1}.

Culture-only microcosms (Delgado et al., 2014c; Delgado et al., 2016) focused on microbiological Cr (VI) reduction were established in 160 mL serum bottles containing 100 mL anaerobic mineral medium as used in soil microcosms. The inoculum (4% v v^{-1}) was a mixed culture grown on Cr (VI) and lactate. The culture-only microcosms were amended with 1 g L^{-1} yeast extract and 3 mM lactate (~260 mg L^{-1}). The initial concentration of Cr (VI) was 15 mg L^{-1}. All (soil and culture-only) microcosms were established in triplicates, were incubated in the dark at 30°C, and were shaken on a platform shaker at 125 rpm. Liquid samples from the soil microcosms were collected for IC analysis during the experiment at 0.2, 3.7 and 8.2 hours. Liquid samples from the culture-only microcosms were collected at 0, 2, 7, 10, 11, 14, and 17 days. The liquid

samples were filtered using 0.2 µm syringe filters (mdi Membrane Technologies Inc., Harrisburg, PA) and analyzed for anions by IC.

5.4 Results and Discussion

In this study, we report an isocratic IC method with suppressed conductivity detection for simultaneous quantification of Cr (VI), F^-, Cl^-, NO_2^-, NO_3^-, SO_4^{2-}, Se (VI), As (V), and ClO_4^-. A typical chromatogram of the analytes (50 µg L^{-1} each in DI water) is shown in Figure 5.1. Most analytes showed good separation (defined as $R > 1.5$ (Harris, 2010)). All analytes were eluted within 20 min of sample injection (Figure 5.1).

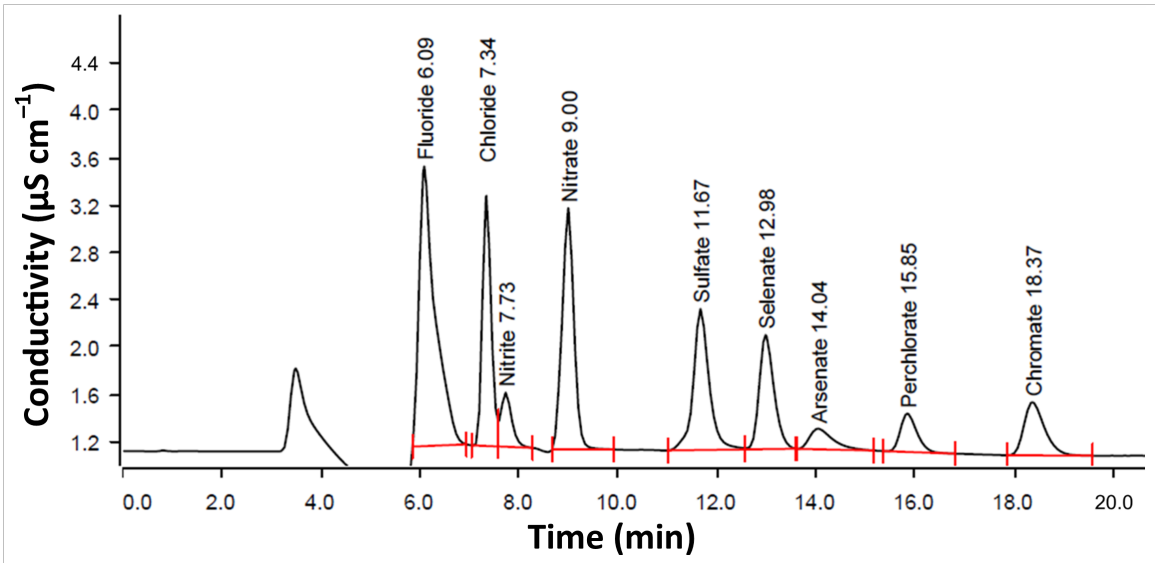

Figure 5.1. IC chromatogram of a mixture of 50 µg L^{-1} each of Cr (VI), ClO_4^-, SO_4^{2-} and other anions spiked to DI water with a Metrohm Metrosep A Supp 7 analytical column and mobile phase containing 10.8 mM Na_2CO_3 eluent and 35% (v/v) acetonitrile.

Table 5.1 compiles the resolution of the peaks, linear regression equation, determination coefficient, LOD and LOQ for the analytes. The determination coefficient of every analyte was > 0.99 and the LOD was in the range of 0.1–7.5 µg L^{-1} (Table 5.1). These data demonstrate the capability of the method to quantify trace concentrations of the analytes. For Cr (VI), the LOD and LOQ were 0.2 µg L^{-1} and 0.6 µg L^{-1},

respectively, which are three orders of magnitude lower than EPA's current MCL of 100 μg L^{-1} Cr.

Table 5.1. Resolution, regression equation, determination coefficient, quantification range, LOQ, and LOD of 9 analytes using the method from this study. R values greater than 1.5 are baseline resolutions. Y = peak area ((μS cm^{-1}) × min); X = concentration (μg L^{-1}). NA = Not applicable (Cr (VI) was the last analyte in the method run).

Elution order	Analyte	Resolution (R)	Regression equation	R^2	Quantification range (μg L^{-1})	LOD (μg L^{-1})	LOQ (μg L^{-1})
1	F^-	3.05	Y = 0.0071X + 0.1517	0.9986	24.9-1000	7.5	24.9
2	Cl^-	1.03	Y = 0.0083X + 0.0541	0.9984	14.4-10000	4.3	14.4
3	NO_2^-	2.92	Y = 0.002X + 0.0082	0.9979	1.5-5000	0.4	1.5
4	NO_3^-	5.51	Y = 0.0122X + 0.0009	0.9981	1.9-10000	0.6	1.9
5	SO_4^{2-}	2.45	Y = 0.0067X + 0.0903	0.9983	9.5-10000	2.9	9.5
6	Se (VI)	1.55	Y = 0.0066X + 0.0024	0.9999	0.5-9000	0.2	0.5
7	As (V)	2.51	Y = 0.0023X – 0.009	0.9988	2.1-7000	0.6	2.1
8	ClO_4^-	3.71	Y = 0.0025X – 0.0045	0.9992	0.5-10000	0.1	0.5
9	Cr (VI)	NA	Y = 0.0041X + 0.0046	0.9998	0.6-10000	0.2	0.6

A comparison of published IC methods for measurement of Cr (VI) in aqueous samples is shown in Table 5.2. The contribution of our method over previously published IC methods for Cr (VI) quantification is that ClO_4^- can also be quantified. I validated my method by demonstrating linearity, precision, and accuracy for simultaneous quantification of all the anion analytes, which was not reported previously by other IC methods (Bruzzoniti et al., 1999; Kończyk et al., 2018). The LOD and LOQ for Cr (VI) determined in this study was lowest among IC methods with suppressed conductivity detection (Table 5.2). I was able to achieve this low LOD and LOQ for Cr (VI) by using a 1000 μL injection loop, which is employed in the EPA Method for trace analysis of ClO_4^- in drinking water (Hautman et al., 1999). Methods that use UV-Vis spectroscopy, chemiluminescence, and thermal lens spectroscopy detection systems can achieve lower LOD for Cr (VI) but cannot quantify other anions.

Table 5.2. Comparison of various IC methods for Cr (VI) quantification in aqueous samples. NR = not reported.

Detection system	Post-column derivatization	LOD (µg L^{-1})	LOQ (µg L^{-1})	Sample injection volume (µL)	Simultaneous detection of other anions	Reference
UV-Vis spectroscopy	Yes	[a]0.01	[a]0.036	[a]1250	No	EPA method 218.7 (Zaffiro et al., 2011)
Chemiluminescence detection	Yes	0.09	NR	50	No	(Gammelgaard et al., 1997)
Thermal lens spectrometry	Yes	0.1	NR	200	No	[b](Šikovec et al., 2001)
Direct UV detection	No	0.2	1.2	100	No	(Michalski, 2003)
Suppressed conductivity	No	13.5	44.7	10	Cyanide, thiocyanate, cyanate	(Destanoğlu and Gümüş Yılmaz, 2016)
Suppressed conductivity	No	2	NR	200	Cl^-, NO_3^-, SO_4^{2-}, Se (IV), Se (VI), W (VI), As (V), Mo (VI)	[b](Bruzzoniti et al., 1999)
Suppressed conductivity	No	NR	NR	100	F^-, Cl^-, Br^-, NO_3^-, PO_4^{3-}, SO_4^{2-}	[b](Kończyk et al., 2018)
Suppressed conductivity	No	0.2	0.6	1000	F^-, Cl^-, NO_2^-, NO_3^-, SO_4^{2-}, Se (VI), As (V), ClO_4^-	This study

[a]Values from carbonate/bicarbonate eluent system.
[b]Linear regression equation, precision, and trueness were not reported.

SO_4^{2-} is among the most abundant anions in many environmental media.(Miao et al., 2012) In our analytical method, As (V) and Se (VI) elute within 3 min after SO_4^{2-} (Figure 5.1). Thus, high SO_4^{2-} concentrations could potentially interfere with quantification of As (V) and Se (VI) through this method. In such cases, samples would require dilution, making it challenging for trace analysis of the analytes using a conductivity detector. Alternatively, pre-treatment of the sample matrix to remove SO_4^{2-} can be employed using pre-treatment cartridges, but these can severely affect the

recovery of other analytes like Cr (VI) (Thermo Scientific, 2013). To elucidate SO_4^{2-} interference, we evaluated the effect of SO_4^{2-} concentration (up to 500 mg L^{-1}) on recovery of co-analytes. SO_4^{2-} concentration had no effect on recovery of F^-, Cl^-, NO_2^- and NO_3^- as these analytes eluted before SO_4^{2-} in my method (Figure 5.1). Se (VI) and As (V) recovery was < 80 % when SO_4^{2-} concentration was > 10 mg L^{-1} (data not shown). A recovery of 80% or greater is an acceptable criterion for quantification of chemical analytes (Hautman et al., 1999; US EPA, 2007). Hence, Se (VI) and As (V) cannot be quantified with accuracy in samples containing SO_4^{2-} at concentrations > 10 mg L^{-1}. Cr (VI) and ClO_4^- recovery was ≥ 85% in the presence of up to 500 mg L^{-1} SO_4^{2-} (Figure 5.2). These data demonstrate that the method can be used to quantify low concentrations of Cr (VI) and ClO_4^- in matrices with a high concentration of SO_4^{2-} without requiring pre-treatment or dilution of the sample.

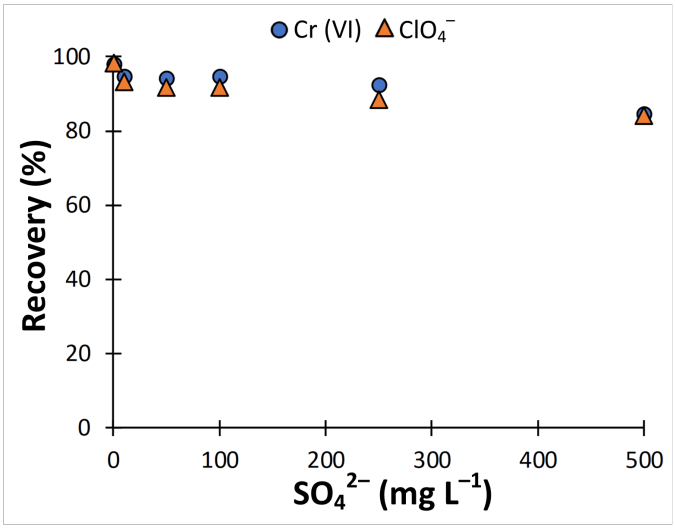

Figure 5.2. Effect of SO_4^{2-} concentration on recovery of Cr (VI) and ClO_4^-.

I evaluated the analytical accuracy (precision and trueness) for quantification of the anions at three concentration levels (2 µg L^{-1}, 10 µg L^{-1}, and 100 µg L^{-1}) using the

developed IC method. In reagent water or DI water, US EPA's acceptance criterion for RSD is ≤ 10%. The acceptance criterion for recovery is 80–120% for mid-level check standards (US EPA, 1996; Hautman et al., 1999). The acceptance criterion for recovery is 50–150% at concentrations close to the LOD of the analyte (low-level check standard) (US EPA, 1996). Table 5.3 documents the recovery of all anion analytes. At 100 μg L^{-1}, all analytes were quantified with RSD < 2.3% and the recovery was in the range of 96.2–107.9%, showing precision and trueness (accuracy) for quantification (Table 5.3). At 10 μg L^{-1}, the RSD and recovery for F^- and Cl^- were substantially affected (RSD values > 10% and recovery of 47.5–90.6% (Table 5.3)). These results are expected as 10 μg L^{-1} is within a factor of 3 from the LOD of F^- and Cl^- (US EPA, 1996). All other analytes were quantified with RSD < 7.4% and recovery of 92.6–105.3% using 10 μg L^{-1} standard (Table 5.3). At 2 μg L^{-1} concentration, all analytes except NO_3^- were quantified with RSD < 6 % and recovery in the range of 95.8–106.4% (Table 5.3). Overall, the method accomplished accuracy in quantification of NO_2^-, Se (VI), As (V), ClO_4^- and Cr (VI) at concentrations as low as 2 μg L^{-1}. At 100 μg L^{-1}, the RSD and recovery for all analytes are well within the acceptance accuracy criteria (Hautman et al., 1999; Munch et al., 2005).

Table 5.3. Analyte accuracy of quantification using the method from this study. NA = not applicable (concentration below LOD).

Elution order	Analyte	Spiked concentration 2 µg L^{-1} (n = 6)		Spiked concentration 10 µg L^{-1} (n = 6)		Spiked concentration 100 µg L^{-1} (n = 6)	
		Precision (RSD (%))	Trueness (recovery (%))	Precision (RSD (%))	Trueness (recovery (%))	Precision (RSD (%))	Trueness (recovery (%))
1	F^-	NA	NA	20.3	47.5	2.2	99.5
2	Cl^-	NA	NA	12.2	90.6	0.9	96.2
3	NO_2^-	0.0	95.8	2.4	97.2	1.3	97.6
4	NO_3^-	60.7	42.6	3.1	99.1	0.9	96.3
5	SO_4^{2-}	NA	NA	7.3	92.6	1.5	101.0
6	Se (VI)	3.2	106.4	1.3	100.8	0.8	102.2
7	As (V)	0.0	102.2	0.0	101.7	0.7	107.9
8	ClO_4^-	0.0	104.6	1.6	105.3	0.7	103.1
9	Cr (VI)	5.2	98.3	1.7	100.1	0.7	98.7

To test the applicability of the developed IC method on environmental aqueous samples, I evaluated the recovery of all analytes in deionized water, tap water, surface water, groundwater, and wastewater. The US EPA's acceptance criteria for recovery of analytes in environmental samples is 80–120% (Hautman et al., 1999). As seen in Table 5.4, the recovery of Cr (VI) in all environmental samples tested was in the range of 97.2–102.8%. The recovery of the other analytes was within the acceptable recovery criterion in most environmental samples (Table 5.4). These data support the applicability of this method for simultaneous quantification of the analytes in environmental aqueous samples.

Table 5.4. Recovery of all anion analytes in environmental samples. The data are averages with standard deviation of triplicates. The spiking concentration for all anions was 100 μg L^{-1}. ND = Not determined.

Samples	Cr (VI) recovery (%)	F^- recovery (%)	Cl^- recovery (%)	NO_2^- recovery (%)	NO_3^- recovery (%)	SO_4^{2-} recovery (%)	Se (VI) recovery (%)	As (V) recovery (%)	ClO_4^- recovery (%)
DI water	100.9 ± 0.5	94.5 ± 1.2	93.5 ± 0.8	98.1 ± 1.3	96.5 ± 0.6	102.1 ± 1.5	104.3 ± 0.9	103.2 ± 0.7	103.3 ± 0.6
RO water (Tempe, AZ)	100.1 ± 0.3	ND	ND	ND	ND	ND	ND	ND	ND
Tap water (Tempe, AZ)	102.1 ± 0.3	ND	ND	ND	ND	ND	ND	ND	ND
Tap water (Mesa, AZ)	100.5 ± 0.6	ND	ND	ND	ND	ND	ND	ND	ND
Groundwater (Goodyear, AZ)	97.6 ± 0.3	ND	ND	ND	ND	ND	ND	ND	ND
Groundwater (confidential site 1)	100.2 ± 0.0	107.8 ± 7.0	101.5 ± 3.0	92.7 ± 2.3	109.2 ± 6.1	104.2 ± 2.8	94.3 ± 2.6	84.9 ± 4.9	95.9 ± 0.5
Groundwater (confidential site 2)	99.7 ± 0.6	82.6 ± 3.6	100.3 ± 2.5	85.0 ± 0.7	109.7 ± 1.9	111.8 ± 3.1	89.1 ± 0.2	71.0 ± 4.9	93.2 ± 0.4
Surface water (Tamilnadu, India)	102.8 ± 0.6	86.1 ± 4.6	95.5 ± 0.4	92.5 ± 2.1	90.7 ± 2.7	89.5 ± 1.4	108.8 ± 0.2	98.7 ± 7.2	92.3 ± 0.6
Wastewater (confidential site 3, Eastern United States)	99.5 ± 0.3	ND	ND	ND	ND	ND	ND	ND	ND
Wastewater (Water Reclamation Plant, Mesa, AZ)	97.2 ± 0.2	107.8 ± 3.7	108.8 ± 5.2	76.1 ± 2.4	103.7 ± 2.9	84.2 ± 0.3	97.0 ± 0.8	97.0 ± 0.5	101.2 ± 0.4

I evaluated the trueness of Cr (VI) concentration in the surface water sample measured with our IC method by comparing it with the measured value using the EPA method 7196A (diphenylcarbazide based colorimetry method). The concentration of Cr (VI) in the surface water was 20.6 ± 0.2 mg L^{-1} using the diphenylcarbazide method (EPA Method 7196A). Assuming this was the true Cr (VI) concentration, the recovery of Cr (VI) concentration using the IC method was 100.2 ± 3.4 % (data not shown), demonstrating trueness for Cr (VI) quantification in the surface water sample. For Cr (VI) quantification using the IC method, the surface water was diluted 1000 times with reagent water to fit the Cr (VI) concentration within the calibration range.

I further applied the IC analytical method to simultaneously track concentrations of anions in typical batch microcosms used commonly in laboratory settings. The microcosms in this study were focused on abiotic and microbiological Cr (VI) reduction. Figure 5.3 shows the time course concentrations of Cr (VI) (naturally-present and spiked) and SO_4^{2-}, NO_3^- and Cl^- (naturally-present anions in the soil matrix). The concentration of Cr (VI) decreased from 90 mg L^{-1} to below detection limit in ~8 hours, likely from abiotic reduction by reducing agents in the soil such as sulfide and iron bearing minerals and/or microbial reduction to Cr (III) (Chen and Hao, 1998; Kim et al., 2001; Joe-Wong et al., 2017). The concentrations of SO_4^{2-} and Cl^- did not change significantly during the incubation time in the soil microcosms (Figure 5.3). Figure 5.4 tracks concentrations of Cr (VI) in culture-only microcosms focused on microbial reduction of Cr (VI) using a mixed culture. Cr (VI) concentration was reduced from ~15 mg L^{-1} to < 1 mg L^{-1} in ~18 days. Data from Figures 5.3 and 5.4 highlight the applicability of the IC method in

laboratory experiments using both complex matrices containing multiple analytes and simple matrices focused only on Cr (VI).

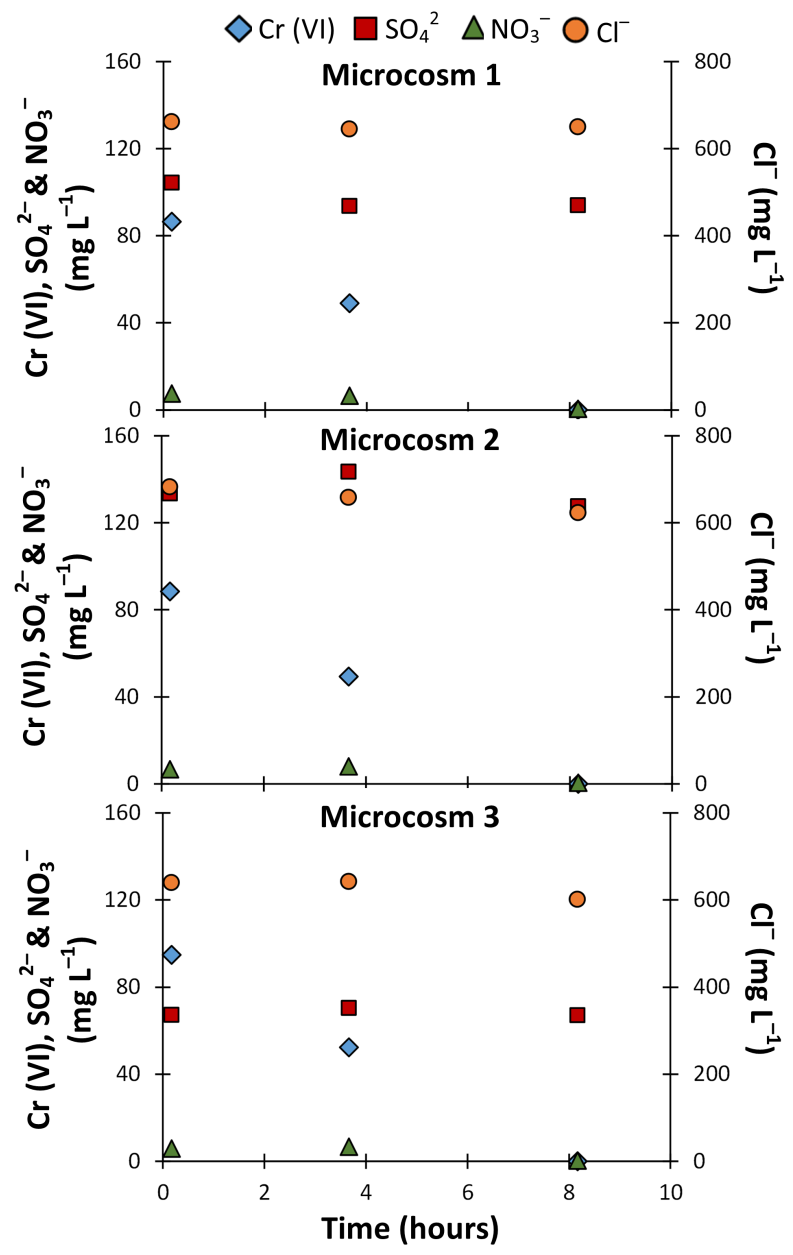

Figure 5.3. Concentrations of Cr (VI), SO_4^{2-}, NO_3^- and Cl^- during incubation in replicate soil microcosms. Note that Cl^- is plotted on the secondary y axis.

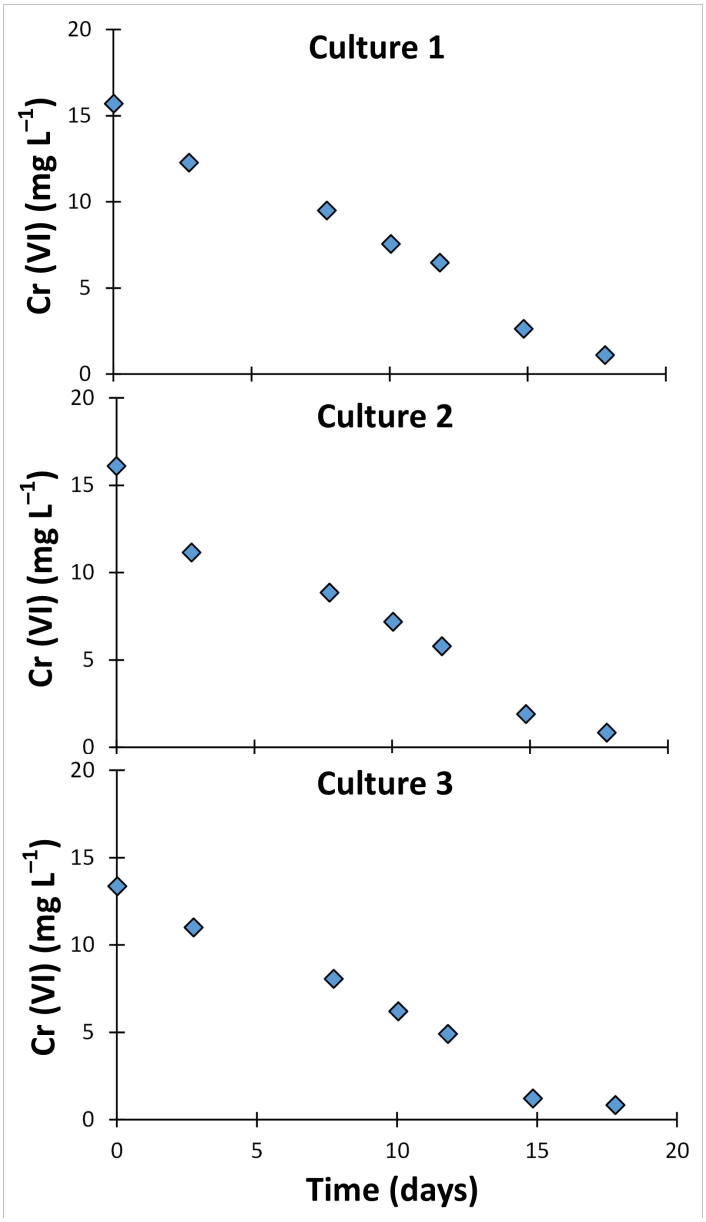

Figure 5.4. Concentrations of Cr (VI) during incubation in replicate culture-only microcosms.

Due to the capability of quantifying several anions simultaneously, the IC method developed in this study is useful to environmental practitioners, academic and research organizations, and other industries that routinely measure Cr (VI) and co-occurring anions. An ion chromatograph equipped with a suppressed conductivity detector is a

common instrumentation that many laboratories possess for quantification of common inorganic anions (e.g., Cl^-, NO_3^-, SO_4^{2-}) by EPA Method 9056A. Thus, the method developed can be easily adapted by laboratories that use the most common IC instrument. Our study shows that Cr (VI), As (V), Se (VI) and ClO_4^- in the low μg L^{-1} concentration range can be measured without pre-treatment of the sample or post column derivatization. The IC method from this work was shown to be reliable, precise, accurate, and suitable for monitoring important anions in environmental aqueous media, industrial wastewaters, and laboratory experiments.

5.5 References

Allegrini, F., Olivieri, A.C., 2014. IUPAC-consistent approach to the limit of detection in partial least-squares calibration. Analytical Chemistry 86, 7858-7866.

Bhandari, N., Reeder, R.J., Strongin, D.R., 2011. Photoinduced oxidation of arsenite to arsenate on ferrihydrite. Environmental Science & Technology 45, 2783-2789.

Bruzzoniti, M.C., Mentasti, E., Sarzanini, C., 1999. Simultaneous determination of inorganic anions and metal ions by suppressed ion chromatography. Analytica Chimica Acta 382, 291-299.

California State Water Quality Control Board, 2020. Chromium-6 Drinking Water MCL. https://www.waterboards.ca.gov/drinking_water/certlic/drinkingwater/Chromium6.html.

Chen, J.M., Hao, O.J., 1998. Microbial chromium (VI) reduction. Critical Reviews in Environmental Science and Technology 28, 219-251.

Cohen, M.D., Kargacin, B., Klein, C.B., Costa, M., 1993. Mechanisms of chromium carcinogenicity and toxicity. Critical Reviews in Toxicology 23, 255-281.

Costa, M., 1997. Toxicity and carcinogenicity of Cr (VI) in animal models and humans. Critical Reviews in Toxicology 27, 431-442.

Delgado, A.G., Fajardo-Williams, D., Bondank, E., Esquivel-Elizondo, S., Krajmalnik-Brown, R., 2017. Coupling bioflocculation of Dehalococcoides mccartyi to high-rate reductive dehalogenation of chlorinated ethenes. Environmental Science & Technology 51, 11297-11307.

Delgado, A.G., Fajardo-Williams, D., Kegerreis, K.L., Parameswaran, P., Krajmalnik-Brown, R., 2016. Impact of ammonium on syntrophic organohalide-respiring and fermenting microbial communities. Msphere 1, e00053-00016.

Delgado, A.G., Kang, D.-W., Nelson, K.G., Fajardo-Williams, D., Miceli III, J.F., Done, H.Y., Popat, S.C., Krajmalnik-Brown, R., 2014. Selective enrichment yields robust ethene-producing dechlorinating cultures from microcosms stalled at cis-dichloroethene. PloS One 9, e100654.

Delgado, A.G., Parameswaran, P., Fajardo-Williams, D., Halden, R.U., Krajmalnik-Brown, R., 2012. Role of bicarbonate as a pH buffer and electron sink in microbial dechlorination of chloroethenes. Microbial Cell Factories 11, 128.

El-Shahawi, M., Bashammakh, A., Abdelmageed, M., 2011. Chemical speciation of chromium (III) and (VI) using phosphonium cation impregnated polyurethane foams prior to their spectrometric determination. Analytical Sciences 27, 757-757.

Gandhi, S., Oh, B.-T., Schnoor, J.L., Alvarez, P.J., 2002. Degradation of TCE, Cr (VI), sulfate, and nitrate mixtures by granular iron in flow-through columns under different microbial conditions. Water Research 36, 1973-1982.

Harris, D.C., 2010. Quantitative chemical analysis, 8th ed. W. H. Freeman and Company, New York.

Hautman, D.P., Munch, D.J., Eaton Andrew, D., Haghani Ali, W., 1999. EPA Method 314.0: Determination of perchlorate in drinking water using ion chromatography.

Ike, M., Miyazaki, T., Yamamoto, N., Sei, K., Soda, S., 2008. Removal of arsenic from groundwater by arsenite-oxidizing bacteria. Water Science and Technology 58, 1095-1100.

Inczedy, J., Lengyel, T., Ure, A.M., Gelencsér, A., Hulanicki, A., 1998. Compendium of analytical nomenclature. Hoboken: Blackwell Science.

Joe-Wong, C., Brown Jr, G.E., Maher, K., 2017. Kinetics and products of chromium (VI) reduction by iron (II/III)-bearing clay minerals. Environmental Science & Technology 51, 9817-9825.

Joshi, S., Robles, A., Aguiar, S., Delgado, A.G., 2021. The occurrence and ecology of microbial chain elongation of carboxylates in soils. The ISME Journal.

Karlson, U., Frankenberger Jr, W., 1986. Determination of selenate by single-column ion chromatography. Journal of Chromatography A 368, 153-161.

Khamkhash, A., Srivastava, V., Ghosh, T., Akdogan, G., Ganguli, R., Aggarwal, S., 2017. Mining-related selenium contamination in Alaska, and the state of current knowledge. Minerals 7, 46.

Kim, C., Zhou, Q., Deng, B., Thornton, E.C., Xu, H., 2001. Chromium (VI) reduction by hydrogen sulfide in aqueous media: stoichiometry and kinetics. Environmental Science & Technology 35, 2219-2225.

Kończyk, J., Muntean, E., Michalski, R., 2018. Simultaneous determination of chromate and common inorganic anions using suppressed ion chromatography. Chemistry, Environment, Biotechnology 21, 11-13.

Lee, H., Choi, W., 2002. Photocatalytic oxidation of arsenite in TiO2 suspension: kinetics and mechanisms. Environmental Science & Technology 36, 3872-3878.

McNaught, A.D., Wilkinson, A., 1997. Compendium of chemical terminology. Blackwell Science Oxford.

Mehra, H., Frankenberger, W., 1988. Simultaneous analysis of selenate and selenite by single-column ion chromatography. Chromatographia 25, 585-588.

Metrohm USA, Determination of Hexavalent Chromium (Cr+6) by US EPA Method 218.7 https://www.metrohm.com/en-us/applications/AN-U-US-001.

Miao, Z., Brusseau, M.L., Carroll, K.C., Carreón-Diazconti, C., Johnson, B., 2012. Sulfate reduction in groundwater: characterization and applications for remediation. Environmental Geochemistry and Health 34, 539-550.

Munch, D.J., Wasko, M., Flynt, E., Wendelken, S.C., Scifres, J., Mario, J.R., Hunt, M., Gregg, D., Schaeffer, T., Clarage, M., 2005. Validation and Peer Review of US Environmental Protection Agency Chemical Methods of Analysis.

Onchoke, K.K., Sasu, S.A., 2016. Determination of Hexavalent Chromium (Cr (VI)) concentrations via ion chromatography and UV-Vis spectrophotometry in samples collected from nacogdoches wastewater treatment plant, East Texas (USA). Advances in Environmental Chemistry 2016.

Parker, D.R., Seyfferth, A.L., Reese, B.K., 2008. Perchlorate in groundwater: a synoptic survey of “pristine” sites in the coterminous United States. Environmental Science & Technology 42, 1465-1471.

Pyrzyńska, K., 2002. Determination of selenium species in environmental samples. Microchimica Acta 140, 55-62.

Rakhunde, R., Deshpande, L., Juneja, H., 2012. Chemical speciation of chromium in water: a review. Critical Reviews in Environmental Science and Technology 42, 776-810.

Rangan, S.M., Mouti, A., LaPat-Polasko, L., Lowry, G.V., Krajmalnik-Brown, R., Delgado, A.G., 2020. Synergistic Zerovalent Iron (Fe0) and Microbiological Trichloroethene and Perchlorate Reductions Are Determined by the Concentration and Speciation of Fe. Environmental Science & Technology 54, 14422-14431.

Riley, R.G., 1992. Chemical contaminants on DOE lands and selection of contaminant mixtures for subsurface science research. US Department of Energy, Office of Energy Research, Subsurface Science Program.

Salnikow, K., Zhitkovich, A., 2008. Genetic and epigenetic mechanisms in metal carcinogenesis and cocarcinogenesis: nickel, arsenic, and chromium. Chemical Research in Toxicology 21, 28-44.

Shrivastava, A., Gupta, V.B., 2011. Methods for the determination of limit of detection and limit of quantitation of the analytical methods. Chronicles of Young Scientists 2, 21.

Steinmaus, C.M., 2016. Perchlorate in water supplies: sources, exposures, and health effects. Current Environmental Health Reports 3, 136-143.

Thermo Fisher Scientific, Sensitive Determination of Hexavalent Chromium in Drinking Water. Sunnyvale, CA, USA.

Thermo Scientific, 2013. Dionex onguard II cartridges product manual. Waltham, MA.

Urbansky, E.T., 2002. Perchlorate as an environmental contaminant. Environmental Science and Pollution Research 9, 187-192.

US EPA, 1992. Method 7196A: Chromium, Hexavalent (Colorimetric). United States Environmental Protection Agency.

US EPA, 1996. DBP/ICR Analytical Methods Manual. United States Environmental Protection Agency.

US EPA, 2007. Method 9056A: Determination of inorganic anions by ion chromatography. United States Environmental Protection Agency.

US EPA, 2010. Chromium in Drinking Water. https://www.epa.gov/sdwa/chromium-drinking-water.

Wang, Z., Bush, R.T., Sullivan, L.A., Liu, J., 2013. Simultaneous redox conversion of chromium (VI) and arsenic (III) under acidic conditions. Environmental Science & Technology 47, 6486-6492.

Weiss, J., 2016. Handbook of Ion Chromatography, 3 Volume Set. John Wiley & Sons.

WHO, 2003. Guidelines for Drinking-water Quality | Chromium. World Health Organization.

WHO, 2018. Arsenic - Fact sheets. World Health Organization. https://www.who.int/news-room/fact-sheets/detail/arsenic.

Yeo, J., Choi, W., 2009. Iodide-mediated photooxidation of arsenite under 254 nm irradiation. Environmental Science & Technology 43, 3784-3788.

Yoon, J., Amy, G., Chung, J., Sohn, J., Yoon, Y., 2009. Removal of toxic ions (chromate, arsenate, and perchlorate) using reverse osmosis, nanofiltration, and ultrafiltration membranes. Chemosphere 77, 228-235.

Zaffiro, A., Zimmerman, M., Wendelken, S., Smith, G., Munch, D., 2011. METHOD 218.7: Determination of hexavalent chromium in drinking water by ion chromatography with post-column derivatization and UV-Visible spectroscopic detection. United States Environmental Protection Agency.

Zhitkovich, A., 2011. Chromium in drinking water: sources, metabolism, and cancer risks. Chemical Research in Toxicology 24, 1617-1629.

Ziv-El, M., Delgado, A.G., Yao, Y., Kang, D.-W., Nelson, K.G., Halden, R.U., Krajmalnik-Brown, R., 2011. Development and characterization of DehaloR^2, a novel anaerobic microbial consortium performing rapid dechlorination of TCE to ethene. Applied Microbiology and Biotechnology 92, 1063-1071.

CHAPTER 6

KEY FINDINGS AND RECOMMENDATIONS FOR FUTURE WORK

6.1 Key Findings

The ability of Fe^0 to remove dissolved O_2 and generate H_2 makes it an attractive chemical reductant to enhance bioremediation of TCE and ClO_4^-. However, the reactive oxygen species generated by Fe^0 and its oxidation product, Fe^{2+} can potentially inhibit microbial activity. In chapter 2, I investigated the effect of Fe^0 and Fe^{2+} at field relevant concentrations on microbial TCE and ClO_4^- reduction. The results from Chapter 2 showed that high Fe^0 concentration (16.5 g L^{-1}), expected during Fe^0 injection in the field, yielded rapid abiotic TCE dechlorination to ethene and ethane. However, microbiological TCE reductive dechlorination was hampered and microbiological ClO_4^- was inhibited at the high Fe^0 concentration. These results suggested that simultaneous injection of Fe^0 and *D. mccartyi*-containing cultures in contaminated sites could be detrimental for microbial TCE and ClO_4^- reduction. Fe^{2+} at 0.25 g L^{-1} delayed microbial TCE dechlorination, with limited production of ethene, implying a possibility of incomplete TCE dechlorination to *cis*-DCE and VC, downstream of Fe^0 application. However, a low concentration of aged-Fe^0 synergistically promoted microbiological TCE dechlorination to ethene while achieving complete microbiological ClO_4^- reduction. Collectively, these data suggested that Fe^0 abiotic reactions may benefit microbial TCE and ClO_4^- reductions if performed sequentially downstream of Fe^0 injection points.

Based on the results from Chapter 2, I evaluated an experimental approach where biostimulation and bioaugmentation with *D. mccartyi*-containing cultures was performed

sequentially downstream of Fe^0 addition using continuous-flow soil columns. I hypothesized that a decoupled Fe^0 and biostimulation/bioaugmentation treatment will mitigate the Fe^0-induced toxicity to the bioaugmented microbial cells while the Fe^0-reduced anaerobic groundwater will support microbial TCE reductive dechlorination. To evaluate this treatment approach, I used a soil column amended with Fe^0 (Fe^0 column) was used as a proxy for an upstream Fe^0 injection zone. Fe^0-reduced groundwater (effluent of Fe^0-column) was flown into soil packed columns with added organic substrates and a *D. mccartyi* mixed culture; these Bio-columns were a proxy for a downstream biostimulation and bioaugmentation zone. Results from Chapter 3 showed that Bio-columns flown with Fe^0-reduced groundwater yielded complete microbial TCE reductive dechlorination to ethene. These results provide evidence for enhanced microbial TCE reductive dechlorination in a decoupled Fe^0 and biostimulation/bioaugmentation treatment approach by inducing the required anoxic conditions, while likely mitigating Fe^0-induced oxidative stress to the bioaugmented microorganisms. After achieving complete microbial TCE dechlorination to ethene, the Bio-columns' influent was switched from Fe^0-reduced groundwater to aerobic groundwater "as collected" from the field, to mimic subsurface conditions after Fe^0 exhaustion. The microbial community established with Fe^0-reduced groundwater sustained TCE reductive dechlorination to ethene when challenged with aerobic groundwater. During this phase, distinct changes in the microbial community structure provided insights on the potential mechanisms of O_2 removal in the Bio-columns: (i) enrichment of iron-reducing bacteria suggested Fe^{2+}/Fe^{3+} cycling as a O_2 scavenging

mechanism, (ii) enrichment of sulfate-reducing bacteria and sulfur-oxidizing bacteria hinted on sulfur cycling as a O_2 scavenging mechanism, and (iii) enrichment of facultative anaerobic bacteria suggested occurrence of microbial O_2 reduction in the Bio-columns. These results suggest that in aerobic aquifers, microbial TCE reductive dechlorination to ethene could be sustained after Fe^0 exhaustion by addition of organic substrates.

Hundreds of chlorinated ethenes contaminated sites have benefited from bioaugmentation with *D. mccartyi*-containing cultures. However, bioremediation of heavy metals such as Cr (VI) still relies on biostimulation of indigenous soil microorganisms with organic substrates. The primary reason for bioaugmentation being overlooked for Cr (VI) bioremediation is due to the fact that NADH produced during microbial fermentation reactions can directly reduce Cr (VI) to Cr (III). In the presence of mixed microbial communities, the benefits of metabolic Cr (VI) bio-reduction (*via* respiration) by enriched Cr (VI)-reducing microorganisms is often obscured by fermentation-mediated Cr (VI) reduction. The contribution of metabolic Cr (VI) reduction by enriched Cr (VI)-reducing microorganisms in a mixed microbial consortium is poorly understood. In Chapter 4, I addressed this knowledge gap by evaluating the effect of microbial mixed culture enriched with Cr (VI)-reducing microorganisms on the rate and extent of Cr (VI) reduction and comparing it to microbial fermentation mediated Cr (VI) reduction. Specifically, I developed a microbial mixed culture using soil and groundwater from a Superfund site. Exposing the soil microorganisms to a high Cr (VI) concentration prior to enrichment process proved to be advantageous for selective

enrichment of Cr (VI)-resistant and Cr (VI)-reducing bacteria. The enriched microbial mixed culture grew with Cr (VI) as the sole electron acceptor and sustained Cr (VI) reduction up to 4 additions of 0.3 mM Cr (VI). A fermentative subculture grown with lactate (without Cr (VI)) was inhibited after 2 additions of ~0.3 mM Cr (VI). Cr (III) compounds ($Cr(OH)_3$ and/or Cr_2O_3) were precipitated extracellularly from microbial Cr (VI) reduction by the enriched Cr (VI)-reducing mixed culture. *Morganella* and *Pleomorphomonas* were the most abundant genera in the Cr (VI) reducing mixed culture, constituting up to 66.3% and 25.4% of the microbial communities. Species of *Morganella* are known to reduce Cr (VI), while the role of *Pleomorphomonas* in microbial Cr (VI) reduction is unclear. Overall, the results from this study suggest that bioaugmentation with enriched metabolic Cr (VI)-reducing bacteria has potential for Cr (VI) bioremediation.

Due to high toxicity and carcinogenicity of Cr (VI), the World Health Organization has set a maximum allowable limit of 50 $\mu g\ L^{-1}$ in groundwater and drinking water. For quantification of such low concentrations, the standard EPA method using ion chromatography (IC) (Method 218.7) requires special modifications to the instrumentation such as post column derivatization reactor and UV-Vis detector. Moreover, IC methods based on EPA method 218.7 are Cr (VI)-specific and does not allow quantification of other co-occurring anions. In Chapter 5, I developed an isocratic IC method with suppressed conductivity detection, a Metrohm Metrosep A Supp 7 column, and sodium carbonate/acetonitrile as mobile phase for simultaneous quantification of Cr (VI), ClO_4^-, As (V) as arsenate, Se (VI) as selenate, and the common

inorganic anions F^-, Cl^-, NO_2^-, NO_3^-, and SO_4^{2-}. The determination coefficient for every analyte was >0.99 and the method showed good accuracy in quantification. For Cr (VI), As (V), Se (VI), and ClO_4^-, limit of detection and limit of quantification were in the range of 0.1–0.6 µg/L and 0.5–2.1 µg/L, respectively. Overall, most analytes showed acceptable recovery (80–120%) in the environmental samples tested. An ion chromatograph equipped with a suppressed conductivity detector is a common instrumentation that laboratories possess for routine quantification of common inorganic anions. Hence, the method developed in this chapter is applicable to laboratories that possess the most common IC instrumentation.

6.2 Recommendations for Future Work

Field application of Fe^0 and bioaugmentation for chlorinated ethenes

Based on my research and review of the literature, combining Fe^0 with *in situ* anaerobic reductive dechlorination of chlorinated ethenes in the field has only focused on biostimulation of native indigenous *D. mccartyi* in the soil. Fe^0 particles coated with organic polymers (He et al., 2010a; Kocur et al., 2015) or Fe^0 particles with emulsions of organic substrates (Su et al., 2012; Sheu et al., 2016; Yang et al., 2018a) have increasingly being used in chlorinated ethenes contaminated sites. In contaminated sites that lack native *D. mccartyi*, bioaugmentation with *D. mccartyi*-containing cultures is essential to achieve complete microbial reductive dechlorination of chlorinated ethenes to non-toxic ethene. The results from Chapters 2 and 3 strongly suggest that bioaugmentation with *D. mccartyi*-containing cultures should be performed downstream of Fe^0 injection points for remediation of chlorinated ethenes.

Fe^0-mediated H_2 delivery is expected to decrease the requirement for organic carbon substrates, but the extent to which they do remains to be investigated. Future research should focus on using Fe^0 as the major H_2-delivery method and decreasing the concentrations of organic substrates. Decreasing the requirement of organic substrates can potentially alleviate bio-clogging of aquifers and injection wells, which is a frequently encountered issue in *in situ* bioremediation techniques (Han et al., 2020). Further, a low H_2 concentration was likely delivered to the bioaugmented microorganisms in this decoupled Fe^0 and biostimulation/bioaugmentation treatment approach. A low H_2 concentration favors microbial TCE reductive dechlorination over SO_4^{2-} reduction and methanogenesis (Ballapragada et al., 1997). Future research should focus on understanding how the potentially low concentration of H_2 delivered *via* upstream Fe^0 injection affects competing electron accepting microbial processes.

Microbial mixed culture studies for Cr (VI) bio-reduction

The results from Chapter 4 highlight the benefits of mixed culture enriched with Cr (VI)-reducing bacteria compared to fermentation-mediated Cr (VI) reduction for sustained remediation of Cr (VI). Most microbial Cr (VI) reduction studies in the peer-reviewed literature are concerned with isolation and enrichment of pure cultures. Mixed culture studies for Cr (VI) bio-reduction are limited in the peer-reviewed literature. While pure culture studies are essential for fundamental knowledge on Cr (VI)-reducing microbial isolates, future investigations should be focused on understanding these microorganisms in their natural environment, as members of mixed microbial communities, and in the presence aquifer materials with other co-occurring electron

acceptors. Specifically, presence of Fe^{3+} and SO_4^{2-} can enhance Cr (VI) reduction. Microbial reduction of Fe^{3+}-bearing minerals in soil generates Fe^{2+}, which can rapidly reduce Cr (VI). Similarly, microbial SO_4^{2-} reduction yields sulfite/sulfide, which are potent reducers of Cr (VI). Furthermore, iron reducing bacteria such as *Geobacter* (Lovley et al., 1993) and sulfate-reducing bacteria such as *Desulfotomaculum* (Tebo and Obraztsova, 1998) have shown to cometabolically reduce Cr (VI) to Cr (III). Future studies should focus on assessing the impact of Fe^{3+}-minerals and SO_4^{2-} on microbial Cr (VI) reduction by enriched metabolic Cr (VI)-reducing microorganisms. Such studies would provide useful insights to achieve synergistic biotic and abiotic Cr (VI) bioremediation in the field.

Analytical methods for simultaneous quantification of multiple anions

In Chapter 5, I demonstrated a novel method for simultaneous quantification of 9 important anions in the environment at low $\mu g\ L^{-1}$ concentration in aqueous samples. I would expand on this analytical method in Chapter 5 to potentially increase the array of analytes by modifications in the stationary phase (analytical separation columns) and/or mobile phase (eluent). Increasing the analytical capability of this method would significantly benefit a wide range of applications including but not limited to environmental research, environmental monitoring, wastewater-based epidemiology, and municipal and industrial wastewater treatment.

REFERENCES

ATSDR's Substance Priority List.

Abu-Amero, K.K., Abu-Groun, E.A., Halablab, M.A., Miles, R.J., 2000. Kinetics and distribution of alcohol oxidising activity in Acholeplasma and Mycoplasma species. *FEMS Microbiology Letters* 183, 147-151.

Ahmad, W.A., Ahmad, W.H.W., Karim, N.A., Raj, A.S., Zakaria, Z.A., 2013. Cr (VI) reduction in naturally rich growth medium and sugarcane bagasse by Acinetobacter haemolyticus. *International Biodeterioration & Biodegradation* 85, 571-576.

Allegrini, F., Olivieri, A.C., 2014. IUPAC-consistent approach to the limit of detection in partial least-squares calibration. *Analytical Chemistry* 86, 7858-7866.

Amos, B.K., Christ, J.A., Abriola, L.M., Pennell, K.D., Löffler, F.E., 2007. Experimental evaluation and mathematical modeling of microbially enhanced tetrachloroethene (PCE) dissolution. *Environmental Science & Technology* 41, 963-970.

Amos, B.K., Ritalahti Kirsti, M., Cruz-Garcia, C., Padilla-Crespo, E., Loffler Frank, E., 2008a. Oxygen effect on Dehalococcoides viability and biomarker quantification. *Environmental Science and Technology* 42, 5718--5726.

Amos, B.K., Ritalahti, K.M., Cruz-Garcia, C., Padilla-Crespo, E., Loffler, F.E., 2008b. Oxygen effect on Dehalococcoides viability and biomarker quantification. *Environmental Science and Technology* 42, 5718--5726.

Ancona, V., Campanale, C., Tumolo, M., De Paola, D., Ardito, C., Volpe, A., 2020. Enhancement of chromium (VI) reduction in microcosms amended with lactate or yeast extract: A laboratory-scale Study. *International Journal of Environmental Research and Public Health* 17, 704.

Arizona Department of Environmental Quality, 2017. , Phoenix-Goodyear Airport North | Site History.

Arnold, W.A., Roberts, A.L., 2000. Pathways and kinetics of chlorinated ethylene and chlorinated acetylene reaction with Fe (0) particles. *Environmental Science & Technology* 34, 1794-1805.

Aronniemi, M., Sainio, J., Lahtinen, J., 2005. Chemical state quantification of iron and chromium oxides using XPS: the effect of the background subtraction method. *Surface Science* 578, 108-123.

ATSDR, 2019. Substance Priority List 2019 | Agency of Toxic Substances and Disease Registry.

Auffan, M., Achouak, W., Rose, J., Roncato, M.-A., Chaneac, C., Waite, D.T., Masion, A., Woicik, J.C., Wiesner, M.R., Bottero, J.-Y., 2008. Relation between the redox state of iron-based nanoparticles and their cytotoxicity toward *Escherichia coli*. *Environmental Science & Technology* 42, 6730-6735.

Bae, W.-C., Lee, H.-K., Choe, Y.-C., Jahng, D.-J., Lee, S.-H., Kim, S.-J., Lee, J.-H., Jeong, B.-C., 2005. Purification and characterization of NADPH-dependent Cr (VI) reductase from Escherichia coli ATCC 33456. *Journal of Microbiology* 43, 21-27.

Bai, Y.-N., Lu, Y.-Z., Shen, N., Lau, T.-C., Zeng, R.J., 2018. Investigation of Cr (VI) reduction potential and mechanism by Caldicellulosiruptor saccharolyticus under glucose fermentation condition. *Journal of hazardous materials* 344, 585-592.

Ballapragada, B.S., Stensel, H.D., Puhakka, J., Ferguson, J.F., 1997. Effect of hydrogen on reductive dechlorination of chlorinated ethenes. *Environmental science & technology* 31, 1728-1734.

Barak, Y., Ackerley, D., Dodge, C., Banwari, L., Alex, C., Francis, A., Matin, A., 2006. Analysis of novel soluble chromate and uranyl reductases and generation of an improved enzyme by directed evolution. *Applied and Environmental Microbiology* 72, 7074-7082.

Bardiya, N., Bae, J.-H., 2011. Dissimilatory perchlorate reduction: a review. *Microbiological research* 166, 237-254.

Baric, M., Majone, M., Beccari, M., Papini, M.P., 2012. Coupling of polyhydroxybutyrate (PHB) and zero valent iron (ZVI) for enhanced treatment of chlorinated ethanes in permeable reactive barriers (PRBs). *Chemical Engineering Journal* 195, 22-30.

Barnes, R.J., van der Gast, C.J., Riba, O., Lehtovirta, L.E., Prosser, J.I., Dobson, P.J., Thompson, I.P., 2010. The impact of zero-valent iron nanoparticles on a river water bacterial community. *Journal of Hazardous Materials* 184, 73-80.

Bencheikh-Latmani, R., Obraztsova, A., Mackey, M.R., Ellisman, M.H., Tebo, B.M., 2007. Toxicity of Cr (III) to Shewanella sp. strain MR-4 during Cr (VI) reduction. *Environmental science & technology* 41, 214-220.

Bennett, P., He, F., Zhao, D., Aiken, B., Feldman, L., 2010. In situ testing of metallic iron nanoparticle mobility and reactivity in a shallow granular aquifer. *Journal of Contaminant Hydrology* 116, 35-46.

Bhandari, N., Reeder, R.J., Strongin, D.R., 2011. Photoinduced oxidation of arsenite to arsenate on ferrihydrite. *Environmental Science & Technology* 45, 2783-2789.

Biedermann, K.A., Landolph, J.R., 1990. Role of valence state and solubility of chromium compounds on induction of cytotoxicity, mutagenesis, and anchorage independence in diploid human fibroblasts. *Cancer Research* 50, 7835-7842.

Biel-Maeso, M., Burke, V., Greskowiak, J., Massmann, G., Lara-Martin, P.A., Corada-Fernandez, C., 2021. Mobility of contaminants of emerging concern in soil column experiments. *Science of The Total Environment* 762, 144102.

Biesinger, M.C., Payne, B.P., Grosvenor, A.P., Lau, L.W., Gerson, A.R., Smart, R.S.C., 2011. Resolving surface chemical states in XPS analysis of first row transition metals, oxides and hydroxides: Cr, Mn, Fe, Co and Ni. *Applied Surface Science* 257, 2717-2730.

Blowes, D.W., Ptacek, C.J., Jambor, J.L., 1997. In-situ remediation of Cr (VI)-contaminated groundwater using permeable reactive walls: laboratory studies. *Environmental Science & Technology* 31, 3348-3357.

Bokulich, N.A., Kaehler, B.D., Rideout, J.R., Dillon, M., Bolyen, E., Knight, R., Huttley, G.A., Caporaso, J.G., 2018a. Optimizing taxonomic classification of marker-gene amplicon sequences with QIIME 2's q2-feature-classifier plugin. *Microbiome* 6, 90.

Bokulich, N.A., Kaehler Benjamin, D., Rideout Jai, R., Dillon, M., Bolyen, E., Knight, R., Huttley Gavin, A.a., 2018b. Optimizing taxonomic classification of marker-gene amplicon sequences with QIIME 2's q2-feature-classifier plugin. *Microbiome*.

Bolyen, E., Rideout Jai, R., Dillon Matthew, R., Bokulich Nicholas, A., Abnet Christian, C., Al-Ghalith Gabriel, A., Alexander, H., Alm Eric, J., Arumugam, M., Asnicar, F., Bai, Y., Bisanz Jordan, E., Bittinger, K., Brejnrod, A., Brislawn Colin, J., Brown, C.T., Callahan Benjamin, J., Caraballo-Rodrguez Andrs, M., Chase, J., Cope Emily, K.a., 2019a. Reproducible, interactive, scalable and extensible microbiome data science using QIIME 2. *Nature Biotechnology*.

Bolyen, E., Rideout, J.R., Dillon, M.R., Bokulich, N.A., Abnet, C.C., Al-Ghalith, G.A., Alexander, H., Alm, E.J., Arumugam, M., Asnicar, F., 2019b. Reproducible, interactive, scalable and extensible microbiome data science using QIIME 2. *Nature Biotechnology* 37, 852-857.

Borden, R.C., 2007. Concurrent bioremediation of perchlorate and 1,1,1-trichloroethane in an emulsified oil barrier. *Journal of Contaminant Hydrology* 94, 13--33.

Boutry, S., Forge, D., Burtea, C., Mahieu, I., Murariu, O., Laurent, S., Vander Elst, L., Muller, R.N., 2009. How to quantify iron in an aqueous or biological matrix: a technical note. *Contrast media & molecular imaging* 4, 299-304.

Brown, R.A., Mueller, J.G., Seech, A.G., Henderson, J.K., Wilson, J.T., 2009. Interactions between biological and abiotic pathways in the reduction of chlorinated solvents. *Remediation Journal: The Journal of Environmental Cleanup Costs, Technologies & Techniques* 20, 9-20.

Bruzzoniti, M.C., Mentasti, E., Sarzanini, C., 1999. Simultaneous determination of inorganic anions and metal ions by suppressed ion chromatography. *Analytica Chimica Acta* 382, 291-299.

California State Water Quality Control Board, 2020. Chromium-6 Drinking Water MCL. https://www.waterboards.ca.gov/drinking_water/certlic/drinkingwater/Chromium6.html.

Callahan, B.J., McMurdie, P.J., Rosen, M.J., Han, A.W., Johnson, A.J.A., Holmes, S.P., 2016. DADA2: high-resolution sample inference from Illumina amplicon data. *Nature Methods* 13, 581-583.

Camacho, C., Coulouris, G., Avagyan, V., Ma, N., Papadopoulos, J., Bealer, K., Madden, T.L., 2009. BLAST+: architecture and applications. *BMC bioinformatics* 10, 1-9.

Cao, F., Jaunat, J., Sturchio, N., Cances, B., Morvan, X., Devos, A., Barbin, V., Ollivier, P., 2019. Worldwide occurrence and origin of perchlorate ion in waters: A review. *Science of the Total Environment* 661, 737-749.

Caporaso, J.G., Lauber Christian, L., Walters William, A., Berg-Lyons, D., Huntley, J., Fierer, N., Owens Sarah, M., Betley, J., Fraser, L., Bauer, M., Gormley, N., Gilbert Jack, A., Smith, G., Knight, R., 2012a. Ultra-high-throughput microbial community analysis on the Illumina HiSeq and MiSeq platforms. *The ISME Journal* 6, 1621--1624.

Caporaso, J.G., Lauber, C.L., Walters, W.A., Berg-Lyons, D., Huntley, J., Fierer, N., Owens, S.M., Betley, J., Fraser, L., Bauer, M., 2012b. Ultra-high-throughput microbial community analysis on the Illumina HiSeq and MiSeq platforms. *The ISME Journal* 6, 1621-1624.

Caro-Quintero, A., Ritalahti, K., Cusick, K., Löffler, F., Konstantinidis, K., 2012. The chimeric genome of Sphaerochaeta: nonspiral spirochetes that break with the prevalent dogma in spirochete biology. *MBio* 3, e00025-00012.

Cefalu, W.T., Hu, F.B., 2004. Role of chromium in human health and in diabetes. *Diabetes Care* 27, 2741-2751.

Chang, I.S., Kim, B.H., 2007. Effect of sulfate reduction activity on biological treatment of hexavalent chromium [Cr (VI)] contaminated electroplating wastewater under sulfate-rich condition. *Chemosphere* 68, 218-226.

Chen, G., Kara Murdoch, F., Xie, Y., Murdoch, R.W., Cui, Y., Yang, Y., Yan, J., Key, T.A., Löffler, F.E., 2022. Dehalogenation of Chlorinated Ethenes to Ethene by a Novel Isolate,"Candidatus Dehalogenimonas etheniformans". *Applied and Environmental Microbiology*, e00443-00422.

Chen, J., Xiu, Z., Lowry, G.V., Alvarez, P.J., 2011. Effect of natural organic matter on toxicity and reactivity of nano-scale zero-valent iron. *Water Research* 45, 1995-2001.

Chen, J.M., Hao, O.J., 1998. Microbial chromium (VI) reduction. *Critical Reviews in Environmental Science and Technology* 28, 219-251.

Chowdhury, A.I., Krol, M.M., Kocur, C.M., Boparai, H.K., Weber, K.P., Sleep, B.E., O'Carroll, D.M., 2015. nZVI injection into variably saturated soils: Field and modeling study. *Journal of Contaminant Hydrology* 183, 16-28.

Coates, J.D., Achenbach, L.A., 2004. Microbial perchlorate reduction: rocket-fuelled metabolism. *Nature Reviews Microbiology* 2, 569-580.

Coates, J.D., Michaelidou, U., Bruce Royce, A., Oapos, Connor, S.M., Crespi Jill, N., Achenbach Laurie, A., 1999. Ubiquity and diversity of dissimilatory (per)chlorate-reducing bacteria. *Applied and Environmental Microbiology* 65, 5234-5241.

Cohen, M.D., Kargacin, B., Klein, C.B., Costa, M., 1993. Mechanisms of chromium carcinogenicity and toxicity. *Critical Reviews in Toxicology* 23, 255-281.

Costa, M., 1997. Toxicity and carcinogenicity of Cr (VI) in animal models and humans. *Critical Reviews in Toxicology* 27, 431-442.

Csákberényi-Malasics, D., Rodriguez-Blanco, J.D., Kis, V.K., Rečnik, A., Benning, L.G., Pósfai, M., 2012. Structural properties and transformations of precipitated FeS. *Chemical Geology* 294, 249-258.

Czinnerová, M., Vološčuková, O., Marková, K., Ševců, A., Černík, M., Nosek, J., 2020. Combining nanoscale zero-valent iron with electrokinetic treatment for remediation of chlorinated ethenes and promoting biodegradation: A long-term field study. *Water Research* 175, 115692.

Dang, H., Kanitkar, Y.H., Stedtfeld, R.D., Hatzinger, P.B., Hashsham, S.A., Cupples, A.M., 2018. Abundance of chlorinated solvent and 1, 4-dioxane degrading microorganisms at five chlorinated solvent contaminated sites determined via shotgun sequencing. *Environmental science & technology* 52, 13914-13924.

Davies, K.J., 2000. Oxidative stress, antioxidant defenses, and damage removal, repair, and replacement systems. *IUBMB life* 50, 279-289.

Davison, W., Seed, G., 1983. The kinetics of the oxidation of ferrous iron in synthetic and natural waters. *Geochimica et Cosmochimica Acta* 47, 67-79.

de Guzmán, G.T.N., Hapeman, C.J., Millner, P.D., Torrents, A., Jackson, D., Kjellerup, B.V., 2018. Presence of organohalide-respiring bacteria in and around a permeable reactive barrier at a trichloroethylene-contaminated Superfund site. *Environmental Pollution* 243, 766-776.

Delgado, A.G., Fajardo-Williams, D., Bondank, E., Esquivel-Elizondo, S., Krajmalnik-Brown, R., 2017. Coupling bioflocculation of *Dehalococcoides mccartyi* to high-rate reductive dehalogenation of chlorinated ethenes. *Environmental Science & Technology* 51, 11297-11307.

Delgado, A.G., Fajardo-Williams, D., Kegerreis, K.L., Parameswaran, P., Krajmalnik-Brown, R., 2016. Impact of ammonium on syntrophic organohalide-respiring and fermenting microbial communities. *Msphere* 1, e00053-00016.

Delgado, A.G., Fajardo-Williams, D., Popat, S.C., Torres, C.I., Krajmalnik-Brown, R., 2014a. Successful operation of continuous reactors at short retention times results in high-density, fast-rate *Dehalococcoides* dechlorinating cultures. *Applied Microbiology and Biotechnology* 98, 2729-2737.

Delgado, A.G., Kang, D.-W., Nelson, K.G., Fajardo-Williams, D., Miceli III, J.F., Done, H.Y., Popat, S.C., Krajmalnik-Brown, R., 2014b. Selective enrichment yields robust ethene-producing dechlorinating cultures from microcosms stalled at *cis*-dichloroethene. *PloS one* 9.

Delgado, A.G., Kang, D.-W., Nelson, K.G., Fajardo-Williams, D., Miceli III, J.F., Done, H.Y., Popat, S.C., Krajmalnik-Brown, R., 2014c. Selective enrichment yields robust ethene-producing dechlorinating cultures from microcosms stalled at cis-dichloroethene. *PLOS ONE* 9, e100654.

Delgado, A.G., Parameswaran, P., Fajardo-Williams, D., Halden, R.U., Krajmalnik-Brown, R., 2012. Role of bicarbonate as a pH buffer and electron sink in microbial dechlorination of chloroethenes. *Microbial Cell Factories* 11, 128.

Desimoni, E., Malitesta, C., Zambonin, P., Riviere, J., 1988. An x-ray photoelectron spectroscopic study of some chromium–oxygen systems. *Surface and interface analysis* 13, 173-179.

Destanoğlu, O., Gümüş Yılmaz, G., 2016. Determination of cyanide, thiocyanate, cyanate, hexavalent chromium, and metal cyanide complexes in various mixtures by ion chromatography with conductivity detection. *Journal of Liquid Chromatography & Related Technologies* 39, 465-474.

Dhal, B., Thatoi, H., Das, N., Pandey, B., 2013. Chemical and microbial remediation of hexavalent chromium from contaminated soil and mining/metallurgical solid waste: a review. *Journal of hazardous materials* 250, 272-291.

Dong, H., Li, L., Lu, Y., Cheng, Y., Wang, Y., Ning, Q., Wang, B., Zhang, L., Zeng, G., 2019. Integration of nanoscale zero-valent iron and functional anaerobic bacteria for groundwater remediation: a review. *Environment international* 124, 265-277.

El-Shahawi, M., Bashammakh, A., Abdelmageed, M., 2011. Chemical speciation of chromium (III) and (VI) using phosphonium cation impregnated polyurethane foams prior to their spectrometric determination. *Analytical Sciences* 27, 757-757.

Elangovan, R., Abhipsa, S., Rohit, B., Ligy, P., Chandraraj, K., 2006. Reduction of Cr (VI) by a Bacillus sp. *Biotechnology Letters* 28, 247-252.

Ellis, D.E.a.L.E.J.a.O.J.M.a.B.R.J.a.B.C.L.a.L.M.D.a.H.M.R.a., 2000. Bioaugmentation for accelerated in situ anaerobic bioremediation. *Environmental Science and Technology* 34, 2254--2260.

Environmental Toxicology Section., 2004. Perchlorates. Oregon department of human services.

Ergul-Ulger, Z., Ozkan, A.D., Tunca, E., Atasagun, S., Tekinay, T., 2014. Chromium (VI) biosorption and bioaccumulation by live and acid-modified biomass of a novel Morganella morganii isolate. *Separation Science and Technology* 49, 907-914.

Esquivel-Elizondo, S., Maldonado, J., Krajmalnik-Brown, R., 2018. Anaerobic carbon monoxide metabolism by Pleomorphomonas carboxyditropha sp. nov., a new mesophilic hydrogenogenic carboxydotroph. *FEMS microbiology ecology* 94, fiy056.

Evans, P.J., Koenigsberg, S., 2001. A bioavailable ferric iron assay and relevance to reductive dechlorination. *Bioaugmentation, biobarriers, and biogeochemistry. Battelle Press, Columbus, Ohio*, 209-215.

Farrell, J., Kason, M., Melitas, N., Li, T., 2000a. Investigation of the long-term performance of zero-valent iron for reductive dechlorination of trichloroethylene. *Environmental Science & Technology* 34, 514-521.

Farrell, J., Melitas, N., Kason, M., Li, T., 2000b. Electrochemical and column investigation of iron-mediated reductive dechlorination of trichloroethylene and perchloroethylene. *Environmental Science & Technology* 34, 2549-2556.

Fernández, P.M., Viñarta, S.C., Bernal, A.R., Cruz, E.L., Figueroa, L.I., 2018. Bioremediation strategies for chromium removal: current research, scale-up approach and future perspectives. *Chemosphere* 208, 139-148.

Franco, L.C., Steinbeisser, S., Zane, G.M., Wall, J.D., Fields, M.W., 2018. Cr (VI) reduction and physiological toxicity are impacted by resource ratio in Desulfovibrio vulgaris. *Applied microbiology and biotechnology* 102, 2839-2850.

Freim, J., Optimization of ZVI Technology for In-Situ Remediation of Chlorinated Contaminants. OnMaterials, LLC.

Fu, F., Dionysiou, D.D., Liu, H., 2014. The use of zero-valent iron for groundwater remediation and wastewater treatment: a review. *Journal of Hazardous Materials* 267, 194-205.

Gadd, G.M., White, C., 1993. Microbial treatment of metal pollution—a working biotechnology? *Trends in biotechnology* 11, 353-359.

Gadkari, J., Goris, T., Schiffmann, C.L., Rubick, R., Adrian, L., Schubert, T., Diekert, G., 2018. Reductive tetrachloroethene dehalogenation in the presence of oxygen by Sulfurospirillum multivorans: physiological studies and proteome analysis. *FEMS Microbiology Ecology* 94, fix176.

Gammelgaard, B., Liao, Y.-p., Jøns, O., 1997. Improvement on simultaneous determination of chromium species in aqueous solution by ion chromatography and chemiluminescence detection. *Analytica Chimica Acta* 354, 107-113.

Gandhi, S., Oh, B.-T., Schnoor, J.L., Alvarez, P.J., 2002. Degradation of TCE, Cr (VI), sulfate, and nitrate mixtures by granular iron in flow-through columns under different microbial conditions. *Water Research* 36, 1973-1982.

Garrigues, C., Loubiere, P., Lindley, N.D., Cocaign-Bousquet, M., 1997. Control of the shift from homolactic acid to mixed-acid fermentation in Lactococcus lactis: predominant role of the NADH/NAD+ ratio. *Journal of Bacteriology* 179, 5282-5287.

Gong, L., Lv, N., Qi, J., Qiu, X., Gu, Y., He, F., 2020. Effects of non-reducible dissolved solutes on reductive dechlorination of trichloroethylene by ball milled zero valent irons. *Journal of Hazardous Materials* 396, 122620.

Goris, T., Diekert, G., 2016. The genus *Sulfurospirillum*. Organohalide-respiring Bacteria. Springer, pp. 209-234.

Goris, T., Schubert, T., Gadkari, J., Wubet, T., Tarkka, M., Buscot, F., Adrian, L., Diekert, G., 2014. Insights into organohalide respiration and the versatile

catabolism of S ulfurospirillum multivorans gained from comparative genomics and physiological studies. *Environmental Microbiology* 16, 3562-3580.

Gregory, K.B., Mason, M.G., Picken, H.D., Weathers, L.J., Parkin, G.F., 2000. Bioaugmentation of Fe (0) for the remediation of chlorinated aliphatic hydrocarbons. *Environmental Engineering Science* 17, 169-181.

Guan, X., Sun, Y., Qin, H., Li, J., Lo, I.M., He, D., Dong, H., 2015. The limitations of applying zero-valent iron technology in contaminants sequestration and the corresponding countermeasures: the development in zero-valent iron technology in the last two decades (1994–2014). *Water Research* 75, 224-248.

Guha, H., Jayachandran, K., Maurrasse, F., 2001. Kinetics of chromium (VI) reduction by a type strain Shewanella alga under different growth conditions. *Environmental Pollution* 115, 209-218.

Gullick, R.W., Lechevallier, M.W., Barhorst, T.S., 2001. Occurrence of perchlorate in drinking water sources. *Journal-American Water Works Association* 93, 66-77.

Gutiérrez-Corona, J., Romo-Rodríguez, P., Santos-Escobar, F., Espino-Saldaña, A., Hernández-Escoto, H., 2016. Microbial interactions with chromium: basic biological processes and applications in environmental biotechnology. *World Journal of Microbiology and Biotechnology* 32, 191.

Han, K., Park, S., Kwon, S., Kim, Y., 2020. Evaluating a new injection method of liquid/gas mixture spray injection via performing long-term in situ bioremediation tests. *Journal of Environmental Management* 268, 110691.

Han, R., Li, F., Liu, T., Li, X., Wu, Y., Wang, Y., Chen, D., 2016. Effects of incubation conditions on Cr (VI) reduction by c-type cytochromes in intact Shewanella oneidensis MR-1 cells. *Frontiers in microbiology* 7, 746.

Han, Z., Salawu, O.A., Zenobio, J.E., Zhao, Y., Adeleye, A.S., 2021. Emerging investigator series: immobilization of arsenic in soil by nanoscale zerovalent iron: role of sulfidation and application of machine learning. *Environmental Science: Nano* 8, 619-633.

Hanajima, D., Aoyagi, T., Hori, T., 2015. Survival of free-living Acholeplasma in aerated pig manure slurry revealed by 13C-labeled bacterial biomass probing. *Frontiers in Microbiology* 6, 1206.

Harris, D.C., 2010. Quantitative chemical analysis, 8th ed. W. H. Freeman and Company, New York.

Hassan, A., Pariatamby, A., Ossai, I., Ahmed, A., Muda, M., Wen, T., Hamid, F., 2022. Bioaugmentation-assisted bioremediation and kinetics modelling of heavy metal-

polluted landfill soil. *International Journal of Environmental Science and Technology* 19, 6729-6754.

Hatzinger, P., Diebold, J., 2009. In situ bioremediation of perchlorate in groundwater. Shaw Environmental, Inc., Lawrenceville, NJ.

Hautman, D.P., Munch, D.J., Eaton Andrew, D., Haghani Ali, W., 1999. EPA Method 314.0: Determination of perchlorate in drinking water using ion chromatography.

He, F., Zhao, D., Paul, C., 2010a. Field assessment of carboxymethyl cellulose stabilized iron nanoparticles for in situ destruction of chlorinated solvents in source zones. *Water Research* 44, 2360-2370.

He, Y.T., Wilson, J.T., Wilkin, R.T., 2010b. Impact of iron sulfide transformation on trichloroethylene degradation. *Geochimica et Cosmochimica Acta* 74, 2025-2039.

He, Z., Gao, F., Sha, T., Hu, Y., He, C., 2009. Isolation and characterization of a Cr (VI)-reduction Ochrobactrum sp. strain CSCr-3 from chromium landfill. *Journal of hazardous materials* 163, 869-873.

Heidelberg, J.F., Seshadri, R., Haveman, S.A., Hemme, C.L., Paulsen, I.T., Kolonay, J.F., Eisen, J.A., Ward, N., Methe, B., Brinkac, L.M., 2004. The genome sequence of the anaerobic, sulfate-reducing bacterium Desulfovibrio vulgaris Hildenborough. *Nature biotechnology* 22, 554-559.

Hem, J.D., 1985. Study and interpretation of the chemical characteristics of natural water. Department of the Interior, US Geological Survey.

Henn, K.W., Waddill, D.W., 2006. Utilization of nanoscale zero-valent iron for source remediation—A case study. *Remediation Journal: The Journal of Environmental Cleanup Costs, Technologies & Techniques* 16, 57-77.

Holmes, V.F., He, J., Lee, P.K., Alvarez-Cohen, L., 2006. Discrimination of multiple Dehalococcoides strains in a trichloroethene enrichment by quantification of their reductive dehalogenase genes. *Applied and Environmental Microbiology* 72, 5877-5883.

Hora, A., Shetty, V.K., 2015. Partial purification and characterization of chromate reductase of a novel Ochrobactrum sp. strain Cr-B4. *Preparative Biochemistry and Biotechnology* 45, 769-784.

Huang, H., Wu, K., Khan, A., Jiang, Y., Ling, Z., Liu, P., Chen, Y., Tao, X., Li, X., 2016. A novel Pseudomonas gessardii strain LZ-E simultaneously degrades naphthalene and reduces hexavalent chromium. *Bioresource technology* 207, 370-378.

Huang, J., Ye, Y., Fu, Z., Dun, W.J., Wang, Y., Fang, L., Ye, S., Ye, X., Jin, J., Hu, Q., 2019. Synergetic effects of zero-valent iron and Morganella morganii on the removal of Cr (VI) from Wastewater. *Nature Environment and Pollution Technology* 18, 871-877.

Huang, Y., Feng, H., Lu, H., Zeng, Y., 2017. A thorough survey for Cr-resistant and/or-reducing bacteria identified comprehensive and pivotal taxa. *International Biodeterioration & Biodegradation* 117, 22-30.

Huang, Y.H., Zhang, T.C., 2005. Effects of dissolved oxygen on formation of corrosion products and concomitant oxygen and nitrate reduction in zero-valent iron systems with or without aqueous Fe^{2+}. *Water Research* 39, 1751-1760.

Ibarrolaza, A., Coppotelli, B.M., Del Panno, M.T., Donati, E.R., Morelli, I.S., 2009. Dynamics of microbial community during bioremediation of phenanthrene and chromium (VI)-contaminated soil microcosms. *Biodegradation* 20, 95-107.

Ike, M., Miyazaki, T., Yamamoto, N., Sei, K., Soda, S., 2008. Removal of arsenic from groundwater by arsenite-oxidizing bacteria. *Water Science and Technology* 58, 1095-1100.

Inczedy, J., Lengyel, T., Ure, A.M., Gelencsér, A., Hulanicki, A., 1998. Compendium of analytical nomenclature. *Hoboken: Blackwell Science*.

Islam, S., Han, Y., Yan, W., 2020. Reactions of chlorinated ethenes with surface-sulfidated iron materials: reactivity enhancement and inhibition effects. *Environmental Science: Processes & Impacts* 22, 759-770.

Jeong, H.Y., Hayes, K.F., 2007. Reductive dechlorination of tetrachloroethylene and trichloroethylene by mackinawite (FeS) in the presence of metals: reaction rates. *Environmental science & technology* 41, 6390-6396.

Jobby, R., Jha, P., Yadav, A.K., Desai, N., 2018. Biosorption and biotransformation of hexavalent chromium [Cr (VI)]: a comprehensive review. *Chemosphere* 207, 255-266.

Joe-Wong, C., Brown Jr, G.E., Maher, K., 2017. Kinetics and products of chromium (VI) reduction by iron (II/III)-bearing clay minerals. *Environmental Science & Technology* 51, 9817-9825.

Joshi, S., Robles, A., Aguiar, S., Delgado, A.G., 2021. The occurrence and ecology of microbial chain elongation of carboxylates in soils. *The ISME Journal*.

Joutey, N.T., Sayel, H., Bahafid, W., El Ghachtouli, N., 2015. Mechanisms of hexavalent chromium resistance and removal by microorganisms. *Reviews of Environmental Contamination and Toxicology* Volume 233. Springer, pp. 45-69.

Kanel, S.R., Nepal, D., Manning, B., Choi, H., 2007. Transport of surface-modified iron nanoparticle in porous media and application to arsenic (III) remediation. *Journal of Nanoparticle Research* 9, 725-735.

Karlson, U., Frankenberger Jr, W., 1986. Determination of selenate by single-column ion chromatography. *Journal of Chromatography A* 368, 153-161.

Karri, S., Sierra-Alvarez, R., Field, J.A., 2005. Zero valent iron as an electron-donor for methanogenesis and sulfate reduction in anaerobic sludge. *Biotechnology and Bioengineering* 92, 810-819.

Karthik, C., Ramkumar, V.S., Pugazhendhi, A., Gopalakrishnan, K., Arulselvi, P.I., 2017. Biosorption and biotransformation of Cr (VI) by novel Cellulosimicrobium funkei strain AR6. *Journal of the Taiwan Institute of Chemical Engineers* 70, 282-290.

Keenan, C.R., Goth-Goldstein, R., Lucas, D., Sedlak, D.L., 2009. Oxidative stress induced by zero-valent iron nanoparticles and Fe (II) in human bronchial epithelial cells. *Environmental science & technology* 43, 4555-4560.

Keenan, C.R., Sedlak, D.L., 2008. Factors affecting the yield of oxidants from the reaction of nanoparticulate zero-valent iron and oxygen. *Environmental Science & Technology* 42, 1262-1267.

Khamkhash, A., Srivastava, V., Ghosh, T., Akdogan, G., Ganguli, R., Aggarwal, S., 2017. Mining-related selenium contamination in Alaska, and the state of current knowledge. *Minerals* 7, 46.

Kim, C., Zhou, Q., Deng, B., Thornton, E.C., Xu, H., 2001. Chromium (VI) reduction by hydrogen sulfide in aqueous media: stoichiometry and kinetics. *Environmental Science & Technology* 35, 2219-2225.

Kim, J.Y., Park, H.-J., Lee, C., Nelson, K.L., Sedlak, D.L., Yoon, J., 2010. Inactivation of Escherichia coli by nanoparticulate zerovalent iron and ferrous ion. *Applied and Environmental Microbiology* 76, 7668-7670.

Kirschling, T.L., Gregory, K.B., Minkley, J., Edwin G, Lowry, G.V., Tilton, R.D., 2010. Impact of nanoscale zero valent iron on geochemistry and microbial populations in trichloroethylene contaminated aquifer materials. *Environmental Science & Technology* 44, 3474-3480.

Kiyama, M., 1974. Conditions for the Formation of Fe_3O_4 by the Air Oxidation of $Fe(OH)_2$ Suspensions. *Bulletin of the Chemical Society of Japan* 47, 1646-1650.

Kocur, C.M., Chowdhury, A.I., Sakulchaicharoen, N., Boparai, H.K., Weber, K.P., Sharma, P., Krol, M.M., Austrins, L., Peace, C., Sleep, B.E., 2014.

Characterization of nZVI mobility in a field scale test. *Environmental Science & Technology* 48, 2862-2869.

Kocur, C.M., Lomheim, L., Boparai, H.K., Chowdhury, A.I., Weber, K.P., Austrins, L.M., Edwards, E.A., Sleep, B.E., O'Carroll, D.M., 2015. Contributions of abiotic and biotic dechlorination following carboxymethyl cellulose stabilized nanoscale zero valent iron injection. *Environmental Science & Technology* 49, 8648-8656.

Kodama, Y., Watanabe, K., 2004. Sulfuricurvum kujiense gen. nov., sp. nov., a facultatively anaerobic, chemolithoautotrophic, sulfur-oxidizing bacterium isolated from an underground crude-oil storage cavity. *International Journal of Systematic and Evolutionary Microbiology* 54, 2297-2300.

Koelschbach, J.S., Mouttaki, H., Pickl, C., Heipieper, H.J., Rachel, R., Lawson, P.A., Meckenstock, R.U., 2017. Rectinema cohabitans gen. nov., sp. nov., a rod-shaped spirochaete isolated from an anaerobic naphthalene-degrading enrichment culture. *International Journal of Systematic and Evolutionary Microbiology* 67, 1288-1295.

Koenig, J.C., Boparai, H.K., Lee, M.J., O'Carroll, D.M., Barnes, R.J., Manefield, M.J., 2016. Particles and enzymes: Combining nanoscale zero valent iron and organochlorine respiring bacteria for the detoxification of chloroethane mixtures. *Journal of Hazardous Materials* 308, 106-112.

Kończyk, J., Muntean, E., Michalski, R., 2018. Simultaneous determination of chromate and common inorganic anions using suppressed ion chromatography. *Chemistry, Environment, Biotechnology* 21, 11-13.

Krishna, K.R., Philip, L., 2005. Bioremediation of Cr (VI) in contaminated soils. *Journal of Hazardous Materials* 121, 109-117.

Krumholz, L.R., 1997. Desulfuromonas chloroethenica sp. nov. uses tetrachloroethylene and trichloroethylene as electron acceptors. *International Journal of Systematic and Evolutionary Microbiology* 47, 1262-1263.

Kucharzyk, K.H., Meisel, J.E., Kara-Murdoch, F., Murdoch, R.W., Higgins, S.A., Vainberg, S., Bartling, C.M., Mullins, L., Hatzinger, P.B., Löffler, F.E., 2020. Metagenome-Guided Proteomic Quantification of Reductive Dehalogenases in the Dehalococcoides mccartyi-Containing Consortium SDC-9. *Journal of Proteome Research* 19, 1812-1823.

Lampron, K.J., Chiu, P.C., Cha, D.K., 1998. Biological reduction of trichloroethene supported by Fe (0). *Bioremediation Journal* 2, 175-181.

Lash, L.H., Chiu, W.A., Guyton, K.Z., Rusyn, I., 2014. Trichloroethylene biotransformation and its role in mutagenicity, carcinogenicity and target organ toxicity. *Mutation Research/Reviews in Mutation Research* 762, 22-36.

Lazarev, V., Levitskii, S., Basovskii, Y., Chukin, M., Akopian, T., Vereshchagin, V., Kostrjukova, E., Kovaleva, G., Kazanov, M., Malko, D., 2011. Complete genome and proteome of Acholeplasma laidlawii. *Journal of Bacteriology* 193, 4943-4953.

Lee, C., Kim, J.Y., Lee, W.I., Nelson, K.L., Yoon, J., Sedlak, D.L., 2008a. Bactericidal effect of zero-valent iron nanoparticles on Escherichia coli. *Environmental Science & Technology* 42, 4927-4933.

Lee, H., Choi, W., 2002. Photocatalytic oxidation of arsenite in TiO2 suspension: kinetics and mechanisms. *Environmental Science & Technology* 36, 3872-3878.

Lee, P.K., Macbeth, T.W., Sorenson Jr, K.S., Deeb, R.A., Alvarez-Cohen, L., 2008b. Quantifying genes and transcripts to assess the in situ physiology of "Dehalococcoides" spp. in a trichloroethene-contaminated groundwater site. *Applied and Environmental Microbiology* 74, 2728-2739.

Li, P., Karunanidhi, D., Subramani, T., Srinivasamoorthy, K., 2021a. Sources and consequences of groundwater contamination. *Archives of Environmental Contamination and Toxicology* 80, 1-10.

Li, X., Yang, S., Dzakpasu, M., Xu, S., Ding, D., Wang, G., Chen, R., Jin, P., Wang, X.C., 2021b. Galvanic corrosion of zero-valent iron to intensify Fe^{2+} generation for peroxymonosulfate activation. *Chemical Engineering Journal* 417, 128023.

Li, Z., Greden, K., Alvarez, P.J., Gregory, K.B., Lowry, G.V., 2010. Adsorbed polymer and NOM limits adhesion and toxicity of nano scale zerovalent iron to E. coli. *Environmental Science & Technology* 44, 3462-3467.

Lin, W.-H., Chen, C.-C., Ou, J.-H., Sheu, Y.-T., Hou, D., Kao, C.-M., 2022. Bioremediation of hexavalent-chromium contaminated groundwater: Microcosm, column, and microbial diversity studies. *Chemosphere* 295, 133877.

Liu, C., Gorby, Y.A., Zachara, J.M., Fredrickson, J.K., Brown, C.F., 2002. Reduction kinetics of Fe (III), Co (III), U (VI), Cr (VI), and Tc (VII) in cultures of dissimilatory metal-reducing bacteria. *Biotechnology and bioengineering* 80, 637-649.

Liu, Y., Lowry, G.V., 2006. Effect of particle age (Fe^0 content) and solution pH on NZVI reactivity: H_2 evolution and TCE dechlorination. *Environmental science & technology* 40, 6085-6090.

Liu, Y., Phenrat, T., Lowry, G.V., 2007. Effect of TCE concentration and dissolved groundwater solutes on NZVI-promoted TCE dechlorination and H_2 evolution. *Environmental Science & Technology* 41, 7881-7887.

Liu, Y., Wang, Q., Zhang, Y., Ni, B.-J., 2015a. Zero valent iron significantly enhances methane production from waste activated sludge by improving biochemical methane potential rather than hydrolysis rate. *Scientific Reports* 5, 1-6.

Liu, Y., Zhang, Y., Ni, B.-J., 2015b. Zero valent iron simultaneously enhances methane production and sulfate reduction in anaerobic granular sludge reactors. *Water Research* 75, 292-300.

Löffler, F.E., Ritalahti, K.M., Zinder, S.H., 2013. Dehalococcoides and reductive dechlorination of chlorinated solvents. *Bioaugmentation for groundwater remediation*. Springer, pp. 39-88.

Löffler, F.E., Sanford, R.A., Ritalahti, K.M., 2005. Enrichment, cultivation, and detection of reductively dechlorinating bacteria. *Methods in enzymology* 397, 77-111.

Lorah, M.M., Majcher, E.H., Jones, E.J., Voytek, M.A., 2008. Microbial consortia development and microcosm and column experiments for enhanced bioremediation of chlorinated volatile organic compounds, West Branch Canal Creek wetland area, Aberdeen Proving Ground, Maryland. U. S. Geological Survey.

Lovley, D.R., Giovannoni, S.J., White, D.C., Champine, J.E., Phillips, E., Gorby, Y.A., Goodwin, S., 1993. Geobacter metallireducens gen. nov. sp. nov., a microorganism capable of coupling the complete oxidation of organic compounds to the reduction of iron and other metals. *Archives of microbiology* 159, 336-344.

Lovley, D.R., Phillips, E.J., 1994. Reduction of chromate by Desulfovibrio vulgaris and its c3 cytochrome. *Appl. Environ. Microbiol.* 60, 726-728.

Lozupone, C., Hamady, M., Knight, R., 2006. UniFrac–an online tool for comparing microbial community diversity in a phylogenetic context. *BMC bioinformatics* 7, 1-14.

Lu, X., Wilson, J.T., Kampbell, D.H., 2006. Relationship between Dehalococcoides DNA in ground water and rates of reductive dechlorination at field scale. *Water Research* 40, 3131-3140.

Ludwig, R.D., Su, C., Lee, T.R., Wilkin, R.T., Acree, S.D., Ross, R.R., Keeley, A., 2007. In situ chemical reduction of Cr (VI) in groundwater using a combination of ferrous sulfate and sodium dithionite: a field investigation. *Environmental science & technology* 41, 5299-5305.

Lyon, D.Y., Vogel, T.M., 2013. Bioaugmentation for groundwater remediation: an overview. Bioaugmentation for Groundwater Remediation. Springer, pp. 1-37.

Lytras, G., Lytras, C., Argyropoulou, D., Dimopoulos, N., Malavetas, G., Lyberatos, G., 2017. A novel two-phase bioreactor for microbial hexavalent chromium removal from wastewater. *Journal of hazardous materials* 336, 41-51.

Ma, L., Xu, J., Chen, N., Li, M., Feng, C., 2019. Microbial reduction fate of chromium (Cr) in aqueous solution by mixed bacterial consortium. *Ecotoxicology and environmental safety* 170, 763-770.

Magga, Z., Tzovolou, D.N., Theodoropoulou, M.A., Dalkarani, T., Pikios, K., Tsakiroglou, C.D., 2008. Soil column experiments used as a means to assess transport, sorption, and biodegradation of pesticides in groundwater. *Journal of Environmental Science and Health, Part B* 43, 732-741.

Mala, J.G.S., Sujatha, D., Rose, C., 2015. Inducible chromate reductase exhibiting extracellular activity in Bacillus methylotrophicus for chromium bioremediation. *Microbiological research* 170, 235-241.

Mao, X., Polasko, A., Alvarez-Cohen, L., 2017. Effects of sulfate reduction on trichloroethene dechlorination by *Dehalococcoides*-containing microbial communities. *Applied and environmental microbiology* 83.

Marsalek, B., Jancula, D., Marsalkova, E., Mashlan, M., Safarova, K., Tucek, J., Zboril, R., 2012. Multimodal action and selective toxicity of zerovalent iron nanoparticles against cyanobacteria. *Environmental Science & Technology* 46, 2316-2323.

Maymo-Gatell, X., Chien, Y., Gossett, J.M., Zinder, S.H., 1997. Isolation of a bacterium that reductively dechlorinates tetrachloroethene to ethene. *Science (New York, N.Y.)* 276, 1568--1571.

McCarty, P.L., 2010. Groundwater contamination by chlorinated solvents: history, remediation technologies and strategies. In situ remediation of chlorinated solvent plumes. Springer, pp. 1-28.

McDonald, D., Price, M.N., Goodrich, J., Nawrocki, E.P., DeSantis, T.Z., Probst, A., Andersen, G.L., Knight, R., Hugenholtz, P., 2012. An improved Greengenes taxonomy with explicit ranks for ecological and evolutionary analyses of bacteria and archaea. *The ISME journal* 6, 610-618.

McNaught, A.D., Wilkinson, A., 1997. Compendium of chemical terminology. Blackwell Science Oxford.

Mehra, H., Frankenberger, W., 1988. Simultaneous analysis of selenate and selenite by single-column ion chromatography. *Chromatographia* 25, 585-588.

Meinel, M., Delgado, A.G., Ilhan, Z.E., Aguero, M.L., Aguiar, S., Krajmalnik-Brown, R., Torres, C.I., 2022. Organic carbon metabolism is a main determinant of hydrogen demand and dynamics in anaerobic soils. *Chemosphere*, 134877.

Melnyk, R.A., Coates, J.D., 2015. The perchlorate reduction genomic island: mechanisms and pathways of evolution by horizontal gene transfer. *BMC genomics* 16, 862.

Melnyk, R.A., Engelbrektson, A., Clark, I.C., Carlson, H.K., Byrne-Bailey, K., Coates, J.D., 2011. Identification of a perchlorate reduction genomic island with novel regulatory and metabolic genes. *Appl. Environ. Microbiol.* 77, 7401-7404.

Metrohm USA, Determination of Hexavalent Chromium (Cr+6) by US EPA Method 218.7 https://www.metrohm.com/en-us/applications/AN-U-US-001.

Miao, Z., Brusseau, M.L., Carroll, K.C., Carreón-Diazconti, C., Johnson, B., 2012. Sulfate reduction in groundwater: characterization and applications for remediation. *Environmental Geochemistry and Health* 34, 539-550.

Miao, Z., Carroll, K.C., Brusseau, M.L., 2013. Characterization and quantification of groundwater sulfate sources at a mining site in an arid climate: The Monument Valley site in Arizona, USA. *Journal of hydrology* 504, 207-215.

Michalski, R., 2003. Ion chromatography method for the determination of trace levels of chromium (VI) in water. *Polish Journal of Environmental Studies* 13, 73-78.

Michel, A., Koch-Koerfges, A., Krumbach, K., Brocker, M., Bott, M., 2015. Anaerobic growth of Corynebacterium glutamicum via mixed-acid fermentation. *Applied and environmental microbiology* 81, 7496-7508.

Michel, C., Brugna, M., Aubert, C., Bernadac, A., Bruschi, M., 2001. Enzymatic reduction of chromate: comparative studies using sulfate-reducing bacteria. *Applied microbiology and biotechnology* 55, 95-100.

Mills, C.T., Morrison, J.M., Goldhaber, M.B., Ellefsen, K.J., 2011. Chromium (VI) generation in vadose zone soils and alluvial sediments of the southwestern Sacramento Valley, California: a potential source of geogenic Cr (VI) to groundwater. *Applied geochemistry* 26, 1488-1501.

Miranda, E.M., Severson, C., Reep, J.K., Hood, D., Hansen, S., Santisteban, L., Hamdan, N., Delgado, A.G., 2021. Continuous-mode acclimation and operation of lignocellulosic sulfate-reducing bioreactors for enhanced metal immobilization from acidic mining-influenced water. *Journal of Hazardous Materials*, 128054.

Moe, W.M., Rainey, F.A., Yan, J., 2016. The genus Dehalogenimonas. *Organohalide-Respiring Bacteria*, 137-151.

Mohana Rangan, S., Krajmalnik-Brown, R., Delgado, A.G., 2021. An Ion Chromatography Method for Simultaneous Quantification of Chromate, Arsenate, Selenate, Perchlorate, and Other Inorganic Anions in Environmental Media. *Environmental Engineering Science* 38, 626-634.

Moore, A.M., De Leon, C.H., Young, T.M., 2003. Rate and extent of aqueous perchlorate removal by iron surfaces. *Environmental science & technology* 37, 3189-3198.

Moratalla, Á., Correia, S.E., Cotillas, S., Lacasa, E., Cañizares, P., Rodrigo, M.A., Sáez, C., 2022. The integration of ZVI-dehalogenation and electrochemical oxidation for the treatment of complex effluents polluted with iodinated compounds. *Journal of Environmental Chemical Engineering* 10, 107587.

Mueller, N.C., Braun, J., Bruns, J., Černík, M., Rissing, P., Rickerby, D., Nowack, B., 2012. Application of nanoscale zero valent iron (NZVI) for groundwater remediation in Europe. *Environmental Science and Pollution Research* 19, 550-558.

Munch, D.J., Wasko, M., Flynt, E., Wendelken, S.C., Scifres, J., Mario, J.R., Hunt, M., Gregg, D., Schaeffer, T., Clarage, M., 2005. Validation and Peer Review of US Environmental Protection Agency Chemical Methods of Analysis.

Naftz, D., Morrison, S.J., Fuller, C.C., Davis, J.A., 2002. Handbook of groundwater remediation using permeable reactive barriers: applications to radionuclides, trace metals, and nutrients. Academic Press.

Nazarova, T., Alessi, D.S., Janssen, D.J., Bernier-Latmani, R., Wanner, C., 2020. In situ biostimulation of Cr (VI) reduction in a fast-flowing oxic aquifer. *ACS Earth and Space Chemistry* 4, 2018-2030.

Nijenhuis, I., Andert, J., Beck, K., Kästner, M., Diekert, G., Richnow, H.-H., 2005. Stable isotope fractionation of tetrachloroethene during reductive dechlorination by Sulfurospirillum multivorans and Desulfitobacterium sp. strain PCE-S and abiotic reactions with cyanocobalamin. *Applied and Environmental Microbiology* 71, 3413-3419.

Noubactep, C., 2013. Metallic iron for water treatment: A critical review. *Clean–Soil, Air, Water* 41, 702-710.

O'Carroll, D., Sleep, B., Krol, M., Boparai, H., Kocur, C., 2013. Nanoscale zero valent iron and bimetallic particles for contaminated site remediation. *Advances in Water Resources* 51, 104-122.

Oleszkiewicz, J., Elektorowicz, M., 1993. Groundwater contamination with trichloroethylene: The problem and some solutions—A review. *Soil and Sediment Contamination* 2, 205-228.

Olson, M.R., Sale, T.C., 2015. Implications of soil mixing for NAPL source zone remediation: Column studies and modeling of field-scale systems. *Journal of Contaminant Hydrology* 177, 206-219.

Onchoke, K.K., Sasu, S.A., 2016. Determination of Hexavalent Chromium (Cr (VI)) concentrations via ion chromatography and UV-Vis spectrophotometry in samples collected from nacogdoches wastewater treatment plant, East Texas (USA). *Advances in Environmental Chemistry* 2016.

Ontañon, O.M., González, P.S., Agostini, E., 2015. Optimization of simultaneous removal of Cr (VI) and phenol by a native bacterial consortium: its use for bioaugmentation of co-polluted effluents. *Journal of Applied Microbiology* 119, 1011-1022.

Ontiveros-Valencia, A., Tang, Y., Krajmalnik-Brown, R., Rittmann, B.E., 2014. Managing the interactions between sulfate-and perchlorate-reducing bacteria when using hydrogen-fed biofilms to treat a groundwater with a high perchlorate concentration. *Water research* 55, 215-224.

Oren, A., 2014. The family *Rhodocyclaceae*. *The Prokaryotes* 11, 975-998.

Oze, C., Bird, D.K., Fendorf, S., 2007. Genesis of hexavalent chromium from natural sources in soil and groundwater. *Proceedings of the National Academy of Sciences* 104, 6544-6549.

Pankow, J.F., Cherry, J.A., 1996. Dense chlorinated solvents and other DNAPLs in groundwater: History, behavior, and remediation.

Pantazidou, M., Panagiotakis, I., Mamais, D., Zikidi, V., 2012. Chloroethene biotransformation in the presence of different sulfate concentrations. *Groundwater Monitoring & Remediation* 32, 106-119.

Parbs, A., Ebert, M., Dahmke, A., 2007. Long-term effects of dissolved carbonate species on the degradation of trichloroethylene by zerovalent iron. *Environmental Science & Technology* 41, 291-296.

Park, J.Y., Yoon, H., Lee, S.-b., Kim, H.J., Jung, Y.H., Choi, C.W., Shin, J.-Y., Park, J.S., Seo, J.-S., 2021. Do Different Samples From Pregnant Women and Their Neonates Share the Common Microbiome: A Prospective Cohort Study.

Parker, D.R., Seyfferth, A.L., Reese, B.K., 2008. Perchlorate in groundwater: a synoptic survey of "pristine" sites in the coterminous United States. *Environmental Science & Technology* 42, 1465-1471.

Patterson, B.M., Lee, M., Bastow, T.P., Wilson, J.T., Donn, M.J., Furness, A., Goodwin, B., Manefield, M., 2016. Concentration effects on biotic and abiotic processes in the removal of 1, 1, 2-trichloroethane and vinyl chloride using carbon-amended ZVI. *Journal of Contaminant Hydrology* 188, 1-11.

Pawlett, M., Ritz, K., Dorey Robert, A., Rocks, S., Ramsden, J., Harris Jim, A., 2013. The impact of zero-valent iron nanoparticles upon soil microbial communities is context dependent. *Environmental Science and Pollution Research* 20, 1041-1049.

Phillips, D., Nooten, T.V., Bastiaens, L., Russell, M., Dickson, K., Plant, S., Ahad, J., Newton, T., Elliot, T., Kalin, R., 2010. Ten year performance evaluation of a field-scale zero-valent iron permeable reactive barrier installed to remediate trichloroethene contaminated groundwater. *Environmental Science & Technology* 44, 3861-3869.

Princy, S., Sathish, S.S., Cibichakravarthy, B., Prabagaran, S.R., 2020. Hexavalent chromium reduction by Morganella morganii (1Ab1) isolated from tannery effluent contaminated sites of Tamil Nadu, India. *Biocatalysis and Agricultural Biotechnology* 23, 101469.

Pushkar, B., Sevak, P., Parab, S., Nilkanth, N., 2021. Chromium pollution and its bioremediation mechanisms in bacteria: A review. *Journal of Environmental Management* 287, 112279.

Pyrzyńska, K., 2002. Determination of selenium species in environmental samples. *Microchimica Acta* 140, 55-62.

Qian, J., Wei, L., Liu, R., Jiang, F., Hao, X., Chen, G.-H., 2016. An exploratory study on the pathways of Cr (VI) reduction in sulfate-reducing up-flow anaerobic sludge bed (UASB) reactor. *Scientific Reports* 6, 23694.

Quast, C., Pruesse, E., Yilmaz, P., Gerken, J., Schweer, T., Yarza, P., Peplies, J., Glöckner, F.O., 2012. The SILVA ribosomal RNA gene database project: improved data processing and web-based tools. *Nucleic Acids Research* 41, D590-D596.

Rakhunde, R., Deshpande, L., Juneja, H., 2012. Chemical speciation of chromium in water: a review. *Critical Reviews in Environmental Science and Technology* 42, 776-810.

Rangan, S.M., 2017. Trade-offs in Utilizing of Zero-Valent Iron for Synergistic Biotic and Abiotic Reduction of Trichloroethene and Perchlorate in Soil and Groundwater. Arizona State University.

Rangan, S.M., Mouti, A., LaPat-Polasko, L., Lowry, G.V., Krajmalnik-Brown, R., Delgado, A.G., 2020. Synergistic Zerovalent Iron (Fe^0) and Microbiological Trichloroethene and Perchlorate Reductions Are Determined by the Concentration and Speciation of Fe. *Environmental Science & Technology* 54, 14422-14431.

Reinke, L.A., Rau James, M., McCay Paul, B., 1994. Characteristics of an oxidant formed during iron (II) autoxidation. *Free Radical Biology and Medicine* 16, 485-492.

Riley, R.G., 1992. Chemical contaminants on DOE lands and selection of contaminant mixtures for subsurface science research. US Department of Energy, Office of Energy Research, Subsurface Science Program.

Ritalahti, K.M., Löffler, F.E., Rasch, E.E., Koenigsberg, S.S., 2005. Bioaugmentation for chlorinated ethene detoxification: bioaugmentation and molecular diagnostics in the bioremediation of chlorinated ethene-contaminated sites. *Industrial Biotechnology* 1, 114-118.

Robles-Camacho, J., Armienta, M., 2000. Natural chromium contamination of groundwater at Leon Valley, Mexico. *Journal of Geochemical Exploration* 68, 167-181.

Robles, A., 2019. Reductive Dechlorination Sustained by Microbial Chain Elongation. Arizona State University.

Robles, A., Yellowman, T.L., Joshi, S., Mohana Rangan, S., Delgado, A.G., 2021. Microbial Chain Elongation and Subsequent Fermentation of Elongated Carboxylates as H2-Producing Processes for Sustained Reductive Dechlorination of Chlorinated Ethenes. *Environmental Science & Technology* 55, 10398-10410.

Rosenthal, H., Adrian, L., Steiof, M., 2004. Dechlorination of PCE in the presence of Fe^0 enhanced by a mixed culture containing two Dehalococcoides strains. *Chemosphere* 55, 661-669.

Ruhl, A.S., Naubert, A., Titze, D., Steiof, M., Jekel, M., 2008. Bioactivity and NOM distribution in horizontal columns with two alternative Fe0 materials after bioaugmentation. Remediation of Chlorinated and Recalcitrant Compounds. Battelle, Monterey, CA, pp. A-032.

Russell, H.H., Matthews, J.E., Guy, W.S., 1992. TCE removal from contaminated soil and groundwater. *EPA Environmental Engineering Sourcebook*, 87-100.

Saha, R., Nandi, R., Saha, B., 2011. Sources and toxicity of hexavalent chromium. *Journal of Coordination Chemistry* 64, 1782-1806.

Salnikow, K., Zhitkovich, A., 2008. Genetic and epigenetic mechanisms in metal carcinogenesis and cocarcinogenesis: nickel, arsenic, and chromium. *Chemical Research in Toxicology* 21, 28-44.

Sandrin, T.R., Maier, R.M., 2003. Impact of metals on the biodegradation of organic pollutants. *Environmental Health Perspectives* 111, 1093-1101.

Sathishkumar, K., Murugan, K., Benelli, G., Higuchi, A., Rajasekar, A., 2017. Bioreduction of hexavalent chromium by Pseudomonas stutzeri L1 and Acinetobacter baumannii L2. *Annals of Microbiology* 67, 91-98.

Schaefer, C.E., Lippincott, D.R., Steffan, R.J., 2010. Field-scale evaluation of bioaugmentation dosage for treating chlorinated ethenes. *Groundwater Monitoring & Remediation* 30, 113-124.

Schiwy, A., Maes, H.M., Koske, D., Flecken, M., Schmidt, K.R., Schell, H., Tiehm, A., Kamptner, A., Thümmler, S., Stanjek, H., 2016. The ecotoxic potential of a new zero-valent iron nanomaterial, designed for the elimination of halogenated pollutants, and its effect on reductive dechlorinating microbial communities. *Environmental Pollution* 216, 419-427.

Scholz-Muramatsu, H., Neumann, A., Meßmer, M., Moore, E., Diekert, G., 1995. Isolation and characterization of Dehalospirillum multivorans gen. nov., sp. nov., a tetrachloroethene-utilizing, strictly anaerobic bacterium. *Archives of Microbiology* 163, 48-56.

Schumacher, W., Holliger, C., 1996. The proton/electron ration of the menaquinone-dependent electron transport from dihydrogen to tetrachloroethene in" Dehalobacter restrictus". *Journal of Bacteriology* 178, 2328-2333.

Ševců, A., El-Temsah, Y.S., Joner, E.J., Černík, M., 2009. Oxidative stress induced in microorganisms by zero-valent iron nanoparticles. *Microbes and Environments*, 1107220320-1107220320.

Shekhawat, K., Chatterjee, S., Joshi, B., 2015. Chromium toxicity and its health hazards. *International Journal of Advanced Research* 3, 167-172.

Sheu, Y., Lien, P., Chen, K., Ou, J., Kao, C., 2016. Application of NZVI-contained emulsified substrate to bioremediate PCE-contaminated groundwater–A pilot-scale study. *Chemical Engineering Journal* 304, 714-727.

Shi, J., Zhang, B., Qiu, R., Lai, C., Jiang, Y., He, C., Guo, J., 2019. Microbial chromate reduction coupled to anaerobic oxidation of elemental sulfur or zerovalent iron. *Environmental science & technology* 53, 3198-3207.

Shrivastava, A., Gupta, V.B., 2011. Methods for the determination of limit of detection and limit of quantitation of the analytical methods. *Chronicles of Young Scientists* 2, 21.

Shrout, J.D., Williams, A.G., Scherer, M.M., Parkin, G.F., 2005. Inhibition of bacterial perchlorate reduction by zero-valent iron. *Biodegradation* 16, 23-32.

Šikovec, M., Franko, M., Novič, M., Veber, M., 2001. Effect of organic solvents in the on-line thermal lens spectrometric detection of chromium (III) and chromium (VI) after ion chromatographic separation. *Journal of Chromatography A* 920, 119-125.

Singh, R., Misra, V., Singh, R.P., 2012. Removal of Cr (VI) by nanoscale zero-valent iron (nZVI) from soil contaminated with tannery wastes. *Bulletin of Environmental Contamination and Toxicology* 88, 210-214.

Son, A., Lee, J., Chiu Pei, C., Kim Byung, J., Cha Daniel, K., 2006. Microbial reduction of perchlorate with zero-valent iron. *Water Research* 40, 2027-2032.

Song, X., Wang, Q., Jin, P., Chen, X., Tang, S., Wei, C., Li, K., Ding, X., Tang, Z., Fu, H., 2021. Enhanced biostimulation coupled with a dynamic groundwater recirculation system for Cr (VI) removal from groundwater: A field-scale study. *Science of The Total Environment* 772, 145495.

Song, Y., Logan, B.E., 2004. Effect of O2 exposure on perchlorate reduction by Dechlorosoma sp. KJ. *Water Research* 38, 1626-1632.

Srinivasan, A., Viraraghavan, T., 2009. Perchlorate: health effects and technologies for its removal from water resources. *International Journal of Environmental Research and Public Health* 6, 1418-1442.

Statham, T.M., Stark, S.C., Snape, I., Stevens, G.W., Mumford, K.A., 2016. A permeable reactive barrier (PRB) media sequence for the remediation of heavy metal and hydrocarbon contaminated water: A field assessment at Casey Station, Antarctica. *Chemosphere* 147, 368-375.

Steinmaus, C.M., 2016. Perchlorate in water supplies: sources, exposures, and health effects. *Current Environmental Health Reports* 3, 136-143.

Stephenson, J.B., 2007. Department of Defense Activities Related to Trichloroethylene, Perchlorate, and Other Emerging Contaminants. United States Government Accountability Office.

Stevenson, A., Herrera, J., 2018. Role of Zero Valent Iron and Organic Substrates in Chlorinated Solvent Degradation: An Ex-Situ Remediation Case Study. The University of Western Ontario.

Stroo, H.F., Leeson, A., Marqusee Jeffrey, A., Johnson Paul, C., Ward, C.H., Kavanaugh Michael, C., Sale Tom, C., Newell Charles, J., Pennell Kurt, D., Lebrn Carmen, A., Unger, M., 2012. Chlorinated ethene source remediation: Lessons learned. pp. 6438--6447.

Stroo, H.F., West, M.R., Kueper, B.H., Borden, R.C., Major, D.W., Ward, C.H., 2014. In situ bioremediation of chlorinated ethene source zones. Chlorinated solvent source zone remediation. Springer, pp. 395-457.

Stumm, W., Lee, G.F., 1961. Oxygenation of ferrous iron. *Industrial & Engineering Chemistry* 53, 143-146.

Su, C., Puls, R.W., Krug, T.A., Watling, M.T., O'Hara, S.K., Quinn, J.W., Ruiz, N.E., 2012. A two and half-year-performance evaluation of a field test on treatment of source zone tetrachloroethene and its chlorinated daughter products using emulsified zero valent iron nanoparticles. *Water Research* 46, 5071-5084.

Summer, D., Schöftner, P., Watzinger, A., Reichenauer, T.G., 2020. Inhibition and stimulation of two perchloroethene degrading bacterial cultures by nano-and micro-scaled zero-valent iron particles. *Science of The Total Environment* 722, 137802.

Sung, Y., Fletcher, K.E., Ritalahti, K.M., Apkarian, R.P., Ramos-Hernández, N., Sanford, R.A., Mesbah, N.M., Löffler, F.E., 2006. Geobacter lovleyi sp. nov. strain SZ, a novel metal-reducing and tetrachloroethene-dechlorinating bacterium. *Applied and Environmental Microbiology* 72, 2775-2782.

Sutherland, R.A., 2002. Comparison between non-residual Al, Co, Cu, Fe, Mn, Ni, Pb and Zn released by a three-step sequential extraction procedure and a dilute hydrochloric acid leach for soil and road deposited sediment. *Applied Geochemistry* 17, 353-365.

Tebo, B.M., Obraztsova, A.Y., 1998. Sulfate-reducing bacterium grows with Cr (VI), U (VI), Mn (IV), and Fe (III) as electron acceptors. *FEMS Microbiology Letters* 162, 193-199.

Tekerlekopoulou, A.G., Tsiamis, G., Dermou, E., Siozios, S., Bourtzis, K., Vayenas, D.V., 2010. The effect of carbon source on microbial community structure and Cr (VI) reduction rate. *Biotechnology and bioengineering* 107, 478-487.

Thermo Fisher Scientific, Sensitive Determination of Hexavalent Chromium in Drinking Water. Sunnyvale, CA, USA.

Thermo Scientific, 2013. Dionex onguard II cartridges product manual. Waltham, MA.

Todd, G.D., Ruiz, P., Mumtaz, M., Wohlers, D., Klotzbach, J.M., Diamond, G.L., Coley, C., Citra, M.J., 2019. Toxicological profile for trichloroethylene (TCE).

U.S. Department of Defense, 2005. Perchlorate in the Southwestern United States. DOD Environment, Safety and Occupational Health Network and Information Exchange.

U.S. EPA, 2003. Drinking Water Advisory: Consumer Acceptability Advice and

Health Effects Analysis on Sulfate. U.S. Environmental Protection Agency.

Urbansky, E.T., 2000. Perchlorate in the Environment. Springer.

Urbansky, E.T., 2002. Perchlorate as an environmental contaminant. *Environmental Science and Pollution Research* 9, 187-192.

US EPA, 1992. Method 7196A: Chromium, Hexavalent (Colorimetric). United States Environmental Protection Agency.

US EPA, 1996. DBP/ICR Analytical Methods Manual. United States Environmental Protection Agency.

US EPA, 2007. Method 9056A: Determination of inorganic anions by ion chromatography. United States Environmental Protection Agency.

US EPA, 2010. Chromium in Drinking Water. https://www.epa.gov/sdwa/chromium-drinking-water.

US EPA, 2017. Search superfund site information.

Vainberg, S., Condee Charles, W., Steffan Robert, J., 2009. Large-scale production of bacterial consortia for remediation of chlorinated solvent-contaminated groundwater. *Journal of Industrial Microbiology and Biotechnology* 36, 1189-1197.

Velimirovic, M., Simons, Q., Bastiaens, L., 2014. Guar gum coupled microscale ZVI for in situ treatment of CAHs: Continuous-flow column study. *Journal of Hazardous Materials* 265, 20-29.

Velimirovic, M., Simons, Q., Bastiaens, L., 2015. Use of CAH-degrading bacteria as test-organisms for evaluating the impact of fine zerovalent iron particles on the anaerobic subsurface environment. *Chemosphere* 134, 338-345.

Villemur, R., Lanthier, M., Beaudet, R., Lépine, F., 2006. The desulfitobacterium genus. *FEMS Microbiology Reviews* 30, 706-733.

Vincent, J.B., 2017. New evidence against chromium as an essential trace element. *The Journal of Nutrition* 147, 2212-2219.

Viti, C., Pace, A., Giovannetti, L., 2003. Characterization of Cr (VI)-resistant bacteria isolated from chromium-contaminated soil by tannery activity. *Current Microbiology* 46, 0001-0005.

Vogel, T.M., Criddle, C.S., McCarty, P.L., 1987. ES&T critical reviews: transformations of halogenated aliphatic compounds. *Environmental science & technology* 21, 722-736.

Wang, S., Chen, S., Wang, Y., Low, A., Lu, Q., Qiu, R., 2016. Integration of organohalide-respiring bacteria and nanoscale zero-valent iron (Bio-nZVI-RD): a perfect marriage for the remediation of organohalide pollutants? *Biotechnology Advances* 34, 1384-1395.

Wang, Z., Bush, R.T., Sullivan, L.A., Liu, J., 2013. Simultaneous redox conversion of chromium (VI) and arsenic (III) under acidic conditions. *Environmental Science & Technology* 47, 6486-6492.

Wani, R., Kodam, K., Gawai, K., Dhakephalkar, P., 2007. Chromate reduction by Burkholderia cepacia MCMB-821, isolated from the pristine habitat of alkaline crater lake. *Applied Microbiology and Biotechnology* 75, 627-632.

Warren, L.A., Ferris, F.G., 1998. Continuum between sorption and precipitation of Fe (III) on microbial surfaces. *Environmental Science & Technology* 32, 2331-2337.

Weiss, J., 2016. Handbook of Ion Chromatography, 3 Volume Set. John Wiley & Sons.

WHO, 2003a. Chromium in drinking water. World Health Organization, Guidelines for frinking-water quality.

WHO, 2003b. Guidelines for Drinking-water Quality | Chromium. World Health Organization.

WHO, 2004. Sulfate in Drinking-water. World Health Organization.

WHO, 2018. Arsenic - Fact sheets. World Health Organization. https://www.who.int/news-room/fact-sheets/detail/arsenic.

Wolf-Gladrow, D.A., Zeebe, R.E., Klaas, C., Körtzinger, A., Dickson, A.G., 2007. Total alkalinity: The explicit conservative expression and its application to biogeochemical processes. *Marine Chemistry* 106, 287-300.

Xia, S., Song, Z., Jeyakumar, P., Shaheen, S.M., Rinklebe, J., Ok, Y.S., Bolan, N., Wang, H., 2019. A critical review on bioremediation technologies for Cr (VI)-

contaminated soils and wastewater. *Critical reviews in environmental science and technology* 49, 1027-1078.

Xie, Y., Dong, H., Zeng, G., Tang, L., Jiang, Z., Zhang, C., Deng, J., Zhang, L., Zhang, Y., 2017. The interactions between nanoscale zero-valent iron and microbes in the subsurface environment: a review. *Journal of Hazardous Materials* 321, 390-407.

Xin, Y., Yong, K., Duujong, L., Ying, F., 2008. Bioaugmented sulfate reduction using enriched anaerobic microflora in the presence of zero valent iron. *Chemosphere* 73, 1436-1441.

Xiu, Z.-m., Gregory, K.B., Lowry, G.V., Alvarez, P.J., 2010a. Effect of bare and coated nanoscale zerovalent iron on *tceA* and *vcrA* gene expression in *Dehalococcoides* spp. *Environmental Science & Technology* 44, 7647-7651.

Xiu, Z.-m., Jin, Z.-h., Li, T.-l., Mahendra, S., Lowry, G.V., Alvarez, P.J., 2010b. Effects of nano-scale zero-valent iron particles on a mixed culture dechlorinating trichloroethylene. *Bioresource Technology* 101, 1141-1146.

Yang, J., Meng, L., Guo, L., 2018a. In situ remediation of chlorinated solvent-contaminated groundwater using ZVI/organic carbon amendment in China: field pilot test and full-scale application. *Environmental Science and Pollution Research* 25, 5051-5062.

Yang, Y., Guo, J., Hu, Z., 2013. Impact of nano zero valent iron (NZVI) on methanogenic activity and population dynamics in anaerobic digestion. *Water Research* 47, 6790-6800.

Yang, Y., Yan, J., Li, X., Lv, Y., Cui, Y., Kara-Murdoch, F., Chen, G., Löffler, F.E., 2020. Genome Sequence of "Candidatus Dehalogenimonas etheniformans" Strain GP, a Vinyl Chloride-Respiring Anaerobe. *Microbiology Resource Announcements* 9, e01212-01220.

Yang, Y., Yang, F., Huang, W., Huang, W., Li, F., Lei, Z., Zhang, Z., 2018b. Enhanced anaerobic digestion of ammonia-rich swine manure by zero-valent iron: With special focus on the enhancement effect on hydrogenotrophic methanogenesis activity. *Bioresource Technology* 270, 172-179.

Yeo, J., Choi, W., 2009. Iodide-mediated photooxidation of arsenite under 254 nm irradiation. *Environmental Science & Technology* 43, 3784-3788.

Yi, Y., Tu, G., Zhao, D., Tsang, P.E., Fang, Z., 2020. Key role of FeO in the reduction of Cr (VI) by magnetic biochar synthesised using steel pickling waste liquor and sugarcane bagasse. *Journal of Cleaner Production* 245, 118886.

Yoon, J., Amy, G., Chung, J., Sohn, J., Yoon, Y., 2009. Removal of toxic ions (chromate, arsenate, and perchlorate) using reverse osmosis, nanofiltration, and ultrafiltration membranes. *Chemosphere* 77, 228-235.

Yu, X., Amrhein, C., Deshusses, M.A., Matsumoto, M.R., 2006. Perchlorate reduction by autotrophic bacteria in the presence of zero-valent iron. *Environmental science & technology* 40, 1328-1334.

Zaa, C.L.Y., McLean Joan, E., Dupont, R.R., Norton Jeanette, M., Sorensen Darwin, L., 2010. Dechlorinating and iron reducing bacteria distribution in a TCE-contaminated aquifer. *Ground Water Monitoring and Remediation* 30, 46-57.

Zaffiro, A., Zimmerman, M., Wendelken, S., Smith, G., Munch, D., 2011. METHOD 218.7: Determination of hexavalent chromium in drinking water by ion chromatography with post-column derivatization and UV-Visible spectroscopic detection. United States Environmental Protection Agency.

Zhang, B., Wang, Z., Shi, J., Dong, H., 2020. Sulfur-based mixotrophic bio-reduction for efficient removal of chromium (VI) in groundwater. *Geochimica et Cosmochimica Acta* 268, 296-309.

Zhang, T., Lowry, G.V., Capiro, N.L., Chen, J., Chen, W., Chen, Y., Dionysiou, D.D., Elliott, D.W., Ghoshal, S., Hofmann, T., 2019. In situ remediation of subsurface contamination: opportunities and challenges for nanotechnology and advanced materials. *Environmental Science: Nano* 6, 1283-1302.

Zhao, C., Yang, Q., Chen, W., Teng, B., 2012. Removal of hexavalent chromium in tannery wastewater by Bacillus cereus. *Canadian journal of microbiology* 58, 23-28.

Zhao, S., He, J., 2019. Reductive dechlorination of high concentrations of chloroethenes by a Dehalococcoides mccartyi strain 11G. *FEMS microbiology ecology* 95, fiy209.

Zheng, Q., Na, S., Li, X., Li, N., Hai, R., Wang, X., 2019. Acute effects of hexavalent chromium on the performance and microbial community of activated sludge in aerobiotic reactors. *Environmental technology* 40, 1871-1880.

Zhitkovich, A., 2011. Chromium in drinking water: sources, metabolism, and cancer risks. *Chemical Research in Toxicology* 24, 1617-1629.

Zhitkovich, A., Voitkun, V., Costa, M., 1996. Formation of the amino acid− DNA complexes by hexavalent and trivalent chromium in vitro: importance of trivalent chromium and the phosphate group. *Biochemistry* 35, 7275-7282.

Zhou, J., You, X., Niu, B., Yang, X., Gong, L., Zhou, Y., Wang, J., Zhang, H., 2020. Enhancement of methanogenic activity in anaerobic digestion of high solids sludge by nano zero-valent iron. *Science of the Total Environment* 703, 135532.

Ziv-El, M., Delgado, A.G., Yao, Y., Kang, D.-W., Nelson, K.G., Halden, R.U., Krajmalnik-Brown, R., 2011a. Development and characterization of DehaloR^2, a novel anaerobic microbial consortium performing rapid dechlorination of TCE to ethene. *Applied Microbiology and Biotechnology* 92, 1063-1071.

Ziv-El, M., Delgado Anca, G., Yao, Y., Kang Dae, W., Nelson Katherine, G., Halden Rolf, U., Krajmalnik-Brown, R., 2011b. Development and characterization of DehaloR 2, a novel anaerobic microbial consortium performing rapid dechlorination of TCE to ethene. *Applied Microbiology and Biotechnology* 92, 1063--1071.

Ziv-El, M., Kalinowski, T., Krajmalnik-Brown, R., Halden, R.U., 2014. Simultaneous determination of chlorinated ethenes and ethene in groundwater using headspace solid-phase microextraction with gas chromatography. *Journal of chromatographic science* 52, 137-142.

Ziv-El, M., Popat Sudeep, C., Parameswaran, P., Kang Dae, W., Polasko, A., Halden Rolf, U., Rittmann Bruce, E., Krajmalnik-Brown, R., 2012. Using electron balances and molecular techniques to assess trichoroethene-induced shifts to a dechlorinating microbial community. *Biotechnology and Bioengineering* 109, 2230--2239.

Ziv-El, M., Popat, S.C., Cai, K., Halden, R.U., Krajmalnik-Brown, R., Rittmann, B.E., 2012. Managing methanogens and homoacetogens to promote reductive dechlorination of trichloroethene with direct delivery of H2 in a membrane biofilm reactor. *Biotechnology and Bioengineering* 109, 2200-2210.

APPENDIX A

PREVIOUSLY PUBLISHED WORK

Chapters 2 is published in *Environmental Science & Technology* and Chapter 5 is published in *Environmental Engineering Science*. I am the first listed author in these published works and all co-authors have granted permissions to include these published manuscripts as chapters in this dissertation.